Max-Planck-Institut
für Meteorologie

MAX PLANCK
GESELLSCHAFT

International Max Planck Research School
on Earth System Modelling

Decadal prediction of shelf-sea marine ecosystems in the eastern North Atlantic: The role of the Subpolar Gyre

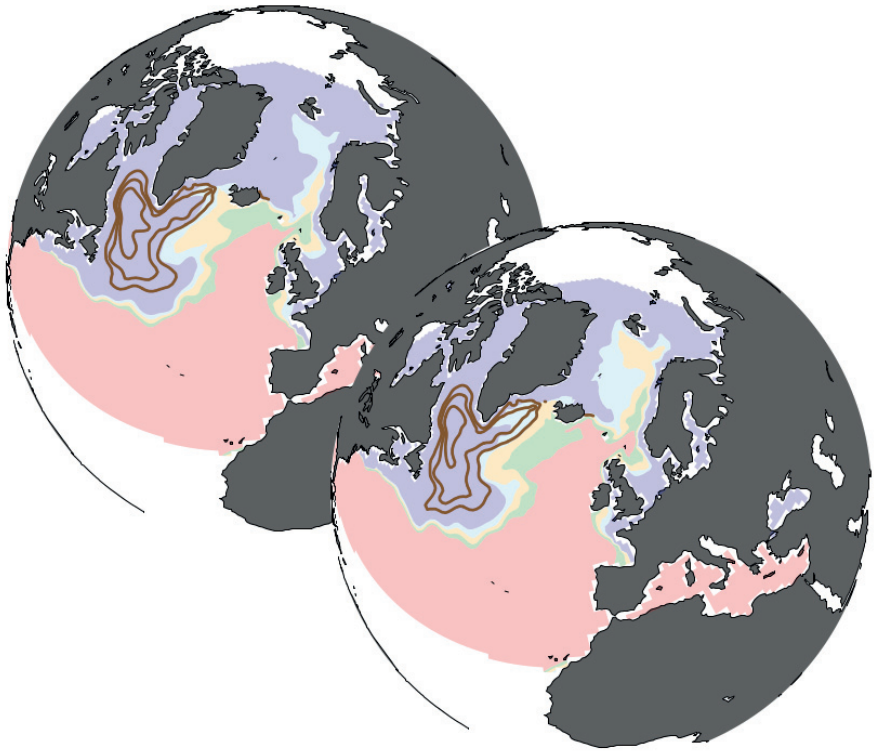

Vimal Koul

Hamburg 2020

Berichte zur Erdsystemforschung
Reports on Earth System Science

236
2020

Hinweis

Die Berichte zur Erdsystemforschung werden vom Max-Planck-Institut für Meteorologie in Hamburg in unregelmäßiger Abfolge herausgegeben.

Sie enthalten wissenschaftliche und technische Beiträge, inklusive Dissertationen.

Die Beiträge geben nicht notwendigerweise die Auffassung des Instituts wieder.

Die "Berichte zur Erdsystemforschung" führen die vorherigen Reihen "Reports" und "Examensarbeiten" weiter.

Notice

The Reports on Earth System Science are published by the Max Planck Institute for Meteorology in Hamburg. They appear in irregular intervals.

They contain scientific and technical contributions, including Ph. D. theses.

The Reports do not necessarily reflect the opinion of the Institute.

The "Reports on Earth System Science" continue the former "Reports" and "Examensarbeiten" of the Max Planck Institute.

Anschrift / Address

Max-Planck-Institut für Meteorologie
Bundesstrasse 53
20146 Hamburg
Deutschland

Tel./Phone: +49 (0)40 4 11 73 - 0
Fax: +49 (0)40 4 11 73 - 298

name.surname@mpimet.mpg.de
www.mpimet.mpg.de

Layout

Bettina Diallo and Norbert P. Noreiks
Communication

Copyright

Decadal prediction of shelf-sea marine ecosystems in the eastern North Atlantic: The role of the Subpolar Gyre

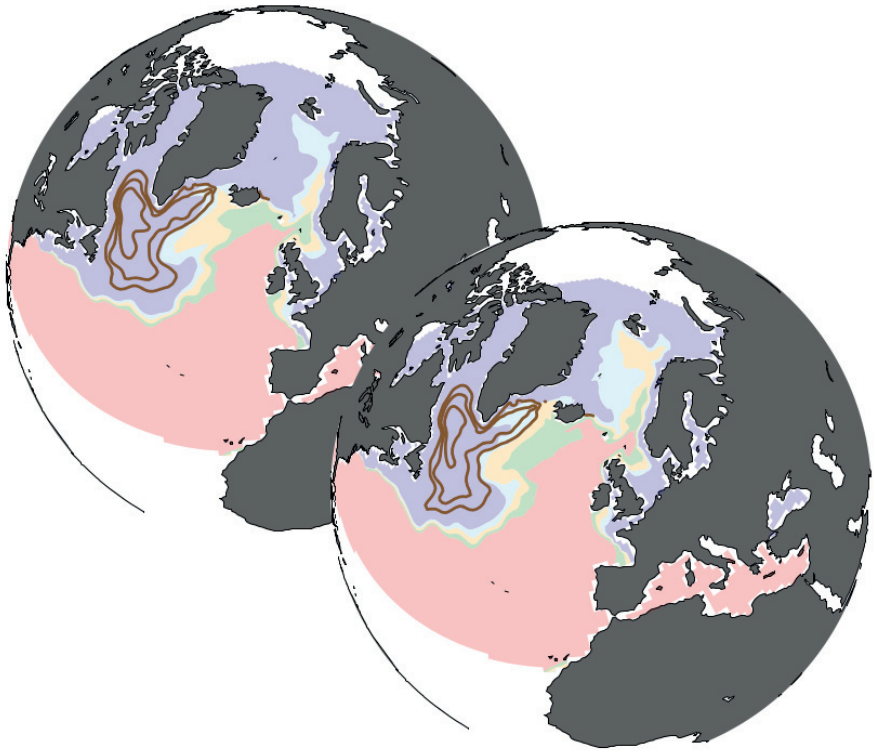

Vimal Koul

Hamburg 2020

Vimal Koul
aus Chittragam, Indien

Max-Planck-Institut für Meteorologie
The International Max Planck Research School on Earth System Modelling
(IMPRS-ESM)
Bundesstrasse 53
20146 Hamburg

Universität Hamburg
Geowissenschaften
Meteorologisches Institut
Bundesstr. 55
20146 Hamburg

Tag der Disputation: 22. Juni 2020

Folgende Gutachter empfehlen die Annahme der Dissertation:
Prof. Dr. Johanna Baehr
Prof. Dr. Corinna Schrum

Vorsitzender des Promotionsausschusses:
Prof. Dr. Dirk Gajewski

Dekan der MIN-Fakultät:
Prof. Dr. Heinrich Graener

Berichte zur Erdsystemforschung / Max-Planck-Institut für Meteorologie 236
Reports on Earth System Science / Max Planck Institute for Meteorology 2020

ISSN 1614-1199

ABSTRACT

Prediction of marine ecosystems is one of the most challenging goals in climate science. Although, over the last century, our understanding of how marine ecosystems change in time has considerably improved, we have had a dismal record on predicting future changes in key aspects of marine ecosystems, such as the fluctuations in fish stocks. In the North Atlantic, one would expect high predictability in marine ecosystems, because, this region is characterized by pronounced variability in oceanic conditions and a strong climate-ecosystem coupling. Such an expectation is reinforced by the remarkably high decadal predictability of oceanic conditions in global coupled models. However, multifaceted challenges have prevented the transfer of high prediction skill from the ocean to fish stocks. Here, using observations and a global coupled model, I reveal that oceanic variability in the North Atlantic Subpolar Gyre (SPG) is the key to decade long predictions in fish stocks in the shelf-seas of the eastern North Atlantic.

I begin with reconciling various conflicting views on SPG variability that have emerged from the application of different SPG indices. While the size and strength of SPG circulation has repeatedly been shown to influence physical and biogeochemical variability in the eastern North Atlantic, recent studies are rather skeptical of an active role of SPG circulation. I illustrate that the variability in the size and strength of SPG circulation is a delayed oceanic response to wind stress variability and involves meridional shifts of advective pathways in the Newfoundland Basin. This insight allows me to clarify the dynamical basis of various SPG indices, and leads to the conclusion that SPG indices based on barotropic streamfunction and largest closed contours of sea surface height should be interpreted with caution. Thus, I establish a close connection between the variability in SPG circulation and oceanic properties in the eastern subpolar North Atlantic.

Further, I illustrate that the influence of SPG circulation also extends to the north of the Greenland-Scotland Ridge. In the Faroe-Shetland Channel and the North Sea, low frequency variability in oceanic properties is mainly driven by variability in SPG circulation. A weak and contracted SPG circulation allows an enhanced throughput of subtropical waters towards far eastern regions of the North Atlantic, including the Barents Sea. Moreover, a volumetric water mass analysis in the regions north of the Greenland-Scotland Ridge suggests that the SPG signal is more pronounced in salinity than in temperature, which has implications on predictability.

Finally, I show that SPG-associated oceanic anomalies influence Barents Sea Cod stock, whereas a long term declining trend in the North Sea Cod stock masks such an influence. The variability in SPG temperature influences Barents Sea Cod biomass 7 years later. I combine this statistical SPG-Cod relationship with the dynamical multi-year prediction of SPG temperature. Using such a dynamical-statistical prediction system, the Barents Sea Cod biomass can be predicted 11 years in advance.

This dissertation, therefore, emphasizes the role of climate variability in the decadal prediction of fish stocks, and also establishes the scope for management decisions at decadal timescales. In this context, the variability in SPG circulation emerges as the key factor in the predictability of Barents Sea Cod stock.

ZUSAMMENFASSUNG

Vorhersagen von Meeresökosystemen sind eine der am schwierigsten zu realisierenden Ziele der Klimawissenschaften. Obwohl sich im Laufe des letzten Jahrhunderts unser Verständnis von temporalen Veränderungen in Meeresökosystemen erheblich verbessert hat, so weisen wir bisher dennoch eine erbärmliche Bilanz in der Vorhersage von Schlüsselaspekten von Meeresökosystemen, wie beispielsweise Fluktuationen von Fischbeständen, auf. Im Nordatlantik würde man ein hohes Vorhersagepotenzial von Meeresökosystemen erwarten weil diese Region von einer ausgeprägten natürlichen Variabilität ozeanischer Bedingungen sowie einer starken Klima-Ökosystem-Kopplung geprägt ist. Diese Erwartung wird durch die bemerkenswert hohe dekadische Vorhersagbarkeit der ozeanischen Bedingungen in global gekoppelten Modellen gestützt. Vielfältige Herausforderungen haben jedoch eine Übertragung dieser hohen Vorhersagekompetenz vom Ozean auf die Fischbestände verhindert. In dieser Dissertation zeige ich anhand von Beobachtungen und in einem global gekoppelten Modell, dass die ozeanische Variabilität im nordatlantischen Subpolaren Gyre (SPG) der Schlüssel zu jahrzehntelangen Vorhersagen über die Fischbestände in den Schelfmeeren des östlichen Nordatlantik ist.

Ich beginne damit, verschiedene widersprüchliche Ansichten über die SPG-Variabilität, die durch die Anwendung unterschiedlicher SPG-Indizes aufgetreten sind, in Einklang zu bringen. Während wiederholt gezeigt wurde, dass die Größe und Stärke der SPG-Zirkulation die physikalische und biogeochemische Variabilität im östlichen Nordatlantik beeinflusst, sind neuere Studien eher skeptisch bezüglich einer aktiven Rolle der SPG-Zirkulation. Ich veranschauliche, dass die Variabilität in Größe und Stärke der SPG-Zirkulation eine verzögerte ozeanische Reaktion auf die Variabilität des Windstresses darstellt und meridionale Verschiebungen von advektiven Strömungen im Neufundlandbecken beinhaltet. Diese Erkenntnisse ermöglichen es mir, die dynamischen Grundlagen verschiedener SPG-Indizes zu verdeutlichen und zu schlussfolgern, dass SPG-Indizes, die auf der barotropen Stromfunktion sowie jene die auf der größten geschlossenenen Kontur der Meeresoberflächenhöhe basieren, mit Vorsicht interpretiert werden sollten. Auf diese Weise stelle ich einen engen Zusammenhang zwischen der Variabilität der SPG-Zirkulation und den ozeanischen Eigenschaften im östlichen subpolaren Nordatlantik her.

Weiterhin veranschauliche ich, dass der Einfluss der SPG-Zirkulation sich auch auf Regionen nördlich des Grönland-Schottland-Rückens erstreckt. Im Färör-Shetland-Kanal und in der Nordsee wird die niederfrequente Variabilität der ozeanischen Eigenschaften hauptsächlich durch die Variabilität der SPG-Zirkulation bestimmt. Eine schwache und zusammengezogene SPG-Zirkulation ermöglicht einen verbesserten Durchfluss von subtropischem Wasser in die fernöstlichen Regionen des Nordatlantiks, einschließlich der Barentssee. Ferner deutet eine volumetrische Wassermassenanalyse in den Regionen nördlich des Grönland-Schottland-Rückens darauf hin, dass sich das SPG-Signal im Salzgehalt stärker als in der Temperatur niederschlägt, was Auswirkungen auf die Vorhersagbarkeit hat.

Abschließend zeige ich, dass SPG-assoziierte ozeanische Anomalien den Barentssee-Kabeljaubestand beeinflussen, wohingegen ein langfristig rückläufiger Trend im Nordsee-Kabeljaubestand einen solchen Einfluss verschleiert. Die Variabilität der SPG-Temperatur beeinflusst die Biomasse des Barentssee-Kabeljau mit einer Zeitverzögerung von 7 Jahren. Ich kombiniere diese statistische SPG-Kabeljau-Beziehung mit der dynamischen mehrjährigen Vorhersage der Temperaturen im SPG. Mit solch einem dynamisch statistischen Vorhersage-System kann die Biomasse des Barentssee-Kabeljaues 11 Jahre im Voraus vorhergesagt werden.

Somit hebt diese Dissertation die bedeutende Rolle von Klimaschwankungen für die dekadische Vorhersage von Fischbeständen im östlichen Nordatlantik hervor und eröffnet ebenso den Spielraum für Managemententscheidungen auf dekadischen Zeitskalen. Hierbei erweist sich insbesondere die Variabilität der SPG-Zirkulation als Schlüsselfaktor für die Vorhersagbarkeit des Barentssee-Kabeljaubestands.

PUBLICATIONS RELATED TO THIS DISSERTATION

Appendix A
Koul, V., Tesdal, J.E., Bersch, M., Hátún, H., Brune, S., Borchert, L., Haak, H., Schrum, C. and Baehr, J. (2019), "Unravelling the Choice of the North Atlantic Subpolar Gyre Index", Scientific Reports (*under review*)

Appendix B
Koul, V., Schrum, C., Düsterhus, A. & Baehr, J. (2019), "Atlantic Inflow to the North Sea Modulated by the Subpolar Gyre in a Historical Simulation with the MPI-ESM", Journal of Geophysical Research: Oceans,124, 1807–1826.

Appendix C
Koul, V., Schrum, C., Arthun, M., Brune, S. and Baehr, J. (2019), "Decadal Prediction of Barents Sea Cod Stock through an Oceanic Linkage with the Subpolar Gyre", Frontiers in Marine Science (*to be submitted*).

Contents

1

DECADAL PREDICTION OF NORTH ATLANTIC MARINE ECOSYSTEMS

1.1 INTRODUCTION

This dissertation is a contribution to the ongoing scientific quest towards the prediction of marine ecosystems. This quest has deep historical roots, and prediction of fluctuations in fish abundance lies at its core. The stage for the prediction of fish abundance was set by the seminal works of Helland-Hansen & Nansen (1909), and Hjort (1914) in the early twentieth century. At that time, the central question that confounded both fishers and scientists alike was – Why does the number of fish caught (fishery yield) fluctuate by a large amount from one year to another? The established explanation at that time was that the fish migrate, and they were not to be found at the usual fishing grounds. Helland-Hansen and Nansen started a systematic assessment and proposed that these fluctuations were related to the variability of Atlantic water properties (Helland-Hansen & Nansen, 1909). Hjort discarded the migration hypothesis, and by accumulating a large piece of evidence, he proposed several hypotheses. In their essence, these hypotheses proposed that survival of early life stages, and hence recruitment – the addition of young individuals to the adult population – determines the large fluctuations in fish abundance (Hjort, 1914). These hypotheses and their corollaries have been a focus of fisheries science over the last century (e.g. Cushing (1990) and Hare (2014)).

In the efforts towards predicting future changes in fish abundance, two main approaches have emerged from various refinements to the aforementioned hypotheses. The first approach considers interannual changes in fishing mortality as the primary cause of fluctuation in fish abundance (Quinn & Deriso, 1999). This approach assumes that variability in recruitment is reflected in the biomass of the sexually mature adult population (Beverton & Holt, 1957), and by knowing the current adult population (spawners) and managing their future harvest rate, the fluctuations in fish abundance can be determined. The second approach emphasizes the importance of changes in environmental conditions as an important precursor to variability in fish abundance (Stenseth et al., 2002; Lehodey et al., 2006; Drinkwater et al., 2010). Despite Hjort's reservations with the migration hypothesis, the concept of environmental niche has gained widespread acceptance and has often been invoked to explain changes in fish distribution and migration in response to changing environment (Nye et al., 2009; Pinsky et al., 2013). This second approach, perhaps, holds the key to long term prediction of fish abundance and distribution, and particularly for those fish stocks which have not borne the brunt of excessive exploitation.

The importance of environmental conditions in determining fish abundance and distribution has emerged from our improved understanding of climate-ecosystem connections over the last century. At seasonal and shorter time scales, variability in ocean currents influences the survival of early life stages by altering their transport towards nursery grounds (Shelton et al., 1982), and through advection of plankton (Hunt Jr et al., 2016). At interannual and longer timescales, climatic modes, such as the El Niño-Southern Oscillation (ENSO) and Pacific Decadal Oscillation (PDO) in the Pacific as well as the North Atlantic Oscillation (NAO) and Atlantic Multidecadal Oscillation (AMO) in the Atlantic, are known to greatly influence diverse fish species (Mantua et al., 1997; Stenseth et al., 2002; Chavez et al., 2003; Drinkwater et al., 2003; Alheit et al., 2014). These species include, for instance, Anchovies, Sardines, Herring, Salmon, Tuna and Cod. Ample evidence has now accumulated which supports direct or indirect influence of large fluctuation in temperature on growth and natural mortality rate of early life stages and adults (Brander, 1995; Michalsen et al., 1998), reproductive capability (Pörtner et al., 2001) and expansion or contraction of habitats (Sundby & Nakken, 2008; Nye et al., 2009; Pinsky et al., 2013). The impact of climate on fish abundance and distribution is not limited to oceanic temperature. Those species which spawn at depth show a preference for certain salinity bounds, and large shifts in spawning distribution of such species have been observed during saline and fresh oceanographic regimes (Miesner & Payne, 2018).

Despite these great strides in our understanding of climate-ecosystem connections, our ability to predict fish abundance or a shift in their distribution has remained poor. Particularly, in the eastern North Atlantic, where some of the world's highly productive fisheries reside (Carmack & Wassmann, 2006), our ability to predict fish stocks lags considerably behind the multiyear predictability of the physical environment of the Subpolar Gyre (SPG, Matei et al. (2012), Robson et al. (2012a), Msadek et al. (2014), and Hermanson et al. (2014)). Challenges have mainly come from the non-linearity associated with biological systems (Glaser et al., 2014; Subbey et al., 2014) and the impact of fishing mortality on many fish stocks in the North Atlantic (Hutchings, 1995; Myers et al., 1997; Frank et al., 2016; Sguotti et al., 2019). However, while the interaction between the inherent non-linearity in biological systems and fishing mortality may limit our ability to predict recruitment or variability at shorter time scales, the integrated impact of pronounced decadal climate variability on fish abundance (biomass) might provide a predictive potential.

In order to predict fish abundance in the eastern North Atlantic, we must consider necessary conditions for achieving reliable predictions of fish stocks. The first condition is the predominance of the physical environment in driving the fluctuation in fish stocks. In the eastern North Atlantic, most of the highly productive and commercially exploited fish stocks, such as the Cod (Gadus morhua), are present in the European continental shelf and Arcto-Norwegian ecosystems including the Barents Sea (Hamre, 1994; Drinkwater, 2005). In the North Sea, major events in the evolution of Cod stock, such as the "gadoid outburst", have been linked to variability in temperature, which impacts metabolism rates and prey availability in this region (Planque & Frédou, 1999; Beaugrand & Kirby, 2010; Olsen et al., 2010). In the Barents Sea, temperature also influences Cod biomass because of its impact on primary production, growth rates, and habitat expansion (Ottersen et al., 1994). Thus, environmental conditions can be a

potential source of predictability in fish stocks at interannual to decadal timescales in the eastern North Atlantic.

The second condition necessitates that the physical environment is predictable. Perhaps, this is where earlier efforts have fallen short. This is because (a) only recently have skillful interannual to decadal predictions emerged in the ocean (e.g. Pohlmann et al. (2004) and Meehl et al. (2014)) and (b) a systematic analysis of multi-year predictability in the eastern North Atlantic shelf seas has been either missing or has started to appear only recently (Tommasi et al., 2017c). If we are to transfer predictability from the physical realm to the biological realm, then we are further restricted by the tools at hand. In this respect, the global coupled models at the core of decadal prediction systems are known to perform poorly in shallow shelf-seas (Holt et al., 2017; Mathis et al., 2017), and in particular, there are known discrepancies in their representation of Atlantic water pathways across the Iceland-Scotland Ridge (Langehaug et al., 2019). Furthermore, we have very little knowledge of what kind of prediction systems, initialization or uninitialized, are best suited for the problem at hand. Then there is the question of quantifying the prediction skill of biological quantities, for which there is very little precedent.

At a more fundamental level, only recently have we started to understand the extent of oceanic linkages between the SPG and biologically important regions in the eastern North Atlantic (see Figure 1.1 for the location of these regions). We have not even arrived at a consensus on how to define the strength of SPG circulation yet, resulting in contradictions in our present understandings of the influence of the SPG in the eastern North Atlantic (Hátún et al., 2005; Foukal & Lozier, 2017). A dynamically consistent and observationally constrained relationship of the influence of SPG strength on hydrography of the regions north of the Greenland-Scotland Ridge has not emerged yet. Furthermore, a large number of earlier studies have focused on the North Atlantic Oscillation (NAO, Hurrell et al. (2003)) and its impact on surface temperatures of the eastern North Atlantic shelf seas (Becker & Pauly, 1996; Schrum, 2001; Drinkwater et al., 2003; Mathis et al., 2015). While the NAO explains a large part of atmospheric variability in the northern latitudes, the NAO is not predictable at multi-year time scales, thus making its application to predictability of fish stocks futile. However, there is scope to analyze the predictive potential emerging from the impact of SPG on large marine ecosystems (Hátún et al., 2009; Hátún et al., 2016).

In this dissertation, I examine these challenges and try to mitigate some of the bottlenecks in the path towards the prediction of fish stocks. While many studies have cautioned about the complexity of the problem and breaking down of correlative relationships between climate and fish stocks (Walters & Collie, 1988; Myers, 1998), analysing predictive potential of fish stocks is not an exercise in futility. This is because such skepticism was partly based on our past inability to predict oceanic conditions reliably, and partly because our past understanding of climate-ecosystem connections was still evolving. This earlier skepticism has, to some degree, now been extinguished by fishery forecasts being made using seasonal to annual forecasts of temperature (Hobday et al., 2011; Eveson et al., 2015; Kaplan et al., 2016). One of the reasons for the success of these forecast products is that rather than predicting recruitment, these products predict changes in fish habitat, which is highly influenced by environmental conditions. However, none of the first generation of marine ecosystem forecast products which exploit dynamical predictability of physical environment, caters to

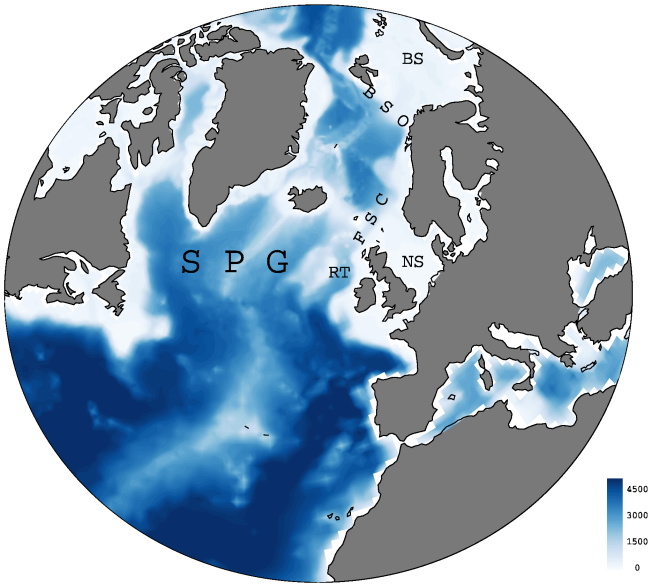

Figure 1.1: North Atlantic bathymetry (meter) in MPI-ESM-LR. SPG–Subpolar Gyre, RT–Rockall Trough, FSC–Faroe -Shetland Channel, BSO–Barents Sea Opening and BS–Barents Sea.

the North Atlantic (Payne et al., 2017). This is ironic because the North Atlantic, particularly the SPG, is one of the hotspots of multi-year predictability (Figure 1.2). This dissertation intends to investigate whether it is possible to transfer such high predictability to marine ecosystems.

The main incentives that motivated this dissertation, or perhaps the quest to predict life in the ocean in general, are the tremendous benefits such predictions would extend to sustainable management and well being of living marine resources. Conventionally, environmental impacts have been excluded from stock assessment procedures (Skern-Mauritzen et al., 2016; Stock et al., 2011), however, experience has shown that reactive policy interventions are inadequate at mitigating the challenges posed by our failure to predict climate-driven response in marine resources (Pershing et al., 2015). Therefore, there is a pressing need to provide reliable predictions on near term climatic shifts which would guide management decisions. At the same time, by demonstrating the power of climate-based predictions of fish stocks, there is a scope to nudge contemporary stock assessment procedures to consider environmental factors.

It is not possible – nor is it necessary – to mitigate all challenges detailed above. But through this cumulative dissertation, I intend to illuminate the path towards the interannual to decadal prediction of marine ecosystems in the eastern North Atlantic. As a first step, I investigate the observed and modelled variability of SPG strength, and provide my assessment on which index is the best suited proxy of SPG strength. In the second step, using the identified SPG index, I investigate the influence of SPG circulation on the eastern North Atlantic. And in the final step, I reveal the prediction skill in the physical environment of the SPG and the eastern North Atlantic, and the Cod biomass in the Barents Sea. The results from these three steps form three research articles and are presented as appendices to this dissertation. In the following sections,

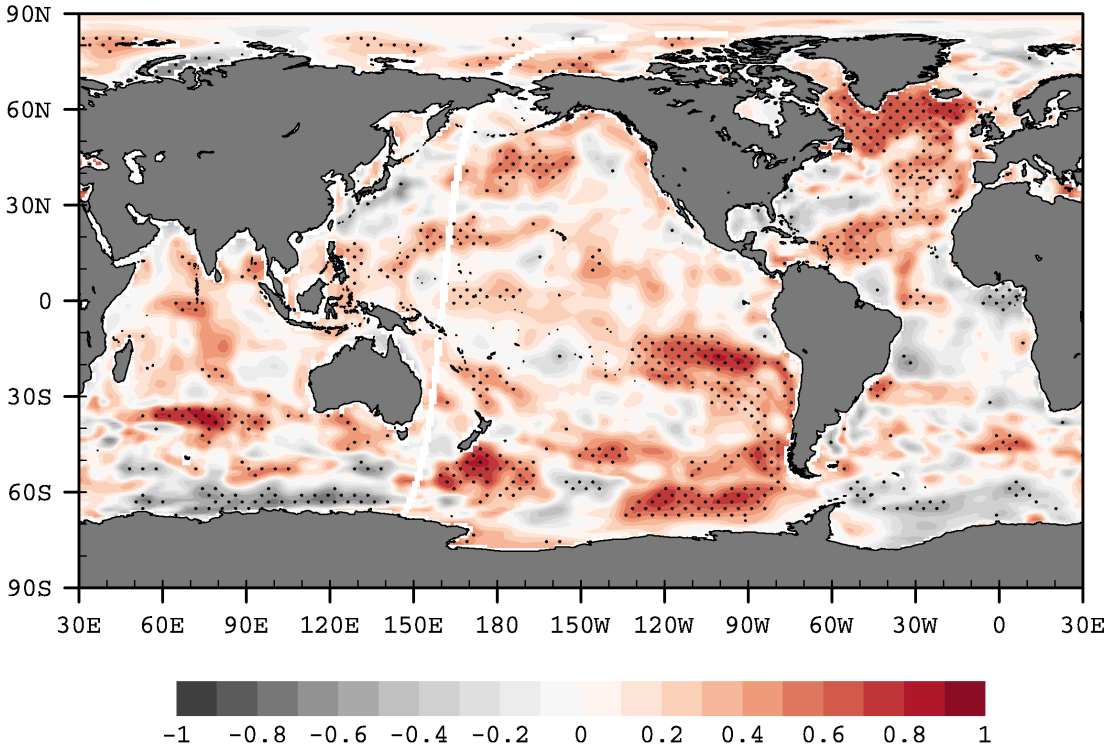

Figure 1.2: Lead-year 1-5 anomaly correlation coefficients for initialized sea surface temperatures against observations. The verification time period is 1970-2016. Stippling denotes statistically significant skill at 95% confidence level.

I provide an overview of the research articles, wherein I derive research questions and provide answers to them. In the end, I provide an outlook wherein I formulate research items for further investigation of the issues highlighted by this dissertations.

1.2 ON THE MECHANISMS UNDERLYING SPG VARIABILITY

In the mid 1990s, a remarkable event occurred in the subpolar North Atlantic. The SPG started warming rapidly and its cyclonic circulation weakened (Bersch, 2002; Häkkinen & Rhines, 2004). Warm and saline water masses which are usually confined to the east of the Rockall-Hatton Bank were traced in the Iceland basin and further west in the late 1990s (Bersch et al., 2007; Sarafanov et al., 2008). These changes in the thermohaline structure of the subpolar North Atlantic coincided with a sharp decrease in the NAO index during the winter of 1995/96. That these changes were observed down to intermediate depths (1000 m) in the water column suggested that heat and freshwater fluxes exchanged at the surface could not have caused these changes. This conjecture was supported by the finding that the magnitude of change in salinity during this time could not be explained by the contribution from air-sea exchanges (Holliday, 2003). Due to scarcity of direct observations of SPG circulation and a very limited satellite altimeter record, the scientific community now had a challenge to explain the cause of such dramatic change.

What came out from subsequent observational and model-based investigations was that the decline in size and strength of the SPG forced by NAO-associated decrease in buoyancy-driven deep convection was responsible for the rapid warming of the SPG (Bersch, 2002; Häkkinen & Rhines, 2004; Hátún et al., 2005; Bersch et al., 2007; Sarafanov et al., 2008). A weaker SPG circulation was thought to also retract westwards in the eastern North Atlantic. This buoyancy-driven contraction of the SPG circulation allowed greater subtropical throughput which warmed the SPG (Hátún et al., 2005). However, later studies discounted the buoyancy forcing and pointed out that wind stress forcing was mainly responsible for the variability in size and strength of the SPG (Lorbacher et al., 2010; Häkkinen et al., 2011b). Despite their disagreements on the forcing mechanism, all of these studies agreed that decline in size and strength of SPG circulation preceded the rapid warming of the SPG in the mid-1990s.

This consensus on size-strength hypothesis was challenged by various modelling studies (Zhang, 2008; Lohmann et al., 2009; Robson et al., 2012b), These studies argued that the rapid warming of the SPG in the mid-1990s was primarily caused by an increase in meridional heat transport, and such increase in heat transport was due to surface buoyancy flux associated with the high NAO index during the previous decade. This mechanism was in line with a negative feedback mechanism characteristic of the subpolar North Atlantic (Delworth et al., 1993): Positive density anomalies in the Labrador Sea, forced by NAO-associated buoyancy fluxes, lead to a lagged response in the overturning circulation, which brings more subtropical water into the SPG, thus inverting the sign of the density anomalies which initiated the change. This mechanism got further support from those modelling studies that showed high skill in retrospective predictions of the mid-1990s warming of the SPG (Robson et al., 2012a; Yeager et al., 2012; Msadek et al., 2014). In their essence, all of these studies attributed the mid-1990s warming and salinification of the SPG to a buoyancy-driven increase in oceanic heat transport from subtropical latitudes, and did not find any active role of the size and strength of SPG circulation.

Criticism of both the size-strength hypothesis and the negative feedback mechanism came from studies that investigated the role of the NAO in driving basin scale variability in SPG circulation (Herbaut & Houssais, 2009; Barrier et al., 2015). These studies argued that, in the eastern North Atlantic, oceanic anomalies in the mid-1990s were primarily created by abrupt changes in local oceanic convergence, due to the wind-driven fast response of oceanic circulation to abrupt changes in the NAO state (Eden & Willebrand, 2001). This is in contrast to connecting oceanic anomalies to the buoyancy-driven strengthening of SPG circulation and also to the strengthening of overturning circulation. More recently, questions were even raised on the methodology of defining the SPG strength through observed proxies (Foukal & Lozier, 2017). Doubts were raised on the "Gyre Index" (Hátún et al., 2005; Berx & Payne, 2017), based on sea surface height, which had been used by various studies to investigate the impact of SPG circulation on physical and biogeochemical variability in the eastern North Atlantic.

It would be a grave oversight to dismiss this background on SPG dynamics as irrelevant for predictability analyses because it is the atmosphere-driven variability in the size and strength of the SPG, proxied by the Gyre Index, that has been shown to influence hydrography, plankton and higher trophic levels in the eastern North

Atlantic (Hátún et al., 2009; Sherwin et al., 2011; Hátún et al., 2016; Larsen et al., 2012), while the promising results on the SPG predictability point towards the dominant role of meridional heat and salt transport. Therefore, in order to investigate the predictability of SPG-ecosystem linkages, there is a need to reconcile the wind-driven and buoyancy-driven changes in SPG circulation. And in order to make sure that future predictions are reliable, it is important to have a mechanistic understanding of the SPG-associated impacts in the eastern North Atlantic. These conflicting views on the variability in SPG circulation, therefore, raise the following two questions:

1. ***Is there a robust relationship between oceanic anomalies in the eastern North Atlantic and size and strength of SPG circulation?***

2. ***Which index or indices are best suited proxies of size and strength of the SPG?***

I answer[1] these questions by analysing four different indices of SPG strength that have been used in observational and modeling studies (Koul et al., 2019c). I also carry out Lagrangian trajectory experiments to incorporate differing viewpoints on SPG dynamics. To be consistent with earlier investigations, I consider changes in salinity to assess the impact of SPG circulation in the eastern subpolar North Atlantic (ENA). Salinity is a passive tracer in the ENA, hence the imprint of circulation variability on salinity is more pronounced than on temperature (Mauritzen et al., 2006).

In observations, I identify latitudinally coherent shifts in isohalines in the ENA. Out of the four analyzed indices of SPG strength, two indices suggest that such variability in isohalines is the manifestation of variability in size and strength of the SPG. Both of these indices reflect the response of subpolar North Atlantic circulation to changes in the NAO. I illustrate this through (a) the similarity in temporal evolution of the NAO index and the two SPG indices, and (b) the similarity of the response of salinity to changes in NAO and the two indices.

To understand the mechanisms behind variability in the size and strength of the SPG and how that is related to shifts in isohalines in the ENA, I analyze model based indices of SPG strength. I complement this analysis with Lagrangian trajectory experiments to compare advective pathways in the subpolar North Atlantic during strong and weak circulation regimes. The results from this model-based analysis reveal meridional shifts of isohalines in the Newfoundland Basin and in the ENA. These meridional shifts of isohalines are accompanied by strong circulation anomalies in the Newfoundland Basin. An analysis of Lagrangian trajectories during strong and weak circulation regimes reveals that the meridional shifts of current pathways in the Newfoundland Basin and in the ENA determine the proportion of subpolar and subtropical water masses arriving in the ENA. It is this variability in the proportion of subtropical and subpolar water masses that leads to variability in salinity in the ENA.

I further illustrate that the meridional shifts in Lagrangian trajectories in the Newfoundland Basin are linked to a decadal variability in the SPG circulation. The second mode of the modelled SSH variability in the North Atlantic has a characteristic dipole pattern (Koul et al., 2019c). While this dipole pattern has been shown to be the fingerprint of AMOC variability (Zhang, 2008), I show that this dipole pattern in the North

1 See appendix A: Koul, V., Tesdal, J.E., Bersch, M., Hátún, H., Brune, S., Borchert, L., Haak, H., Schrum, C. and Baehr, J. (2019), "Unravelling the Choice of the North Atlantic Subpolar Gyre Index", Scientific Reports (under review).

Atlantic SSH can also emerge from wind stress curl variability. Vorticity input from the atmosphere leads to strengthening of SPG circulation which removes fresh surface water from the Labrador Sea. Less fresh water flows southward into the Newfoundland basin and more towards the ENA when the SPG is strong. A sustained removal of fresh water creates density anomalies in the Labrador Sea through westward salt transport, which then initiate anomalous meridional overturning. The anomalous strengthening of the meridional overturning parallels the westward contraction of the SPG in the ENA, the gradual retreat of the North Atlantic Current towards southern latitudes and reversal of density anomalies in the SPG. Thus, the strengthening of SPG circulation precedes the strengthening of the meridional overturning circulation.

Not all indices of SPG strength capture the complexity of the three dimensional SPG circulation. This might lead to errors in interpreting the impact of the SPG circulation on other regions. In light of the mechanisms discussed above, my comparison of various indices shows that those indices which are based on depth average barotropic streamfunction and largest closed contours of SSH should be cautiously used as they do not capture the meridional shifts of the North Atlantic current properly. Finally, the weak-SPG-high-salinity relationship in the ENA should serve as the basis for choosing an index of SPG strength.

These results therefore allow me to put various aforementioned hypotheses into perspective. First, the local oceanic convergence due to abrupt changes in atmospheric conditions might to some extent amplify or damp the low frequency variability. However, I do not find evidence for a dominating role of local (fast) changes in oceanic circulation. This conclusion is supported by high decadal prediction skill in the ENA (Borchert et al., 2018) which would not be possible if the variability in this region was dominated by a local wind-driven barotropic response of ocean circulation. Second, I find that density anomalies in the Labrador Sea are mainly driven by salinity anomalies. This implies that surface heat fluxes associated with the NAO might not fully explain the variability in density and hence would not lead to a lagged response in meridional overturning circulation. Instead, I propose that subpolar basin scale wind stress curl variability modulates the SPG strength. Variability in SPG strength then creates density anomalies in the Labrador Sea through removal of freshwater and westward transport of salt. These salinity anomalies create density anomalies which then lead to a lagged response in the meridional overturning circulation.

In summary, the variability in size and strength of the SPG appears to be a lagged response to the variability in wind stress curl over the subpolar North Atlantic. And such variability in the size and strength of the SPG plays a decisive role in decadal changes in salinity in the ENA. Furthermore, since a lagged oceanic response is involved and provided that the influence of SPG circulation extends to the biological productive shelf seas, the SPG-related impacts on marine ecosystems might be predictable. In the next section, I investigate whether the influence of SPG strength extends north of the Greenland-Scotland Ridge.

1.3 ON THE INFLUENCE OF THE SPG CIRCULATION ON THE PHYSICAL ENVIRONMENT ACROSS THE GREENLAND-SCOTLAND RIDGE

In the eastern North Atlantic, the North Atlantic Current splits into tow main branches. One branch, the Rockall Trough branch, carries Atlantic water through the Faroe-

Shetland Channel (FSC) towards the Nordic Seas. The second branch, the Iceland Branch, carries Atlantic water across the Iceland-Faroe Ridge. North of the Greenland-Scotland Ridge, both of these branches flow as the Norwegian Atlantic Current (NwAC), that carries warm Atlantic water towards the Barents Sea and the Arctic (Orvik & Niiler, 2002). In the Norwegian sea, at interannual timescales, variability in the advection of Atlantic water has emerged as the dominant cause of heat content variability in observations (Mork et al., 2019) as well as reanalysis (Asbjørnsen et al., 2019). However, it remains to be clarified whether the variability in the Atlantic inflow, as it enters the FSC, remains coupled to the variability in SPG circulation (Langehaug et al., 2019).

Another closely related but less investigated aspect is the influence of the SPG circulation on the hydrography of the North Sea. Few observational studies had suggested that part of the variability in the northern North Sea might be linked to oceanic anomalies originating in the Rockall Trough region (Holliday & Reid, 2001). However, no attempts were made to identify whether such oceanic anomalies in the Rockall Trough, later advected to the North Sea, were related to circulation variability associated with the SPG. That was the case because majority of earlier studies analyzed observations and/or employed regional models to study this region due to their superior performance in shelf seas (Winther & Johannessen, 2006; Hjøllo et al., 2009). However, on one hand, these models, due to their limited coverage and issues associated with boundary conditions, could not be used to investigate North Atlantic-North Sea linkages; on the other hand, global coupled models did a poor job at representing important processes in the shelf seas. But a recent comparison suggested that that there is scope to use global models in the northern North Sea, where the impact of Atlantic water is thought to be dominant (Pätsch et al., 2017).

With the refined understanding of SPG dynamics, and given the unexplored impacts of SPG circulation on the shallow shelf seas in the eastern North Atlantic, I frame the following question:

3. ***Is there an influence of SPG circulation on the Atlantic inflow through the FSC and on the North Sea hydrography?***

I investigate[2] this question using a historical simulation (1850-2005) with the Max Planck Institute Earth System Model, run in its low resolution setup (MPI-ESM-LR). While the nominal resolution of the ocean component of MPI-ESM-LR is 1.5 degrees, the setup has a rotated grid configuration for which the singularity at the North Pole is replaced over Greenland. This has the advantage that horizontal resolution is enhanced north of 50N, reaching 50 Km near the northern North Sea. In the model, the connections between North Atlantic and North Sea are represented, which would not be the case in a regional model, and the model provides a long continuous time series of water properties, which is not available from spatially and temporally scarce observations. This simulation provides the base for understanding spatial and temporal modes of variability in the North Atlantic and their connections with the FSC and North Sea. In particular, I focus on the relation between SPG strength and

2 See appendix B: Koul, V., Schrum, C., Düsterhus, A. & Baehr, J. (2019), "Atlantic Inflow to the North Sea Modulated by the Subpolar Gyre in a Historical Simulation with the MPI-ESM", Journal of Geophysical Research: Oceans,124, 1807–1826.

variability in the Rockall Trough, FSC and North Sea and if a similar relationship is seen in observations (Koul et al., 2019a).

On the performance of MPI-ESM-LR in the FSC and the northern North Sea, I find that the model estimates of volume transports into these regions is fairly close to observations. For example, the mean modelled inflow to the North Sea has a strength of 1.6 Sv which is close to the known estimate of 1.7 to 2 Sv. Similarly, the saline core of Atlantic inflow shows remarkable continuity from the Rockall Trough, where the core is close to the shelf edge as observations suggest, to the North Sea entrance. These and other indicators of mean circulation provide confidence that the model is in overall agreement with respect to the location and intensity of various inflows.

The preceding analysis on the dynamics of the SPG allows me to define a dynamically robust index of the SPG strength. By isolating weak and strong circulation regimes using this index, I reveal widespread changes in the spatial extent of subpolar and subtropical water masses from the Rockall Trough to the Barents Sea opening (Figure 1.3). Temperature and salinity anomalies are generated by the variability in SPG strength. These anomalies are then advected by the mean circulation from the Rockall Trough into the FSC and further downstream. A detailed volumetric water mass analysis suggests that, in the FSC and the northern North Sea, the SPG signal is more pronounced in salinity than in temperature. I further emphasize that the interannual variability in the total volume transport of Atlantic water into the North Sea is wind driven and does not co-vary with SPG strength. But the properties of the inflowing Atlantic water (i.e. source water masses) are modulated by the variability in SPG strength at decadal timescales.

This analysis thus builds the case that decadal predictability in these regions can originate in the SPG. It remains to be seen to what extent the SPG signal identified in the Atlantic inflow across the Greenland-Scotland Ridge translates into a robust prediction skill. That is the subject of the final topic of my dissertation.

1.4 ON THE DECADAL PREDICTION OF THE PHYSICAL ENVIRONMENT AND COD STOCKS IN THE EASTERN NORTH ATLANTIC

Having demonstrated that the SPG signal is carried by the Atlantic inflow to the eastern regions of the North Atlantic, including the biologically productive shelf seas, the immediate next step would be to assess the predictability of environmental conditions in these regions. In particular, keeping in mind the stated goal of predicting fish stocks in shelf seas at interannual to decadal timescales, it is necessary to assess whether the multi-year predictability of temperature and salinity in the SPG extends to the North Sea and the Barents Sea.

Earlier attempts at predicting variability in oceanic temperature in these regions have highlighted the presence of a predictability barrier at the Greenland-Scotland Ridge (Langehaug et al., 2017). North of the ridge, models show considerable discrepancies in simulating the propagation of thermal anomalies from the FSC to the Barents Sea. Furthermore, the SPG signal appears to be more pronounced in salinity than in temperature (Koul et al., 2019a; Langehaug et al., 2019). This might lead to substantial differences in prediction skill of temperature and salinity in the regions north of the Greenland-Scotland ridge.

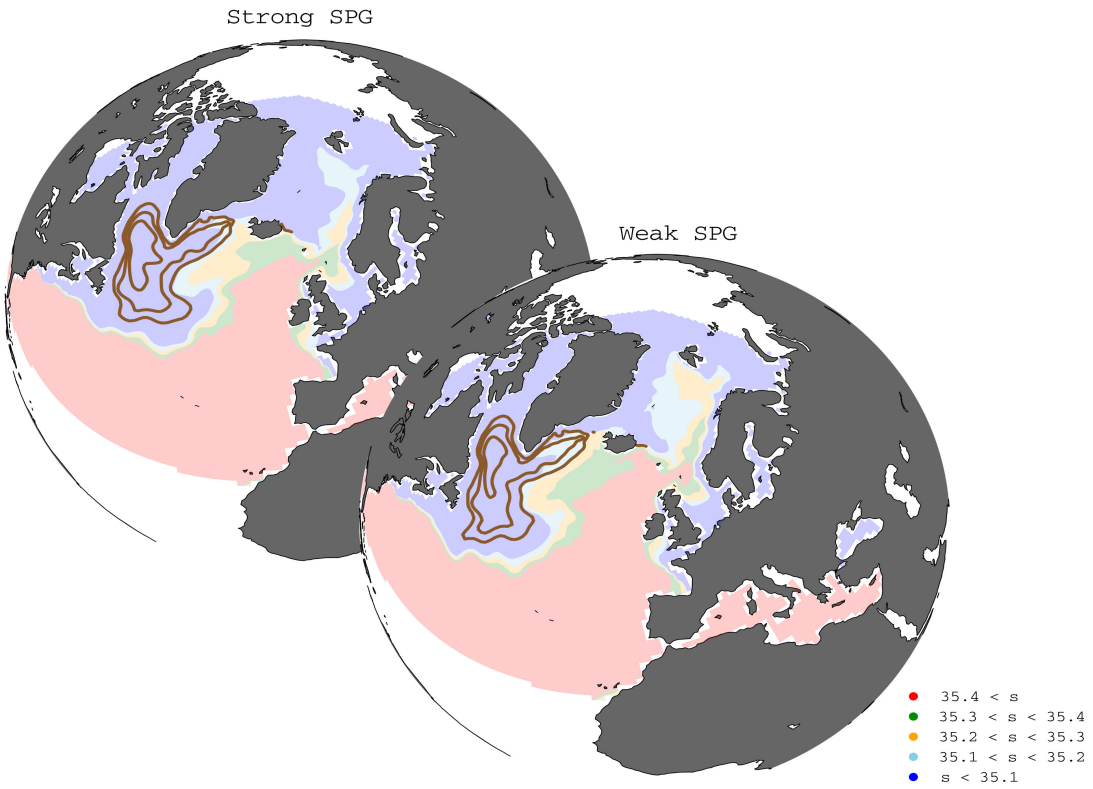

Figure 1.3: Composites of salinity (psu) in the upper 500m based on strong and weak regimes of SPG strength in a historical simulation with MPI-ESM-LR. The thick brown lines show sea surface height contours.

It is commonly understood that the prediction skill at multiyear timescales comes from the oceanic initial conditions. However, at these timescales, part of the skill also comes from the boundary conditions such as radiative effects of the concentration of greenhouse gasses and aerosols in the atmosphere. It is important to find out which of the two sources dominates prediction skill in the shelf seas because such knowledge would determine what kind of prediction systems are best suited for these regions.

As emphasized earlier, the mechanistic understanding of interannual to decadal variability and predictability of the physical conditions (temperature and salinity) in the North Sea and Barents Sea are prerequisites towards investigation of predictability in Cod stocks in these regions. However, we must remain cautious that reliable predictions of Cod biomass are likely to be achieved only when the natural evolution of these Cod stocks has not been drastically altered due to high fishing mortality. In such a scenario, any environment-based prediction system that does not account for fishing mortality is likely to be unreliable.

While temperature and salinity in the SPG have been shown to be predictable at multi-year timescales in various decadal prediction systems (Matei et al., 2012; Robson et al., 2012a; Yeager et al., 2012; Msadek et al., 2014), the status of such predictability in the latest iteration of a decadal prediction system based on MPI-ESM-LR is unknown. In particular, in this prediction system, the status of prediction skill in the regions north of the Greenland-Scotland Ridge must be revealed before we explore the prediction skill in Cod stocks. Such a gap in our knowledge of prediction skill in the eastern North Atlantic allows me to derive the following research question:

4. ***What is the prediction skill of SPG temperature and salinity in MPI-ESM-LR and does the prediction skill extend to the shelf seas in the eastern North Atlantic?***

5. ***What is the source of prediction skill in temperature in these regions?***

6. ***Can the prediction skill of physical environment be translated to reliable predictions of Cod stock biomass?***

To investigate[3] each of these questions, specific tools and methods are required. I use a 16-member decadal prediction system based on MPI-ESM-LR to assess the prediction skill of temperature and salinity (Koul et al., 2019b). It is a common practice in predictability studies to use an ensemble of predictions rather than a single prediction to account for the chaotic nature of the climate system. By averaging over the ensemble members, the hope is that the stochastic noise cancels out while only retaining the predictable signal.

Each of the predictions is started (initialized) from a known state of the climate system and also incorporates the information on external forcings. It is well understood that at interannual to decadal timescales, predictability of the climate system arises from the initial conditions as well as from external forcings associated with changes in the atmospheric composition of gasses and aerosols, land parameters and solar radiation. Therefore to isolate the skill due to external forcings only, I analyze an additional set of 16-member predictions which are not started (uninitialized) from

3 See appendix C: Koul, V., Schrum, C., Arthun, M., Brune, S. and Baehr, J. (2019), "Decadal Prediction of Barents Sea Cod Stock through an Oceanic Linkage with the Subpolar Gyre", Frontiers in Marine Science (to be submitted).

a known state of climate system but incorporate known external forcings only. In my knowledge, such rich sets of ensemble predictions have not been applied before to investigate the source of skill in the eastern North Atlantic shelf sea.

The MPI-ESM-LR, or any other climate model, does not simulate Cod biomass. Therefore, dynamical predictions of environmental conditions (temperature and salinity) by MPI-ESM-LR must be transformed into predictions of Cod biomass through a statistical procedure. Following Årthun et al. (2018), I use a simple linear regression to construct a statistical model to transform predictions of temperature into predictions of Cod. This method relies on the correlative relationship between Cod and temperature to determine the weights of the regression model. However, instead of using a purely statistical model as used in Årthun et al. (2018), I develop a dynamical-statistical prediction system wherein dynamical predictions of temperature as provided by MPI-ESM-LR are fed into a regression model to provide Cod biomass predictions. This method has two benefits: (a) it allows further extension of the prediction horizon and (b) it allows idenfication of the source of skill (Koul et al., 2019b).

I begin with the investigation of prediction skill of environmental conditions. I find that the initialized decadal predictions of the SPG show high skill in both temperature and salinity. And the skill obtained from initialized hindcasts is significantly higher than uninitialized hindcasts, suggesting that internal climate variability in the SPG dominates the forced response. Furthermore, a heat budget analysis suggests that high skill of such predictions is mainly derived from the ocean. In the SPG, there is however difference in the prediction skill between temperature and salinity. While the prediction skill in temperature remains high till lead year 10, in the case of salinity, the skill drops sharply after lead year 4. Further analysis hints at differences in lead-year dependent drift between temperature and salinity hindcasts, which in turn might be related to initialization errors. More detailed analysis is required in this regard.

North of the Greenland-Scotland Ridge, prediction skill in temperature does not remain as high as in the SPG. In the North Sea as well as at the Barents Sea opening, there is no significant difference in prediction skill between initialized and uninitialized temperature hindcasts. However, in the case of salinity, high prediction skill is retained even north of the Greenland-Scotland Ridge. And at the Barents Sea opening, hindcast skill in salinity remains relatively high till lead-year 7. This result is in line with my earlier finding that across the Greenland-Scotland Ridge, the SPG signal is more pronounced in salinity than in temperature.

The low hindcast skill of ambient temperature in the North Sea and at the Barents Sea opening precludes the application of ambient temperatures to Cod predictability. However, there is scope for predicting Cod biomass in the Barents Sea by utilized remote oceanic linkages. In observations, a strong relationship between oceanic temperatures in the North Atlantic and Barents Sea Cod biomass allows a statistical prediction with a 7-year prediction horizon (Årthun et al., 2018). And since dynamical predictions of temperature in the North Atlantic, particularly in the SPG, are skilful up to lead-year 4, it might be possible to combine dynamical and statistical predictions to extend the predictability horizon to 11 years. Indeed, results show that Barents Sea Cod biomass can be skillfully predicted 11 years in advance (Koul et al., 2019b). Furthermore, I illustrate that the statistical model performs better with initialized hindcast of SPG temperature than with uninitialized hindcasts.

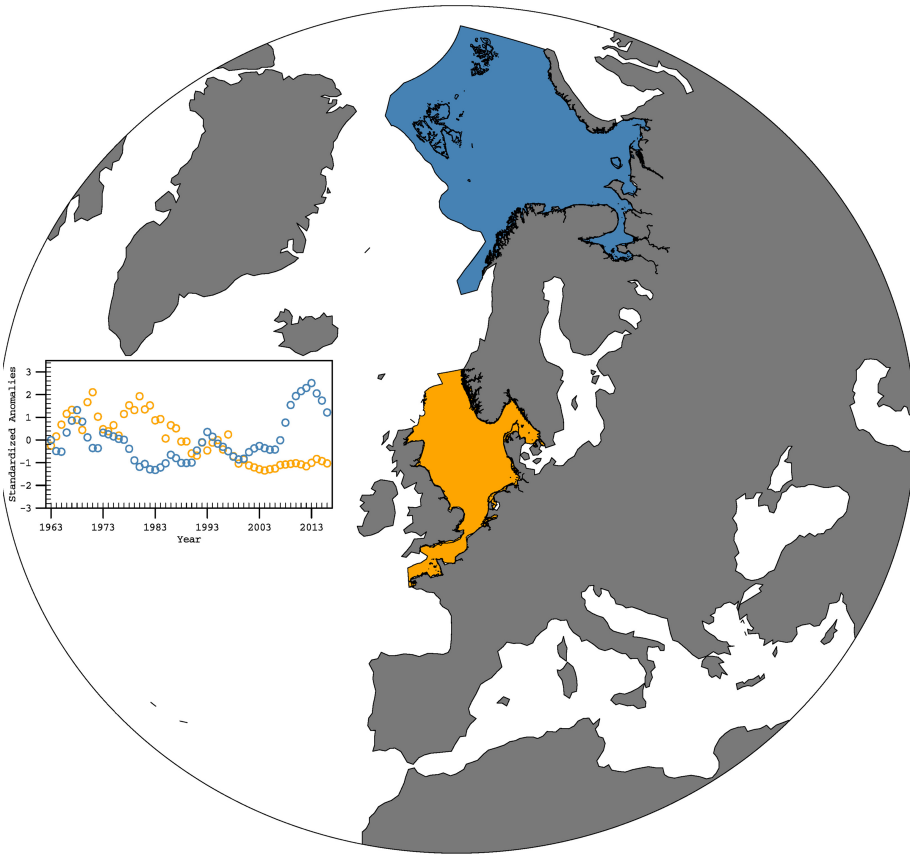

Figure 1.4: The ICES ecoregions in the North Sea (orange) and Barents Sea (blue). The inset shows total stock biomass of North Sea Cod (blue circles) and Barents Sea Cod (blue circles) for the period 1963-2016. Note the strong declining trend in North Sea Cod.

The promising results on Cod predictability in the Barents Sea are attributed to the holistic, yet rigorous, approach adopted in this dissertation. New insight is presented on the dynamics of the SPG, its impact on variability and predictability across the Greenland-Scotland ridge, and finally on the predictability of Cod stocks.

As far as predicting Cod biomass in the North Sea is concerned, the potential for predictability is low. This is attributed to (a) a strong declining trend in the data from early 1970s to the present (Figure 1.4) and (b) unpredictable relationship of North Sea Cod with the ambient temperature. The long term declining trend is most likely due to a combined impact of a high fishing mortality rate and a decline in recruitment success (Daewel et al., 2015), both of which have masked the long term environment-driven variability. Further analysis reveals that when the long term trend is removed, a negative relationship with ambient temperature emerges. Because of low hindcast skill in ambient temperatures in the North Sea, such relationship can not be used in the dynamical-statistical model. Further improvements in the dynamical prediction system are required in this case.

1.5 OUTLOOK

Through this dissertation, I have attempted to remove some of the major bottlenecks in the challenging path towards the decadal prediction of marine ecosystems in the North Atlantic. I investigated variability and predictability of the SPG to reveal predictive potential in Cod stock in the Barents Sea. There is however scope for future research to refine the predictions presented in this dissertation.

While I have mitigated inconsistencies in our understanding of the variability in size and strength of the SPG circulation, further research is required to understand two key issues. The first issue is regarding the low hindcast skill of oceanic temperatures north of the Greenland-Scotland Ridge in MPI-ESM-LR. This issue is closely linked to the apparent discontinuity in thermal anomalies associated with the SPG variability across the Greenland-Scotland Ridge (Koul et al., 2019a). I must make it clear that in observations as well as in coupled models, both thermal and freshwater anomalies originating in the SPG are known to propagate across the Greenland-Scotland Ridge towards the Arctic (Holliday et al., 2008; Jungclaus et al., 2014; Glessmer et al., 2014; Årthun & Eldevik, 2016). Thus it appears that MPI-ESM-LR does not match the observed propagation speed of thermal anomalies across the Greenland-Scotland Ridge. This conjecture is supported by (a) the large drop in hindcast skill of temperature across the Greenland-Scotland ridge which is not seen in salinity, (b) the finding that across the Greenland-Scotland Ridge, the SPG signal is more pronounced in salinity than in temperature and (c) the high correlation between Cod biomass in the Barents Sea and SPG temperature. The second issue concerns the sharp drop in prediction skill of salinity after lead-year 4 in the SPG. It might be due to a strong lead-year dependent drift in hindcasts. Further analysis on the role of model resolution, initialization procedures and drift correction techniques are required to understand and rectify these two issues.

The success of this dissertation depends on whether the predictions presented here can inform policy decision aimed towards marine resource conservation. In this respect, a very relevant research question that emerges directly from this dissertation is regarding the management decisions at interannual to decadal timescales. Both short term (seasonal to annual) and long term (decadal to centennial) predictions have received considerable attention in the past as far as fishery management needs are concerned. Short term predictions cater to tactical management needs whereas climate change projections cater to the strategic management needs (Tommasi et al., 2017b; Haltuch et al., 2019), Thus, in light of the promising results from interannual to decadal forecasts, further research is required to explore management decisions which bridge the gap between tactical and strategic applications.

Fishery managers are often interested in early warnings about abrupt climate shifts. Initialized decadal prediction systems are better poised to predict such climatic shifts than other forecast systems, as has been shown in case of the 1990s climatic shift in the SPG. However, it is equally important to communicate uncertainties associated with decadal prediction skill using a more "fishery-compliant" skill metrics than what has been used in this dissertation. This calls for close collaboration with the end users (having no commercial interests) to understand what kind of predictions, deterministic and/or probabilistic, and skill metrics would be best suited for sustainable management of fish stocks.

This dissertation mainly investigates Cod predictability, however, there is no reason to limit such an investigation to a single species. The high prediction skill in both temperature and salinity in the first few lead years establishes the scope for predicting large shifts in distribution of pelagic fish species such as Blue Whiting and Mackerel. This is because, in the eastern subpolar North Atlantic, large shifts in spawning distribution of Blue Whiting have been observed, which were driven by changes in salinity (Miesner & Payne, 2018). In the case of Mackerel, the westward shift of summer feeding habitat from 2007 to 2016 has been partly linked to temperature (Olafsdottir et al., 2019). In both cases, investigation of retrospective skill in predicting these past shifts can lead to reliable predictions of future shifts in distribution.

Overall, this dissertation presents a template for future studies on climate-based predictability of marine ecosystems. To gain mechanistic understanding, one needs to begin with a robust understanding of the underlying physical variability, then proceed to the evaluation of the sources of, and limits on, prediction skill in the regions of interest. If the application-mandated prediction horizon for marine ecosystems is undefined, these steps should identify the timescales at which uncertainties in future predictions might be minimum. The final step is to assess the predictability in key aspects of marine ecosystems, such as fish abundance or distribution. In the North Atlantic, by applying such a template, this dissertation emphasizes that variability and predictability of SPG circulation plays a central role towards achieving reliable predictions in key aspects of marine ecosystems.

APPENDICES

A

UNRAVELLING THE CHOICE OF THE NORTH ATLANTIC SUBPOLAR GYRE INDEX

This appendix contains a paper, which is under review in Scientific Reports and was submitted as:

Koul, V., Tesdal, J.E., Bersch, M., Hátún, H., Brune, S., Borchert, L., Haak, H., Schrum, C. and Baehr, J. (2019), "Unravelling the Choice of the North Atlantic Subpolar Gyre Index", Scientific Reports (under review).

The contribution of Vimal Koul (V.K.) and others to this paper is as follows:
V.K. conceived the work and wrote the paper. V.K. and J.E.T. conducted Lagrangian experiments with inputs from H.H., M.B. provided observed geostrophic velocities, V.K, M.B., L.B., S.B. and H.H discussed the results. C.S. and J.B. provided guidance on the overall direction of the work. All authors reviewed the manuscript.

Unravelling the Choice of the North Atlantic Subpolar Gyre Index

Vimal Koul[1,2], Jan-Erik Tesdal[3], Mandred Bersch[1],Hjálmar Hátún[4], Sebastian Brune[1], Leonard Borchert[1], Helmuth Haak[5], Corinna Schrum[6] and Johanna Baehr[1]

[1]Institute of Oceanography, Center for Earth System Research and Sustainability, Universität Hamburg, Germany

[2]International Max Planck Research School on Earth System Modelling, Max Planck Institute for Meteorology, Germany

[3]Lamont-Doherty Earth Observatory, Columbia University, Palisades, New York

[4]Faroe Marine Research Institute, Faroe Islands

[5]Max Planck Institute for Meteorology, Germany

[6]Helmholtz Zentrum Geesthacht, Institute of Coastal Research, Germany

(Submitted: 28 August, 2019)

The North Atlantic Subpolar Gyre (SPG) has been widely implicated as the source of large-scale changes in the subpolar marine environment. However, inconsistencies between different indices of SPG strength based on Sea Surface Height (SSH) observations have raised questions about the active role SPG strength and size play in determining water properties in the eastern subpolar North Atlantic (ENA). Here, by analyzing SSH-based and various other SPG-strength indices derived from observations and a global coupled model, we show that the interpretation of SPG strength-salinity relationship is dictated by the choice of the SPG index. Our results emphasize that SPG indices should be interpreted cautiously because they represent variability in different regions of the subpolar North Atlantic. Idealized Lagrangian trajectory experiments illustrate that zonal shifts of main current pathways in the ENA and meridional shifts of the North Atlantic Current (NAC) in the western intergyre region during strong and weak SPG circulation regimes are manifestations of variability in the size and strength of the SPG. Such shifts in advective pathways modulate the proportions of subpolar and subtropical water reaching the ENA, and thus impact salinity. Inconsistency among SPG indices arises due to the inability of some indices to capture the meridional shifts of the NAC in the western intergyre region. Overall, our results imply that salinity variability in the ENA is not exclusively sourced from the subtropics, instead the establishment of a dominant subpolar pathway also points to redistribution within the SPG.

A.1 INTRODUCTION

The northward transport of heat and salt in the North Atlantic is an important aspect of climate variability as it determines the exchanges of heat and salt with the Arctic Mediterranean. Of particular importance is the interannual to decadal variability in salinity of waters headed towards the sites of deep convection. This is because salinity affects buoyancy and density stratification, and can thus influence the formation of dense waters which form the lower limb of the thermohaline circulation. In the eastern subpolar North Atlantic (ENA), the source of interannual to decadal variability in salinity has been a subject of various investigations, and the variability in the North Atlantic Subpolar Gyre (SPG) circulation has emerged as the leading cause. Observations of temperature and salinity suggest that the North Atlantic Oscillation (NAO) drives changes in the size and strength of the SPG (Bersch, 2002; Curry & McCartney, 2001), and that these changes are manifested in the properties of the ENA (Bersch et al., 2007; Sarafanov, 2009). Although variability in the size and strength of the SPG may not always be attributable to the NAO (Häkkinen & Rhines, 2004; Häkkinen et al., 2011a), it has repeatedly been linked to salinity changes in the ENA (Hátún et al., 2005; Frankignoul et al., 2009), leaving a minor role for local air-sea fluxes (Holliday, 2003) and the Atlantic Meridional Overturning Circulation (AMOC) (Häkkinen et al., 2011b; Piecuch et al., 2017).

In contrast to this abundant evidence, recent investigations (Herbaut & Houssais, 2009; Foukal & Lozier, 2017) do not find any relationship between SPG size/strength and salinity in the ENA. At the heart of this discrepancy are (a) the different ways of defining SPG strength and (b) the role of the NAO in driving changes in SPG circulation. The widely-used sea surface height (SSH) based Gyre Index (Häkkinen & Rhines, 2004; Hátún et al., 2005), which is linked to salinity changes in the ENA, does not account for the sea level rise during the altimeter period (Foukal & Lozier, 2017), and is therefore not an appropriate proxy for the size or strength of the SPG. A new index (Foukal & Lozier, 2017) of SPG size and strength based on the largest closed contours of SSH, which accounts for the trend in the SSH data, does not project onto the NAO and does not show any significant relationship with salinity in the ENA at interannual timescales. Moreover, large variations in salinity in the ENA, for example, those seen in the 1990s, are thought to be primarily linked to abrupt changes in local oceanic convergence, due to the wind-driven fast response of oceanic circulation to abrupt changes in the NAO state (Eden & Willebrand, 2001; Herbaut & Houssais, 2009; Barrier et al., 2015). This is in contrast to connecting salinity variations in the ENA to buoyancy-driven strengthening of SPG circulation.

Indices of SPG strength used in coupled model studies do not agree on the SPG strength-salinity relationship either. One explanation for the causes behind salinity variations in the ENA involves a negative internal oceanic feedback mechanism (Delworth et al., 1993; Dong & Sutton, 2005; Jackson et al., 2016; Robson et al., 2016). Under this mechanism, positive (negative) density anomalies in the Labrador Sea lead to a lagged response in the overturning circulation, which brings more (less) subtropical water into the SPG, thus inverting the sign of the density anomalies which initiated the change (Lohmann et al., 2009). As a consequence, the meridional salt transport associated with the overturning circulation, rather than the strength and size of the horizontal gyre circulation, is seen as the dominant cause of variations

in both the salinity in the ENA and SPG strength. The spatial pattern of modelled SSH variability conforming to this mechanism resembles the dipole pattern of SSH variability in observations (Zhang, 2008), and the principal component of the dipole mode in coupled models is viewed more as a proxy of AMOC variability than that of SPG strength. The other contrasting explanation, which defines SPG strength based on depth averaged barotropic streamfunction, emphasises the importance of volume transport associated with SPG strength (Born et al., 2016). In this mechanism, a strong SPG transports freshwater eastwards and thus actively creates freshwater anomalies in the ENA.

These disagreements raise the following question: Is there a robust relationship between SPG circulation and salinity in the ENA? Put differently, does the pathway and proportion of subtropical and subpolar water masses entering the ENA depend on the size and strength of SPG circulation? It is also unclear which index of the SPG strength should be used for examining the relationship of SPG circulation with physical and biogeochemical variability in the ENA and downstream of the Greenland-Scotland ridge. Such ambiguity in the definition of SPG index has resulted in multiple SPG indices being used for investigations while keeping the question of underlying mechanisms behind such indices unanswered (Langehaug et al., 2019).

We address these ambiguities by examining both the barotropic and baroclinic nature of SPG circulation. This is done by examining SSH, density and barotrophic streamfunction-based proxies of SPG strength. Two SSH based indices (PC1 and PC2 SSH) are calculated from the principal component analysis and a third SSH index is based on largest closed contours of SSH. The density based index (DENS) is a measure of subsurface density anomalies in the central SPG and barotropic streamfunction index (BTSF) denotes depth and area averaged streamfunction in the entire SPG. Detailed definitions of all SPG indices are provided in the Methods section. Since a suitably long time series of SSH data before 1993 is not available, and in order to examine the relationship between SPG strength and salinity in a dynamically consistent setting, we complement our analysis of observational data with results from the Max Planck Institute Earth System Model, run in its low resolution setup (MPI-ESM-LR, see Methods). Idealized Lagrangian experiments with MPI-ESM-LR allow us to clarify the SPG strength-salinity relationship and illuminate inconsistencies among SPG indices. By comparing SPG indices, another aim of the present paper is to determine spatial patterns in circulation anomalies and advective pathways that lead to interventions in salinity in the ENA. A detailed analysis of SPG strength-circulation relationship for each SPG index reveals underlying mechanisms which determine SPG strength-salinity relationship in the ENA.

A.2 RESULTS

A.2.1 *Observed SPG Strength-Salinity Relationship*

For the altimeter period (1993-2016), SSH data is often considered as a proxy for the observed variability in the SPG circulation, and can therefore be used to assess the relationship between SPG strength and salinity in the ENA. The patterns of the first two modes of SSH variability in the North Atlantic emphasize different spatial characteristics (Figure A.1a,b). While the first mode displays negative weights

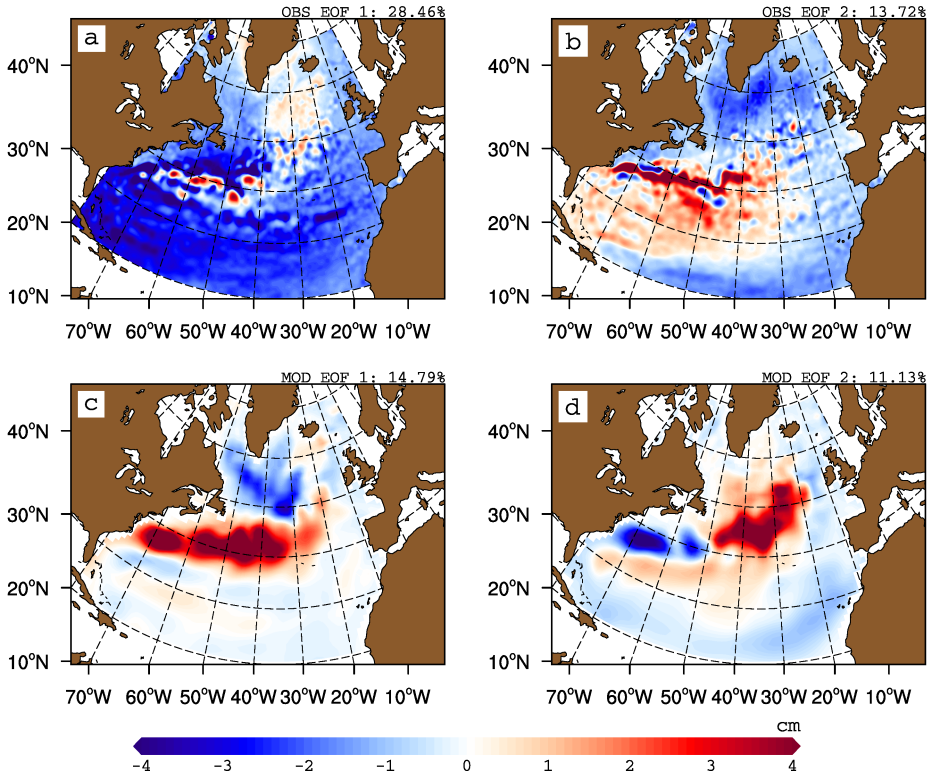

Figure A.1: First and second empirical orthogonal function of sea surface height from non-detrended (a, b) observations (1993-2016) and (c, d) coupled model (last 200 years) respectively.

over most of the North Atlantic, the second mode resembles the well known dipole mode, usually associated with the NAO forcing. A pronounced zonal band of strong positive weights is also present in the western subtropical gyre at 40°N latitude. The relationship between the first principal component of SSH variability in the North Atlantic (PC1 SSH) and salinity in the ENA suggests that with decreasing SSH, salinity in the ENA increases (Figure A.2a). However, the presence of a trend in PC1 SSH (Figure A.3a) together with weak spatial weights in the Irminger Sea and Iceland Basin (Figure A.1a) suggests that PC1 SSH does not represent variability in SPG strength. The second mode of SSH variability shows strong negative weights in the Irminger Sea and Iceland Basin (Figure A.1b), its associated time series (PC2 SSH) does not have a monotonic trend (Figure A.3a), and the relationship between PC2 SSH and salinity suggests that freshening in the ENA is concomitant with a strong SPG (Figure A.2b). Isohalines shift eastward and southward in the ENA when SSH decreases in the Irminger Sea and Iceland Basin.

The index based on the largest closed contours of SSH (hereafter FKL (Foukal & Lozier, 2017)), does not suggest latitudinally coherent shifts in isohalines in the ENA in response to changes in SPG strength (Figure A.2c). This contrasts with the response of salinity to PC2 SSH (Figure A.2b). The FKL index also does not show any shifts in the SPG boundary defined as the largest closed contour of altimeter SSH (Foukal & Lozier, 2017). However, the density-based SPG index (hereafter DENS (Tesdal et al., 2018)), used as a proxy for changes in baroclinic SPG circulation for the period 1993-2016, reveals that the response of upper ocean salinity in the ENA is similar to its response to the PC2 SSH (Figure A.2b, d). Dense upper layers deepen the SPG

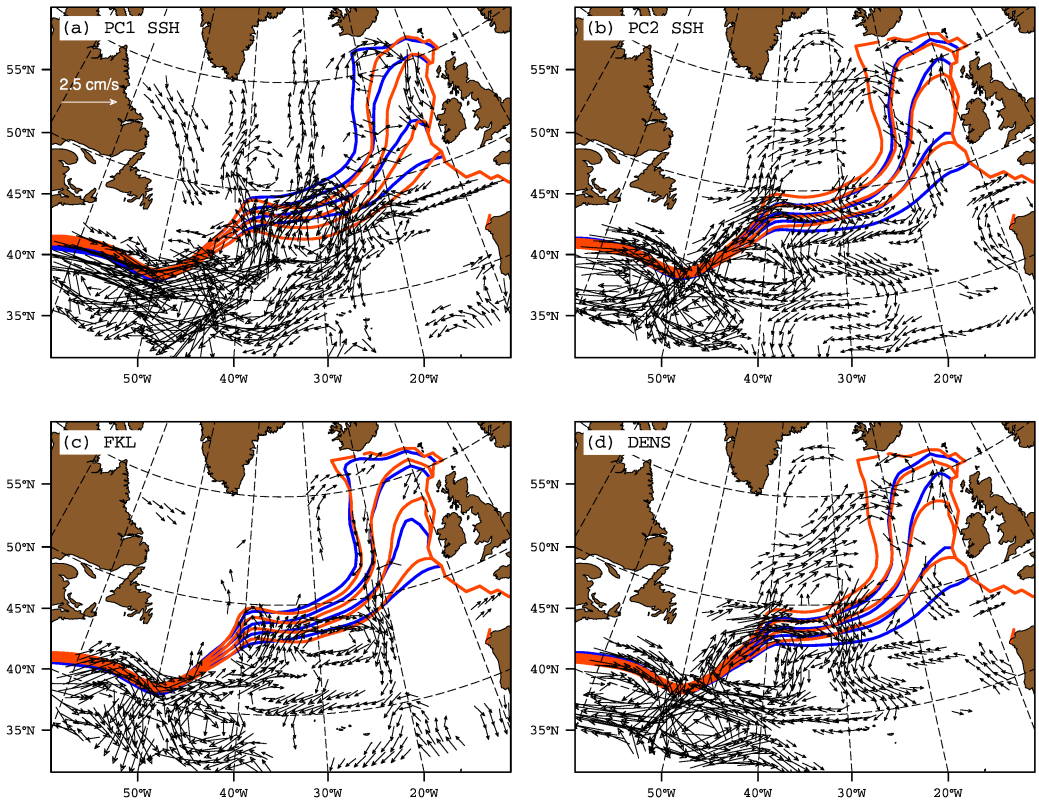

Figure A.2: Strong (blue) and weak (red) composites of annual mean top 500m depth averaged EN4 salinity contours (35.20, 35.30, 35.40 and 35.50 psu) based on strong and weak phases of (a) PC1 SSH, (b) PC2 SSH, (c) FKL and (d) DENS. The SPG indices are not detrended prior to computing composites. Years for compositing are chosen from 1993-2016 and are based on ± 0.5 standard deviation of the respective index. Current vectors denote composites difference (strong-weak) of annual mean upper 500 depth averaged geostrophic currents (cm/s). For clarity, only those geostrophic current vectors with magnitude $\geq$ 0.5 cm/s are shown.

bowl, which spins up the SPG through geostrophic balance, and causes the isohalines to shift eastwards in the ENA. Therefore, DENS also suggests a latitudinally coherent increase or decrease in salinity with changes in SPG strength.

The strong relationship between the NAO and subpolar North Atlantic circulation has also served as a good proxy for variability in SPG circulation (Bersch et al., 2007; Flatau et al., 2003; Sarafanov et al., 2018). During extended periods of positive NAO (NAO+), strong westerlies and increased heat loss across the entire SPG lead to a doming of isopycnals (i.e. a decrease in SSH) and thus spinning up the SPG circulation. The opposite happens during extended periods of negative NAO (NAO-). The response of upper ocean salinity to cases of extended periods of NAO+ (1991-1995) and NAO- (1964-1968) is revealed through shifts in isohalines in the ENA (Figure A.3b). Salinity increases coherently at each latitude in the ENA during a NAO- state and decreases during a NAO+ state. This result is also corroborated by the consistent relationship between DENS and salinity in ENA for the extended time period of 1960-2016 (Figure A.3c).

Changes in the intensity and position of the constituent currents of SPG circulation highlight underlying mechanisms which drive shifts in isohalines in the ENA (Figure A.2). The pattern of baroclinic current anomalies suggests that shifts in isohalines in

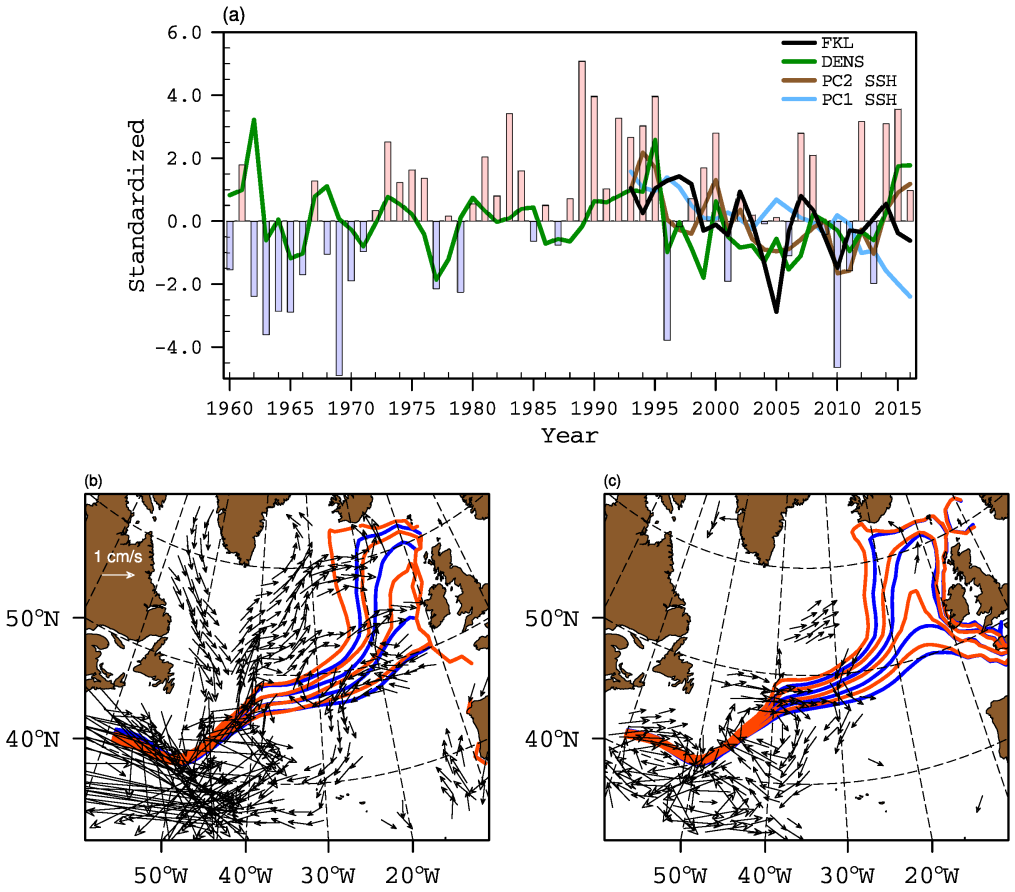

Figure A.3: (a) Time series of SPG indices (lines) and the NAO (bars). (b) Strong (blue) and weak (red) composites of annual mean top 500m depth averaged salinity contours (35.20, 35.30, 35.40 and 35.50 psu) based on strong and weak phases of NAO: 1964-68 for NAO- and 1991-1995 for NAO+. Current vectors denote composites difference (strong-weak) of annual mean upper 500 depth averaged geostrophic currents (cm/s). For clarity, only those geostrophic current vectors with magnitude $\geq$ 0.5 cm/s are shown. (c) same as (b) but for composites based on DENS.

the ENA are linked to the intensification of the cyclonic circulation in the Irminger Sea and Iceland Basin, which is clearly revealed by PC2 SSH and DENS but not by PC1 SSH and FKL (Figure A.2). This is a key distinction as far as the shifts in isohalines in the ENA are concerned because very similar current anomalies emerge as a result of NAO variability (Figure A.3b). Thus it seems that PC2 SSH and DENS are reflecting the NAO driven changes in SPG circulation. Higher heat loss during NAO+ phases increases the density and lowers the SSH in the northern regions. The doming of isopycnals due to a strong wind stress curl associated with NAO+ also lowers the SSH. As a consequence, the baroclinic part of the Irminger, Iceland and Rockall Trough branch strengthens during NAO+ phases. The presence of an anticyclonic circulation anomaly in the southwestern intergyre region suggests a northward shift of the North Atlantic Current (NAC) during NAO+ conditions. Thus, the transport of fresh subpolar water from the western SPG is enhanced, which likely causes the eastward shift in isohalines observed during NAO+ conditions. In addition, the anomalous southwestward current south of ENA restricts the northward penetration of subtropical water, further complimenting the freshening in the ENA (Figure A.3b).

In the case of FKL, along with a weak response in the Irminger Sea, Iceland Basin and the Rockall Trough, the northward shift of the NAC is not represented. Thus, the transport of fresh waters from the western SPG, along the northern flank of the NAC and towards the eastern SPG, is not represented by FKL, and consequently the shifts in isohalines are not realized in the ENA using this index. In summary, observed PC2 SSH, DENS and NAO indices suggest that when the SPG is strong, salinity in the ENA decreases and vice versa, and that there are latitudinally coherent shifts in isohalines. All indices, except PC1 SSH and FKL, relate freshening in the ENA to strong cyclonic circulation anomalies in the northeastern subpolar basins, and to anticyclonic anomalies in the southwestern intergyre region.

A.2.2 *Modelled SPG Strength-Salinity Relationship*

The free model simulation does not exhibit a trend during the period of simulation. As a result there is no equivalent of first mode of observed SSH variability in the model. The dipole pattern of the first mode of modelled SSH variability matches the second mode of observed SSH variability, both of which have negative weights in the SPG and positive weights along the NAC path (Figure A.1). Still, there are some differences: the strong positive weights in the western intergyre region are distributed over much larger domain than in the observations. The negative weights in the SPG are also weaker in the north and stronger in the south. We come back to these differences later. The associated principal component (hereafter SPGI) shows latitudinally coherent shifts in isohalines in the ENA (Figure A.4). However, the SPG strength-salinity relationship depicted by SPGI does not match its observational counterpart but has similarities with the observed relationship depicted by PC2 SSH, DENS and NAO. The meridional shifts in isohalines in western intergyre region also emerge clearly in case of SPGI. Therefore, SPGI suggests that a strong SPG has a more zonal orientation than that of a weak SPG (i.e., when the SPG expands in the ENA, it contracts in the intergyre region). Apart from the SPGI, other indices (see Methods and Table S1), BTSF and FKL do not show any coherent SPG-salinity relationship,

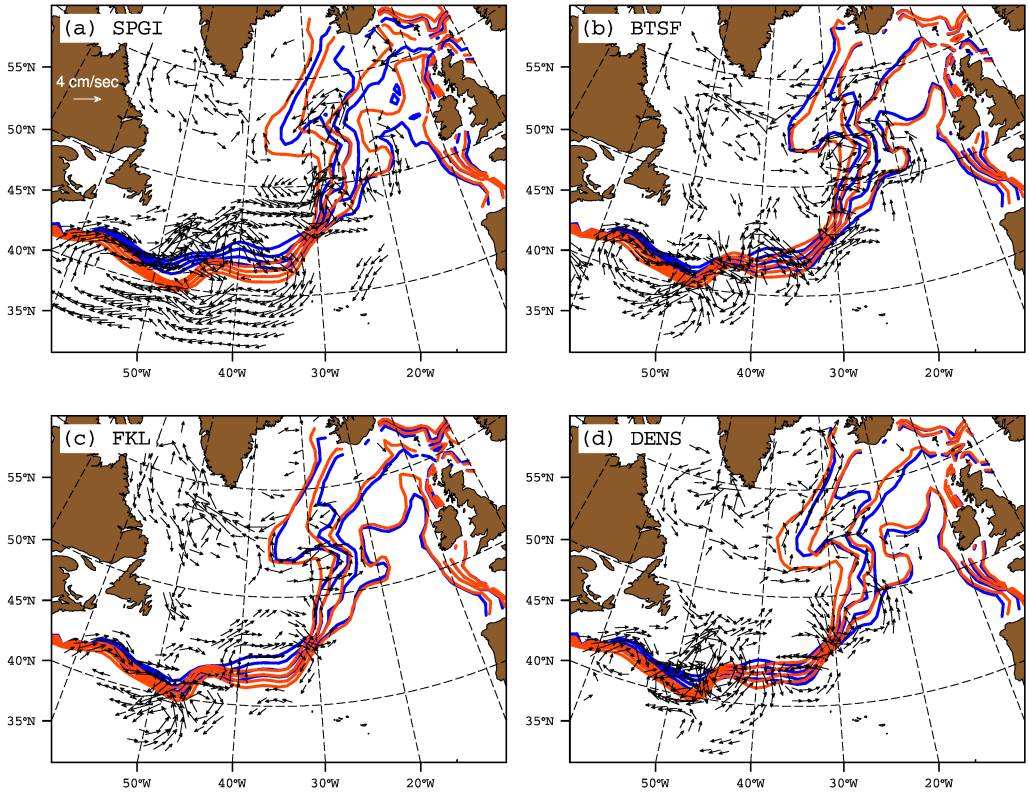

Figure A.4: Strong (blue) and weak (red) composites of annual mean top 500m depth averaged salinity contours (35.20, 35.30, 35.40 and 35.50 psu) based on strong and weak phases of (a) SPGI, (b) BTSF, (c) FKL and (d) DENS. The SPG indices are not detrended prior to computing composites. Years for compositing are chosen from last 200 years of the preindustrial control simulation, and are based on ± 1 standard deviation of the respective index. Current vectors denote composites difference (strong-weak) of annual mean upper 500 depth averaged currents (cm/s). For clarity, only those geostrophic current vectors with magnitude $\geq$ 1.4 cm/s are shown.

while DENS suggests consistent shifts of isohalines in the central SPG region but only subtle shifts in the ENA.

The modelled SPG-salinity relationship depicted by SPGI (i.e., modelled PC1 SSH) matches the observed SPG-salinity relationship depicted by NAO, PC2 SSH and DENS. Therefore, it is of interest to determine if circulation anomalies associated with this modelled index bear any similarity with the observed anomalies. To examine this, we analyzed composites of upper 500 meter currents in the whole North Atlantic computed from weak and strong phases of modeled SPG indices (Figure A.4a). The intensification of cyclonic circulation in the Irminger Sea and Iceland Basin, as emphasized by observed SPG indices, does not seem to determine modelled isohaline shifts in the ENA. However, the anomalous circulation pattern in the southwestern intergyre region emerges as the main circulation anomaly in both observations and the model, which is related to shifts in isohalines in this region and in the ENA. The modelled indices of SPG strength also exhibit regional differences. For example, the anticyclonic circulation anomaly in the western intergyre region is very clearly revealed by the SPGI and not by the modelled DENS, BTSF and FKL indices (Figure A.4). In the western SPG (west of 40°W), all indices show intensification of the

cyclonic circulation during strong index years but BTSF and FKL indices emphasize this intensification more strongly than SPGI and DENS. As discussed later, such differences in modelled SPG indices lead to differences in their relationship with salinity in the ENA.

In summary, the SPG index based on the leading mode of modelled SSH variability (i.e. SPGI) shows latitudinally coherent response of salinity in the ENA to changes in SPG strength; DENS shows changes in salinity as well but only in the central SPG, while BTSF and FKL do not show any latitudinally coherent changes in salinity.

A.2.3 *Lagrangian View of Modelled SPG Circulation Variability*

The results from the composite analysis shown above present a rather static picture of the impact of variability in SPG circulation on salinity in the ENA. Also further insight is sought on the significance of latitudinal shifts of the NAC in western intergyre region. One way to reveal water mass pathways during distinct circulation regimes in the North Atlantic is by analyzing Lagrangian trajectories of virtual floats released in the modelled velocity fields (see Methods). Such view of circulation variability is provided by 4-year backward trajectories of virtual floats released in the upper 100m in the ENA (Figure A.5). First, close to earlier estimates (Burkholder & Lozier, 2014) of the proportion of subtropical and subpolar floats arriving in the ENA, in the present simulation, subtropical floats constitute >60% while subpolar floats constitute <10% of the total floats (Figure A.5). Second, compared to the mean, all indices unambiguously suggest that the number of subtropical floats arriving in the ENA decreases and the number of subpolar floats increases when the SPG circulation is strong. This implies that that a strengthened SPG impedes the subtropical throughput and enhances the subpolar throughput into the ENA. Furthermore, a noticeable feature that emerges from the comparison of backward trajectories is the shift in advective pathway in the western intergyre region. The largest variability in the latitudinal position of the trajectories passing though the western intergyre region is seen in the case of SPGI followed by DENS. This matches well with the largest response of salinity to changes in SPG circulation shown by SPGI followed by DENS. The northward shift of float trajectories in the intergyre region for strong SPGI also corroborates the result from composite analysis of circulation changes which revealed strong anticyclonic circulation anomalies and relatively large meridional shifts in isohalines in the intergyre region.

In the ENA (∼30°W), the trajectories broaden and shift to the west when the SPG weakens (Figure A.5). Except FKL, such a shift in the ENA is represented by other three modelled indices, suggesting that the shift of trajectories in the ENA is a robust feature. Note that the variation in the proportion of subpolar and subtropical floats does not lead to variation in salinity in the ENA in the case of BTSF and FKL, but does in the case of SPGI and DENS, therefore, it implies that along with the proportion of floats, their pathways also influences salinity. As discussed in the following sections, the meridional shifts in advective pathways in the intergyre region and the zonal shifts in the ENA are manifestations of the expansion and contraction of the SPG.

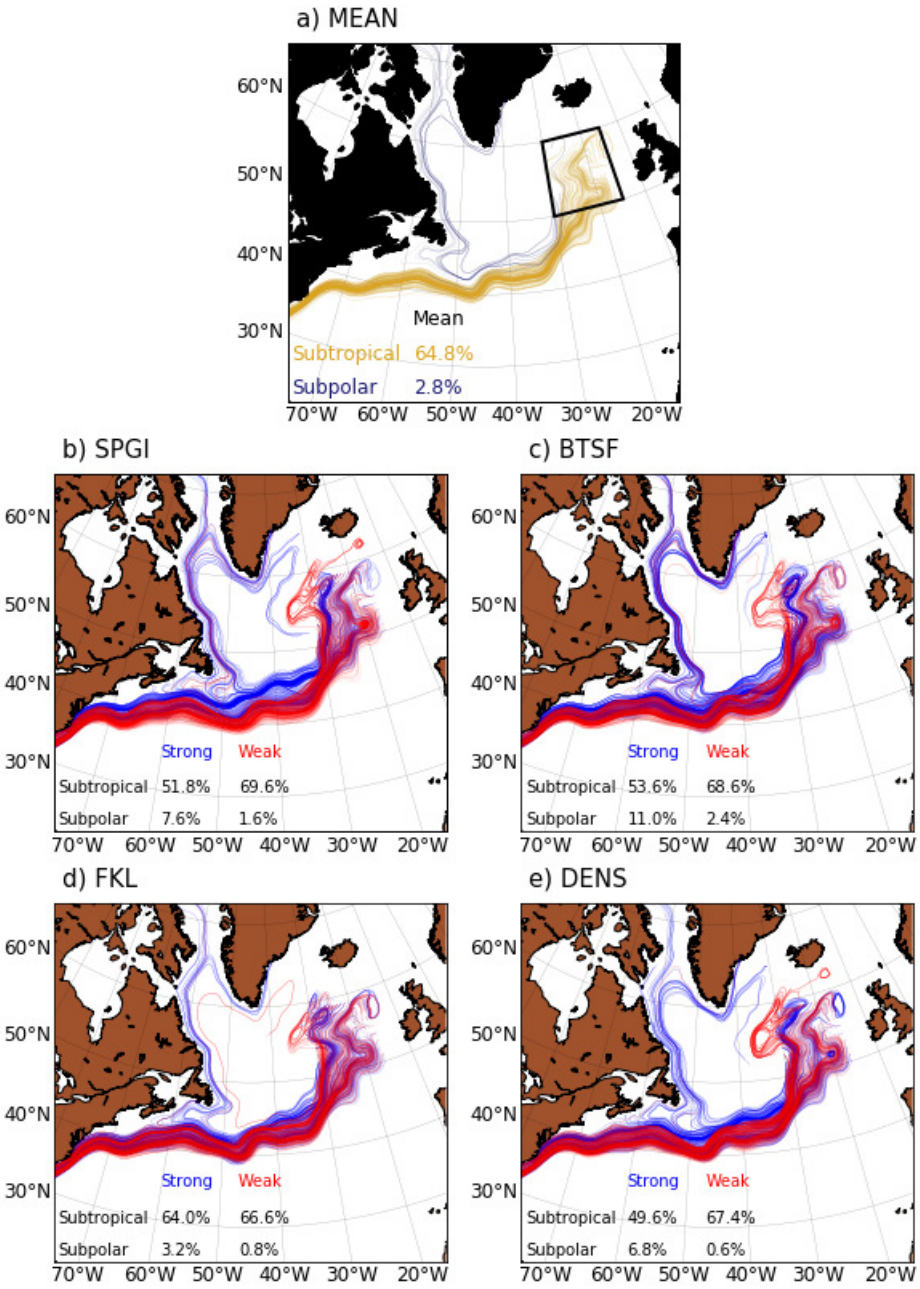

Figure A.5: Four year backward trajectories of all virtual floats released in the eastern SPG during (a) MEAN circulation conditions and during strong (blue) and weak (red) phases of (b) SPGI, (c) BTSF, (d) FKL and (e) DENS. To highlight main features, the trajectory of floats that remain in the ocean throughout their lifetime are drawn by thick lines. The black box in (a) shows the region where 500 virtual floats were released in the upper 100 meter. The subtropical floats are defined (Burkholder & Lozier, 2014) as those floats which move south of 32°N at-least once in their lifetime, while the subpolar floats are defined as those floats which move west of 45°W and north of 60 °N at-least once in their lifetime of 4 years.

A.2.4 *Role of Large Scale Atmospheric Forcing*

Till now we have illustrated that the proportion of subtropical and subpolar floats arriving in the ENA is linked to the state of the SPG circulation as represented by various indices. Now we attend the question of causality. First, the instantaneous relationship between the SSH and large scale atmospheric variability is considered. The instantaneous response of the SSH to the NAO is a decrease in the subpolar latitudes and an increase in the subtropical latitudes (Figure A.6a). This spatial pattern is the characteristic basin scale dipole pattern of the ocean's response to short term atmospheric variability. However, the instantaneous response of SSH to the East Atlantic Pattern, the second mode of modelled sea level pressure variability, is zonally asymmetric (Figure A.6b). Its influence is larger in the ENA than in the western SPG. Nevertheless, none of these regression patterns match the spatial pattern of the leading mode of modelled SSH variability (Figure A.1c).

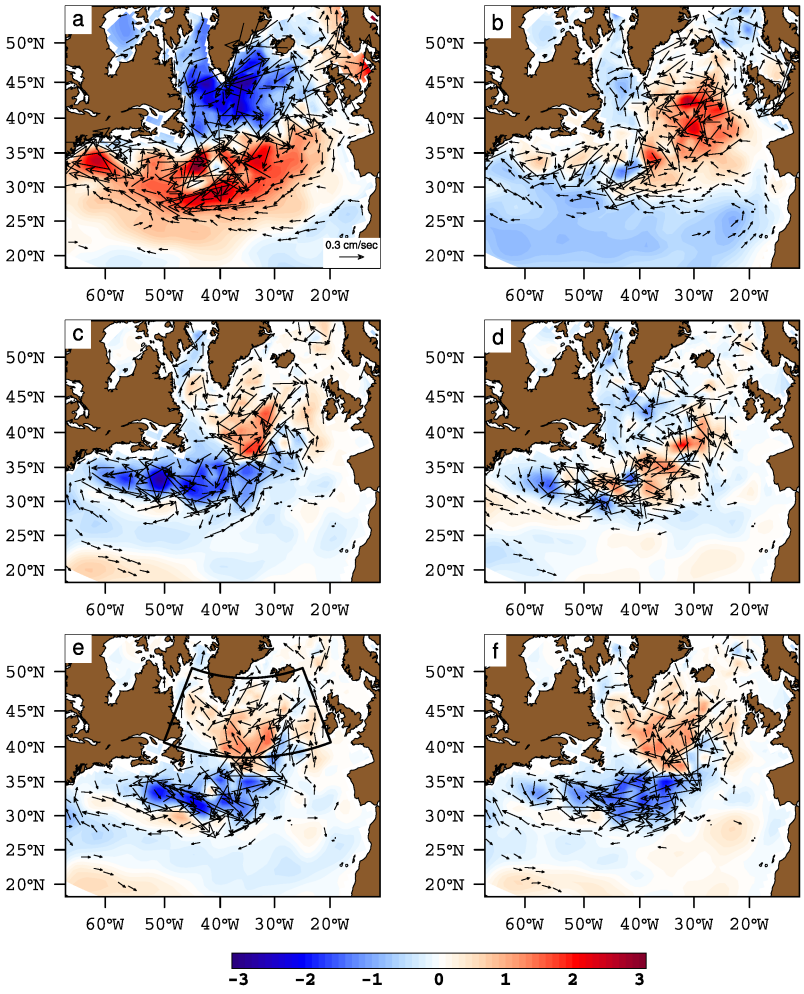

Figure A.6: Lag-0 regression of modelled SSH and currents (upper 500m) on (a) NAO, (b) EAP index and Lag-10 regression of SSH and currents (upper 500m) on leading (c) NAO, (d) EAP, (e) average wind stress curl and (f) average surface heat flux (latent+sensible) over the SPG (black box). Shown are regression coefficients (units/σ(index)). For clarity, only those current vectors with magnitude $\geq$ 0.1 cm/sec are shown. NAO—North Atlantic Oscillation, EAP—East Atlantic Pattern.

When the lagged (decadal) response of the modelled SSH field to the NAO is considered, it emerges that the spatial pattern of the leading mode of modelled SSH variability mirrors the spatial pattern of the lagged response (Figure A.6c). A strong SPG circulation, driven by the NAO, turns into a weak SPG circulation in a decade, suggesting a negative feedback. Such a dipole SSH pattern does not emerge as a lagged response to the East Atlantic Pattern (Figure A.6d). However, a lagged response of SSH, similar to the NAO, emerges if the variability in the winter mean wind stress curl and surface heat fluxes over the subpolar North Atlantic are considered (Figure A.6e,f). Although the pattern of the lagged SSH-response to surface heat fluxes resembles the lagged SSH-response to both the wind stress curl and the NAO, the role of winter mean surface heat flux variability seems to be less important in driving decadal changes in SSH variability. This is because, in the model simulation, changes in surface density in the Labrador Sea are largely driven by changes in salinity and not by temperature (Figure S.1). Thus, the variability in surface heat fluxes over the subpolar North Atlantic would not lead to a lagged response in meridional overturning through changes in density. Therefore, these results suggest that the variability in SPG circulation as represented by SPGI (i.e. modelled PC1 SSH), in particular the latitudinal shift of the NAC in the western intergyre region, is a decadal response to wind stress curl variability over the subpolar North Atlantic.

A.3 DISCUSSION

The decadal meridional shifts in trajectories in the western intergyre region, which seems to explain variability in modelled salinity, can originate from the variability in the NAO (Taylor & Stephens, 1998; Marshall et al., 2001). As a consequence of persistent multi-annual NAO+ state, the upper ocean heat content in the SPG is significantly lower and the SPG strengthens. As a compensating but delayed response, an anomalous anticyclonic intergyre gyre circulation is thought to build up in the western intergyre region as cooling in the SPG progresses (Marshall et al., 2001). However, in the present study, we demonstrate that the changes in the intergyre gyre are mainly driven by the variability in wind stress curl above the subpolar North Atlantic. Since the intergyre gyre circulation is anticyclonic for a strong SPG, the mean circulation would resemble a northward shifted NAC (Figure A.5a). While this might seem like a local circulation anomaly outside of the core SPG, the build-up of this anomalous circulation is due to the same atmospheric forcing that drives the variability in the constituent currents of the core SPG circulation. The intergyre gyre circulation is thus conjectured to be induced by changes in SPG strength itself as a consequence of variability in wind stress curl.

Another mechanism that could explain decadal meridional shifts in the NAC is related to the variability in the AMOC. The dipole pattern of the modelled first EOF of SSH resembles the characteristic fingerprint of decadal AMOC variability (Zhang, 2008). The opposing pattern of SSH variability in the SPG and NAC path is a simple yet robust consequence of heat convergence/divergence in these regions in the MPI-ESM (Borchert et al., 2018). The flow of the deep western boundary current and its associated vortex stretching leads to the formation of a northern recirculation gyre in the upper layers in the NAC region (Zhang & Vallis, 2007). A strong flow in the deep western boundary current enhances the northern recirculation gyre, which

results in higher oceanic heat divergence, and therefore a cooling of the upper layers, and a reduction of SSH in the NAC region. Stronger deep western boundary current leads to a stronger AMOC following a lag of few years which enhances northward heat fluxes, and thus the heat content of the SPG increases and the SSH rises. This creates a characteristic dipole pattern of SSH. This second mechanism thus explains the anomalous circulation pattern in the western intergyre region and the associated weakening and strengthening of the SPG. The NAO is also indirectly involved in this mechanism since it influences both SPG temperature and the deep water formation in the Labrador Sea.

Although the meridional shift of trajectories in the intergyre region in Figure A.5b can be explained by the heat content related mechanisms discussed above, the broadening and shift of trajectories in the ENA can not be explained solely by either of the mechanisms. These mechanisms mainly emphasize external drivers of heat content change as the main source of variability in SPG circulation, however, they overlook the importance of salinity in influencing the stability of water column in the SPG (Figure S.1). This is because our results do not relate the variability in surface density in the Labrador Sea to changes in surface heat fluxes. Instead our results suggest that the initiation of the intergyre gyre circulation anomaly or the northern recirculation gyre in the western intergyre region, both of which relate to latitudinal shifts in the NAC, is due to the wind stress curl driven changes in the SPG circulation. When the vorticity input to the SPG due to winds is anomalously higher and persistent over multiple years, more fresh water is transported along the northern flanks of the NAC towards the ENA and less subpolar water flows southwards (Figure A.5a). Higher surface divergence associated with strong wind stress curl shifts major current pathways eastward, thus explaining the sharpening and eastward shift of simulated trajectories in the ENA. A sustained removal of freshwater from the western SPG leads to a decrease in the thickness of fresh upper layer and consequently salinity increases over multiple years. Such salinification of western SPG creates positive density anomalies which propagate southwards and initiate positive anomalies in the meridional overturning circulation. The anomalous strengthening of the meridional overturning is concomitant with the westward contraction of the SPG in the ENA, the gradual retreat of the NAC towards southern latitudes and reversal of density anomalies in the SPG.

The emergence of negative feedback mechanism in MPI-ESM-LR is consistent with earlier investigations, however, our results suggest that the SPG is not passive in a perpetual negative feedback loop controlled by variability in the meridional overturning circulation. It is important to note that, as compared to the mean, the number of subtropical floats arriving in the ENA does not increase substantially when SPG weakens, but it decreases substantially when the SPG strengthens. The implication being that changes in the SPG size, strength and salinity in the ENA are not exclusively due to changes in subtropical throughput, rather, the variability in SPG circulation modulates the subtropical throughput which then changes the salinity in the ENA. These results are robust and not overly sensitive to the number and deployment depth of virtual floats (Figure S.2 and S.3), Therefore, it is the variability in horizontal SPG circulation, driven by overlying atmospheric variability, that modulates the pathway and proportion of subpolar and subtropical floats arriving

in the ENA, and such variability in the horizontal circulation is mainly captured by the modelled SPGI and to some extent DENS.

This result thus allows us to infer the likely cause of observed salinity changes in the ENA. Intensification of the NAC, the cyclonic circulation and salinity changes in the case of PC2 SSH, DENS, and NAO indices point to the an increased advection of subpolar water from the west. The response of circulation and salinity to long-term changes in the NAO (Figure A.3b) also matches well with SPGI. So, contrary to the recent finding (Foukal & Lozier, 2017), the complex interplay between the variability in the strength and size of the SPG does influence salinity in the ENA.

Having explored the causes of similarity between the SPGI-based and observed SPG-salinity relationship, we now highlight potential causes of discrepancies in modelled FKL and BTSF. In the model, the SPG does expand and contract, however, if one considers the largest closed contour of SSH as the SPG boundary, then the zonal expansion and contraction of the SPG is limited to the western parts (Figure S.4). By definition, this would exclude variability in the ENA and in the western intergyre region, which as discussed above is coupled to the SPG circulation via atmospheric or oceanic forcing, and therefore FKL would neither project onto NAO nor show consistent relationship with salinity in the ENA (Foukal & Lozier, 2017). From the model point of view, the SPG is a cyclonic circulation seen in the two dimensional barotropic stream function in the subpolar North Atlantic. The area and depth averaged BTSF as one of the indices analyzed here only partly captures the complexity of the three dimensional spatial structure of SPG circulation. Furthermore, the BTSF represents circulation strength in the western SPG (Figure S.4), and does not capture the baroclinic component of circulation variability in the intergyre region and the ENA either.

While the results presented here illuminate the SPG-salinity relationship in observations and in an ESM, there are some caveats that must be acknowledged. First, as is the case with various global coupled models, there are known issues in MPI-ESM regarding the zonal position of NAC (Jungclaus et al., 2013). This leads to biases in mean water mass properties. Advection of such biased properties to regions of interest is a concern. Hence, the potential impact model biases could have on the variability of SPG circulation warrants further investigation. Second, the altimeter record is quite short (24 years) compared to the model output (200 years) analyzed here. Thus, the low frequency variability present in modelled SPG indices might not have yet emerged in the observed indices, and thus their comparison must be treated with caution. Third, we have not quantified the contribution of freshwater flux from the atmosphere to salinity changes in the ENA. But the striking similarity between shifts in advective pathways and isohalines suggests that the freshwater flux at the air-sea interface does not dominate. Finally, given the scarcity of long term velocity observations, we have only analyzed the baroclinic part of observed circulation variability. Since the barotropic part of circulation variability is not in phase with the baroclinic part (Eden & Willebrand, 2001), the changes in observed circulation presented in this study must also be carefully interpreted. Nevertheless, the similarity between the response of modelled currents and the observed baroclinic currents suggests that the baroclinic part of circulation variability plays an important role in determining SPG strength-salinity relationship in the ENA.

A.4 CONCLUSIONS

Based on the analysis of observed and modelled SPG indices and Lagrangian trajectory experiments carried out with a global coupled model, we derive the following conclusions:

1. The interpretation of the SPG strength–salinity relationship is dictated by the choice of the SPG index. A dynamically consistent interpretation presented here is that the variability in the proportion and the pathway of subpolar water arriving in the ENA has an influence on salinity. Thus both size and strength of the SPG are related to salinity changes in the ENA.

2. All modelled SPG Indices agree that a stronger SPG is associated with enhanced influence from the fresher western SPG region and impedes the subtropical salinity throughput.

3. The modelled variability in Lagrangian pathways is part of the decadal response of SPG circulation to wind stress curl variability over the subpolar North Atlantic. Latitudinal shifts of the NAC in the western intergyre region and pathways of subpolar water in the ENA are most likely main sources of inconsistency among SPG indices.

4. Constrained by their definitions, SPG indices based on depth integrated barotropic streamfunction and the largest closed contours of SSH should be carefully interpreted as these indices do not capture the variability in the advective pathways from the western intergyre region to the ENA.

5. The observations-based SPG indices–PC2 SSH and DENS, which capture the variability in the strength and position of the NAC and the intensification of cyclonic circulation in Irminger Sea and Iceland basin, are the best-suited proxies of observed SPG circulation variability and associated water mass variability in the ENA.

Finally, the weak-SPG-high-salinity relationship in the eastern subpolar North Atlantic is a robust basis for the choice of SPG indices in observations and models.

A.5 METHODS

Observations of annual mean salinity used in this study are taken from the EN4(Good et al., 2013) gridded dataset and cover the time period 1960-2016. Potential density (σ_0) is calculated from temperature (T) and salinity (S) from the EN4 dataset. We also calculate geostrophic velocities to examine variability in the baroclinic part of observed circulation variability. The geostrophic velocities were calculated from the T and S fields of the EN4 dataset using the geostrophic equation and dynamic topography, while assuming a layer of no motion at 1500 m depth (results do not change substantially if this depth is changed to other reasonable level). The horizontal gradients and velocity components were calculated at the mid point of the original grid boxes. The monthly mean SSH data (i.e., AVISO absolute dynamic topography on a 0.25°x0.25°

grid) was obtained from the Integrated Climate Data Center (http://icdc.cen.uni-hamburg.de/1/daten/ocean/ssh-aviso.html), and covers the time period 1993-2016. Annual means were calculated from monthly mean values.

The model used in this study is the Max Planck Institute Earth System Model, run in a low resolution configuration (MPI-ESM-LR (Giorgetta et al., 2013)). The ocean component of MPI-ESM-LR has a nominal resolution of 1.5 degrees with a gradual increase in resolution towards the subpolar North Atlantic, reaching approximately 18 km near Greenland. We analyzed the last 200 years of a 2000-year pre-industrial control simulation where the model is free to evolve dynamically. This type of simulation is neither initialized from observation nor forced with observed external boundary conditions. This enabled us to examine SPG-salinity relationship in a dynamically consistent setting. The model output was regridded to a 1°x1° regular grid and annual mean values were analyzed in composite analysis. The model output does not exhibit any significant trend, so we present results based on the non-detrended model output. Detrending does not result in any different conclusions.

In the present work, we used multiple indices of SPG strength that have been applied in observational and modelling studies (Table S1). The first index (PC1 SSH) is defined as the principal component of the leading Empirical Orthogonal Function (EOF) of annual mean SSH anomalies in the subpolar North Atlantic, defined in the domain 20-70°N, 0-80°W (Häkkinen & Rhines, 2004), and defined for the altimeter period 1993-2016. Similarly, the second index (PC2 SSH) is defined as the principal component of the second EOF of annual mean SSH anomalies. A third index (DENS) is defined as the annual mean density anomalies at 310 meter depth in the region 50-62°N, 35-55°W (Tesdal et al., 2018). DENS is a proxy for baroclinic strength of the SPG previously used to explain freshening in the western SPG. DENS is defined for two periods: the altimeter period 1993-2016, for comparison with other SSH-based indices, and 1960-2016, to extend the analysis for a longer time period. A fourth index (FKL) is defined as the difference between the largest closed contour of annual mean SSH and the minimum of SSH within the largest closed contour (Foukal & Lozier, 2017). The FKL index is defined for the altimeter period from 1993 to 2016. Additionally, we also use two pentads when the NAO was largely in a high (1991-1995) or a low (1964-1968) state as a proxy of those atmospheric conditions which favor a particular SPG state. The observed NAO index is the Hurrel's station-based index and is obtained from https://climatedataguide.ucar.edu/climate-data/. All observational results presented in this study are based on non-detrended data.

The SPG indices - PC1 SSH, DENS and FKL - defined using observational data are defined identically in the MPI-ESM. Another index (BTSF) is defined in MPI-ESM as the annual mean depth integrated barotropic streamfunction in the region 50-62°N, 10-60°W. Our region of interest for identifying salinity changes is the eastern subpolar North Atlantic (ENA), defined as the region between 50°N to 60°N, 15°W to 30°W.

In order to test whether the variability in advective pathways leads to variability in salinity in the ENA, we performed Lagrangian experiments in MPI-ESM using the offline OceanParcels (Lange & Sebille, 2017; Delandmeter & Van Sebille, 2019) framework for the particle trajectory scheme. First, composite mean monthly horizontal and vertical velocity fields based on strong and weak phases of each index were created. Then the resulting monthly mean 3-dimensional velocity field was used to advect 500 virtual floats deployed randomly in the upper 100 meters in the ENA (50°N to 60°N,

15°W to 30°W) and advected backward in time for four years. The interested reader is referred to http://oceanparcels.org/for more details on the underlying particle trajectory scheme.

A.6 ACKNOWLEDGEMENTS

This work was funded through a research collaboration between Helmholtz Zentrum Geesthacht and Universität Hamburg. The work of J. B. was supported by the Cluster of Excellence CliSAP (EXC177), Universität Hamburg, funded through the Deutsche Forschungsgemeinschaft (DFG, German Research Foundation). This work was also funded by the DFG under Germany's Excellence Strategy EXC 2037 "Climate, Climatic Change, and Society" Project 390683824, contribution to the Center for Earth System Research and Sustainability (CEN) of Universität Hamburg (J. B.). L.B. was supported by the BMBF under the Miklip FlexForDec Project (Grant 01LP1519A). The authors thank Johann Jungclaus for providing helpful comments during the internal review. The authors thank Michael Botzet for carrying out the model simulations. The authors also thank the German Computing Center (DKRZ) for providing their computing resources. The authors do not report any conflict of interest.

A.7 SUPPLEMENTARY INFORMATION

Due to different lengths of observed and modelled time series, for the composite analysis, we have chosen values above and below ± 0.5 standard deviation for observation-based SPG indices and ± 1 standard deviation for model-based SPG indices. This choice of these separate thresholds is guided by the necessity to minimize any bias in the number of strong and weak SPG years. We find that by using the thresholds as they are in this study, this requirement is best fulfilled. We have also compared the observational results based on ± 1 standard deviation, and we find that the conclusions derived in this study do not change.

Table S.1: Indices of SPG strength

	DEFINITION	TIME PERIOD	REFERENCE
PC1-SSH	Principal Component of the first empirical orthogonal function of sea surface height in the North Atlantic (20:70°N, 0:80°W	Observation: 1993:2016 Model: Last 200 years	Häkkinen & Rhines (2004); Hátún et al. (2005)
PC2-SSH	Principal Component of the second empirical orthogonal function of sea surface height in the North Atlantic (20:70°N, 0:80°W	Observation: 1993:2016 Model: Last 200 years	As also used in Hátún & Chafik (2018)
DENS	Weighted area average density anomaly at 314 m depth in the region:50:62°N, 35:55°W	Observation: 1993:2016 Model: Last 200 years	Tesdal et al. (2018)
FKL	Difference between the largest closed contour of annual mean SSH in the subpolar North Atlantic and minimum of SSH within the largest closed contour.	Observation: 1993:2016 Model: Last 200 years	Foukal & Lozier (2017)
BTSF	Weighted area average barotrophic streamfunction in the North Atlantic (50:62°N, 10:60°W)	Model: Last 200 years	As also used in Lohmann et al. (2009)

Table S.2: Strong and weak years (from non-detrended data) of SPG strength

PC1 SSH		PC2 SSH		DENS		FKL	
Strong	Weak	Strong	Weak	Strong	Weak	Strong	Weak
1993	2012	1993	2003	1993	1996	1993	2004
1994	2013	1994	2004	1994	1998	1995	2005
1995	2014	1995	2005	1995	1999	1996	2009
1996	2015	2000	2006	2000	2002	1997	2010
1997	2016	2015	2007	2015	2003	1998	2016
		2016	2010	2016	2004	2002	
			2011		2006	2007	
			2013		2007	2014	
					2011		

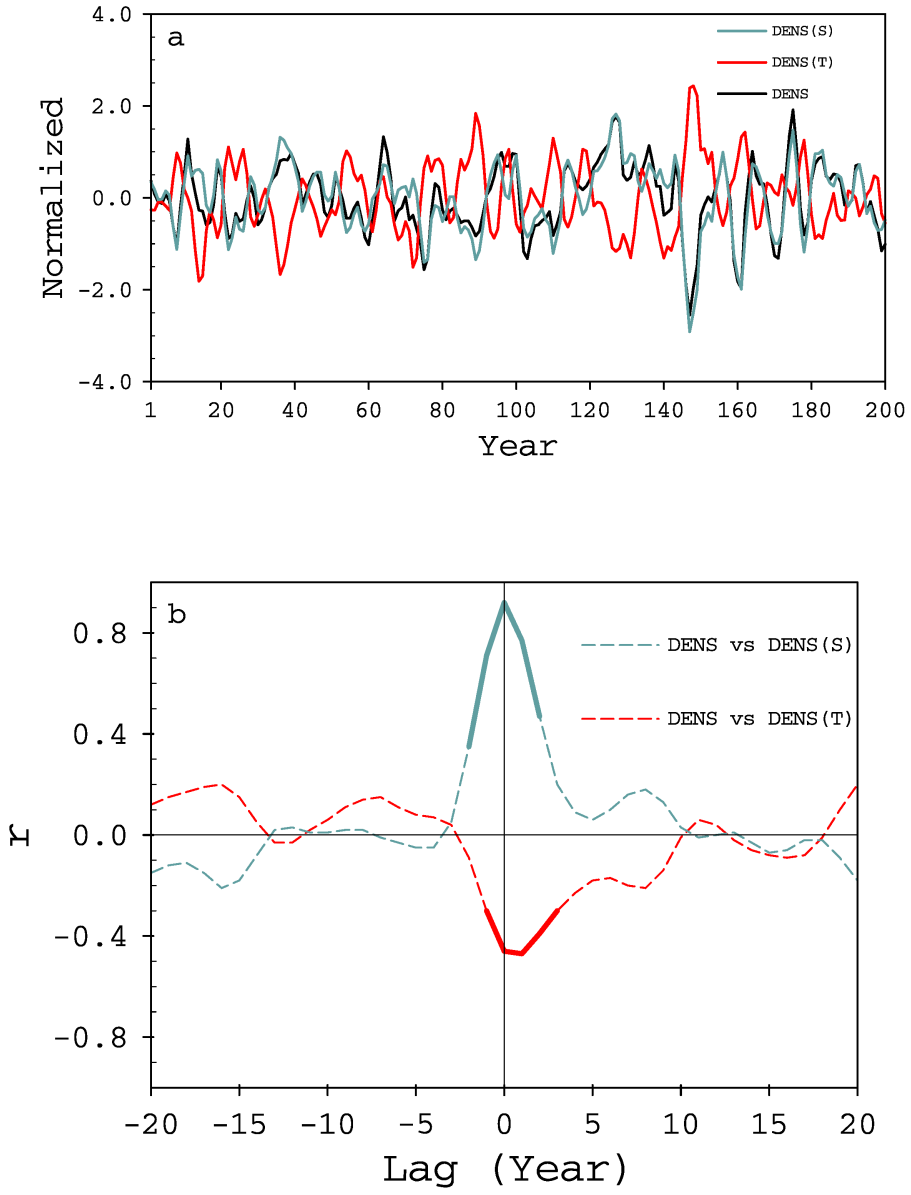

Figure S.1: (a) Time series of modelled surface density (black), density due to variable salinity and mean temperature (blue) and density due to variable temperature and mean salinity (red) in the Labrador Sea (55:65°N, 45:60°W) for the last 200 years of the simulation. (b) Lead-lag correlation between density and density due to variable salinity (blue) and density due to variable temperature (red). Density leads for positive lags. Statistically significant correlations at 95% confidence level are shown in bold. All three time series were smoothed by a 3-year running mean before correlating.

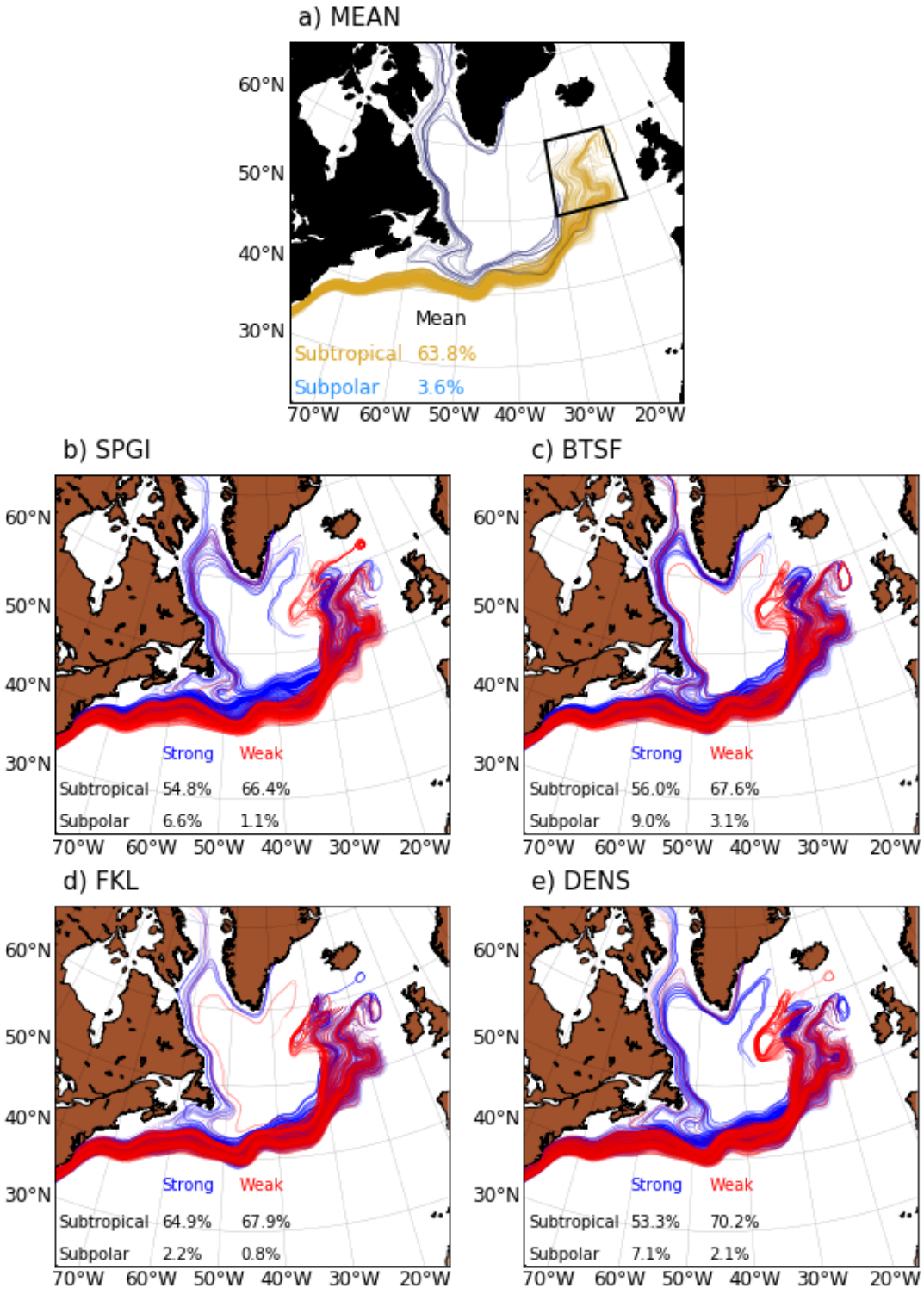

Figure S.2: Same as Figure A.5 in the main text but for 1000 floats deployed in the upper 100m.

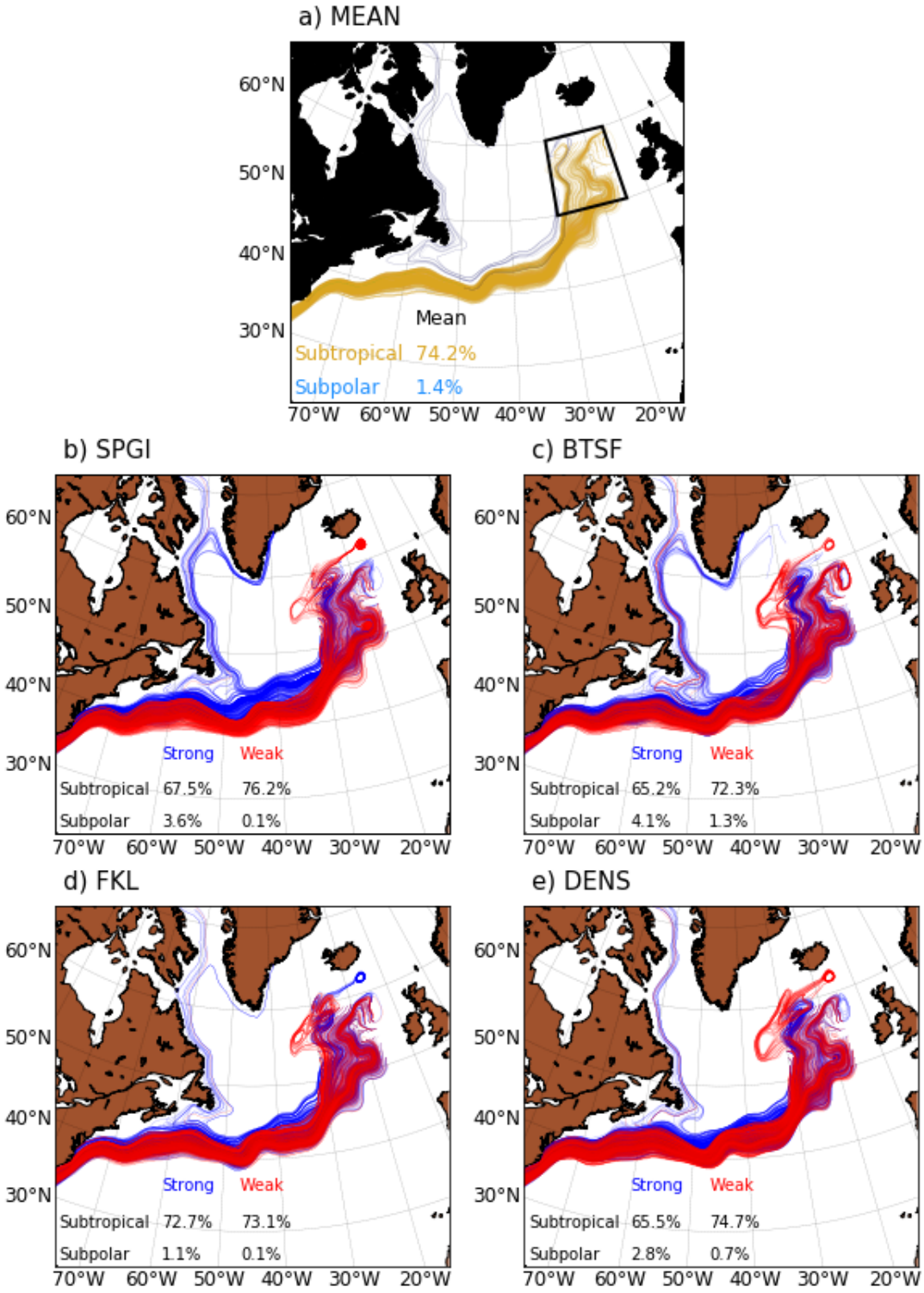

Figure S.3: Same as Figure A.5 in the main text but for 1000 floats deployed in the upper 200m.

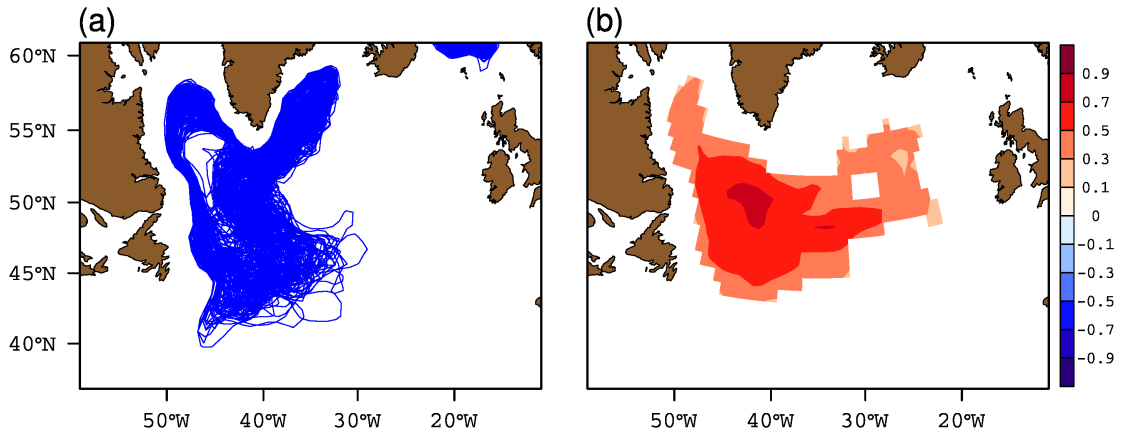

Figure S.4: (a) Largest closed contour of modelled annual mean SSH for each year of the simulation period. (b) Correlation of BTSF index with the annual mean barotropic streamfunction at each grid point. Statistically significant values at 95% confidence level using a t-test are shown.

B

ATLANTIC INFLOW TO THE NORTH SEA MODULATED BY THE SUBPOLAR GYRE IN A HISTORICAL SIMULATION WITH THE MPI-ESM

This appendix contains a paper, which has been published in the journal of Geophysical Research Oceans as:

Koul, V., Schrum, C., Düsterhus, A. & Baehr, J. (2019), "Atlantic Inflow to the North Sea Modulated by the Subpolar Gyre in a Historical Simulation with the MPI-ESM", Journal of Geophysical Research: Oceans,124, 1807–1826.

The contribution of Vimal Koul (V.K.) and others to this paper is as follows:
V.K., C.S and J.B. conceived the work. V.K performed the analysis and wrote the paper. V.K. was guided by A.D. on statistical analysis. C.S. and J.B. provided guidance on the overall direction of the work. All authors reviewed the manuscript.

Atlantic Inflow to the North Sea Modulated by the Subpolar Gyre in a Historical Simulation with the MPI-ESM

Vimal Koul[1,2], Corinna Schrum[3], Andre Düsterhus[1] and Johanna Baehr[1]

[1]Institute of Oceanography, Center for Earth System Research and Sustainability, Universität Hamburg, Germany

[2]International Max Planck Research School on Earth System Modelling, Max Planck Institute for Meteorology, Germany

[3]Helmholtz Zentrum Geesthacht, Institute of Coastal Research, Germany

(Submitted: 7 November, 2018, Revised: 23 January, 2019, Published: 5 March, 2019)

While the influence of the Subpolar Gyre (SPG) on thermohaline variability in the eastern North Atlantic is well documented, the extent and timescale of the influence of the SPG on North Sea is not well understood. This is primarily because earlier investigations on the causes of variability in the North Sea water properties mostly focused on the role of atmosphere, and deployed regional models. Here, using a historical simulation with the Max Planck Institute Earth System Model, we investigate circulation and water mass variability in key regions, namely Rockall Trough and Faroe-Scotland-Channel (FSC) which link the North Atlantic to the North Sea. We find that salinity co-varies with advective lags in these three regions, and that the northern North Sea salinity follows the Rockall Trough with a lag of one year. We show that recurring and persistent excursions of salinity anomalies into the northern North Sea are related to the SPG strength and not to the local acceleration of the inflow. Furthermore, we illustrate that the SPG signal is more pronounced in salinity than in temperature, and that this simulated SPG signal has a period of 30-40 years. Overall, our study suggests that, at low frequency, water mass variability originating in the North Atlantic dominates changes in the North Sea water properties over those due to local wind driven volume transport.

B.1 INTRODUCTION

The North Sea is a shallow adjacent sea of the Atlantic Ocean located on the North-western European continental shelf (NWES). The northern boundary of the North Sea presents an opening for water masses of Atlantic origin to propagate into this region. However, before entering the North Sea, these oceanic anomalies mainly pass through two key upstream regions: the Rockall Trough and the Faroe Shetland Channel (FSC). The Atlantic inflow through these key regions draws water masses from the North Atlantic Current (NAC), the European Slope Current (ESC), and also from the East Icelandic Current (EIC) north of the FSC (Turrell et al., 1996). Therefore, hydrographic changes in the North Sea have often been shown to be influenced by water mass variability originating in the key upstream regions (Holliday & Reid, 2001; Núñez-Riboni & Akimova, 2017). However, given observational and modelling constraints, a robust spatial and temporal characterization of the influence of the North Atlantic on the North Sea is still missing.

Earlier investigations have mostly focused on the atmosphere-driven North Sea variability, and regional models have been used preferably (see for example Winther & Johannessen (2006), Hjøllo et al. (2009), and Daewel & Schrum (2017)). This is because the shallowness of the North Sea makes it more responsive to overlying atmospheric variability. However, being able to identify a variability of North Atlantic (oceanic) origin has the advantage that it not only explains part of the variability in marine ecosystems (Akimova et al., 2016; Holt et al., 2012), but it can also lead to long term hydrographical and biogeochemical predictability. Therefore, of particular interest has been to understand which part of variability in the North Sea is of Atlantic origin (Alheit et al., 2014; Holliday & Reid, 2001). Hence, given the nature of the problem, recent studies have highlighted added value in simulating North Atlantic-North Sea connections using global models (Mathis et al., 2017; Pätsch et al., 2017). This approach has the advantage that it allows a dynamically consistent representation of North Atlantic-North Sea connections, and circumvents the issues associated with specifying lateral boundary conditions in regional models.

The motivation to investigate North Atlantic-North Sea connection in a global coupled model also stems from the fact that no robust conclusion could be drawn from the few observational studies concerning long term North Atlantic-driven variability in the North Sea. For example, by analyzing 65-year surface salinity data for the NWES, Dickson (1971) concluded that the advection of higher proportion of subtropical water was responsible for extended periods of high salinity in the NWES. He linked the periodicity and sustained salinification of the NWES to a persistent pressure-anomaly pattern which was then shown to induce sustained advective changes in the eastern North Atlantic. Becker & Dooley (1995) attributed the 1989/90 high salinity event in the North Sea to increased inflow of Eastern North Atlantic Water (ENAW) in the ESC. They conjectured that large scale circulation changes were responsible for reorganization of water masses in the eastern North Atlantic which in turn had an impact on the inflow stream to the North Sea. While these studies suggest that the causes of salinification events in the NWES are not attributable to a single mechanism, the multi-year persistence of such events also suggests that the causes and characteristics of the large scale oceanic variability which leads to salinification in the NWES needs further investigation.

In the upstream region, i.e. the eastern North Atlantic, abundant observational evidence suggests a role of SPG variability in driving thermohaline changes (Bersch, 2002; Holliday, 2003; Hátún et al., 2005; Sarafanov et al., 2008). A weak SPG circulation allows northward penetration of subtropical water. In the Rockall Trough, long-term observations also suggest an overall warming and salinification from late 1990s till mid 2000s (Holliday et al., 2015), linked to the SPG variability (Sherwin et al., 2011). The SPG-driven changes that have occurred in the Rockall Trough are not limited to thermohaline properties alone; for example, links with nutrient concentrations have also been reported (Johnson et al., 2013). Modelling studies have further suggested that the SPG strength undergoes decadal changes and the mid-1990s event was part of that decadal variability (Böning et al., 2006; Zhang, 2008). Therefore, anomalous SPG circulation is thought to control the proportion of subtropical and subpolar water masses in the Atlantic inflow across the Iceland-Scotland Ridge (ISR).

The SPG-driven thermohaline variability in the Rockall Trough, FSC and the North Sea has not yet been examined in a global model. Hjøllo et al. (2009) did point out that some of the discrepancies in simulating salinity variability at northern North Sea stations in their regional model arose due to the imposed boundary conditions and the limited domain of their model, both of which tend to disregard the SPG signal from open ocean. Using a global model, Mathis et al. (2017) highlighted the importance of North Atlantic in driving future changes in the NWES. Thus there seems to be some hint that the impact of dynamic circulation changes in the North Atlantic extends to the North Sea. However, a comprehensive analysis of the relationship between variability in SPG circulation and Atlantic inflow to the North Sea has remained unexplored.

In the present contribution, we examine North Atlantic-North Sea connections in a historical simulation with a global coupled model. Our aim is to reveal the spatial and temporal characteristics of the influence of the SPG on North Sea properties in such a century long simulation. We use a combination of correlation, composite and water mass analysis to study the key region.

Section B2 describes the model and methods used, results are provided in section B3, section B4 discusses the main findings, and conclusions are presented in section B5.

B.2 MODEL DETAILS, METHODS AND MODEL EVALUATION

B.2.1 *Model Details*

The Max Planck Institute Earth System Model (MPI-ESM) version 1.2 is the latest version of the global Earth system model developed at the Max Planck Institute for Meteorology, and is used in its low resolution (LR) setup in the present study (hereafter MPI-ESM1.2-LR). The ocean general circulation component of MPI-ESM1.2-LR, the Max Planck Institute Ocean Model (MPIOM) (Jungclaus et al., 2013), is a free surface model with primitive equation solved on an Arakawa C-grid, and with hydrostatic and Boussinesq approximations. It has a total of 40 z-levels in the vertical with closely spaced upper levels; the surface layer thickness is 12 meters. Formulations by Pacanowski & Philander (1981) are followed for vertical mixing and diffusion, and tracer transport is parameterized following Gent et al. (1995). Statically unstable flow

over sills and shelves is represented by a slope-convection scheme (Marsland et al., 2003). The MPIOM setup used in the study has a rotated grid configuration (GR15) for which the singularity at the North Pole is replaced over Greenland. This has the advantage that horizontal resolution is enhanced north of 50°N, reaching 15Km near Greenland. The resolution increases gradually to 1.5 degrees towards the equator. Embedded in MPIOM is also the ocean biogeochemistry component, the Hamburg Ocean Carbon Cycle (HAMOCC) model (Ilyina et al., 2013). Among other processes, HAMOCC incorporates phosphate and oxygen cycles, and defines the marine food web based on nutrients, phytoplankton, zooplankton and detritus (NPZD) based approach.

The atmospheric general circulation component of MPI-ESM1.2-LR is the European Center-Hamburg (ECHAM) (Stevens et al., 2013). In MPI-ESM1.2-LR, the ECHAM is run at a horizontal resolution of T63 and with 47 vertical levels, the model top being at 0.01hPa. The land surface-atmosphere interactions are simulated by the land vegetation module JSBACH (Reick et al., 2013) which is embedded in ECHAM. A land hydrology module which contains a river-routing scheme is used for interactive simulation of river runoff (Hagemann & Gates, 2003). MPIOM receives the fresh water fluxes due to river runoff as part of the precipitation field from ECHAM.

B.2.2 *Methods*

In this study, we analyze a historical simulation performed under natural and anthropogenic forcings derived from observations covering a total of 156 years (1850-2005). The natural forcing includes solar insolation, variations of the Earth orbit, tropospheric aerosol, stratospheric aerosols from volcanic eruptions, and seasonally varying ozone. The anthropogenic forcing includes the well mixed gases CO_2, CH_4, N_2O, CFC-11, and CFC-12 as well as O_3, and anthropogenic sulfate aerosols. Tides are not taken into account in this simulation. Atmospheric CO_2 concentrations are prescribed and the carbon cycle is not interactive. It must be noted that as this historical simulation is not initialized from observations, the internal variability in this model simulation may not be in phase with observations, and hence may not reproduce the observed timing of certain climatic events which are related to internal (natural) variability. However, dynamical relationship between variables of interest within the model can be compared to their observed relationship (Langford et al., 2014; Martin et al., 2014; Zhang & Wang, 2013). This simulation provides the base for understanding spatial and temporal modes of variability and their connections with North Sea. Here we focus on the relation between SPG circulation and North Sea variability, and if similar relationship is seen in observations.

Annual mean values of model output variables are first computed, and detrended (linear trend is removed at each grid point) prior to subsequent analysis. Anomalies are calculated by removing the mean of the entire simulation period (1850-2005). The climatological (1850-2005 mean) bias of modelled salinity is calculated against KLIWAS North Sea Climatology (KNSC) data set (1873-2013 mean) available from Integrated Climate Data Center (https://icdc.cen.uni-hamburg.de/1/daten/ocean/knsc-hydrographic.html).

Throughout this study, correlation coefficients are calculated from detrended anomalies. To estimate the uncertainty in correlation, we modify the strategy of McCarthy

et al. (2015) wherein they use a parametric and a non-parametric approach. As the data are auto-correlated, we first calculate the effective degrees of freedom. For this we use the equation given by Pyper & Peterman (1998) to determine the degree of freedom on the basis of auto-correlation coefficients at various lags.

For the non-parametric approach, we use block bootstrapping. While the t-test assumes the data to be normally distributed, the block bootstrap method does not make such an assumption. In this method, a set of 10000 bootstrap samples, each having the same length as the parent time series, is constructed by block-wise sampling with replacement from the parent time series. The block length L is given by: $L = \frac{N}{min(N^*)}$, where N^* is the effective degrees of freedom and N is the length of the time series. This choice of block length ensures that the most conservative estimate of confidence intervals is obtained. The resulting distribution of correlations is then investigated for significance. The sensitivity of the significance bounds to block length is also tested by changing the block length to a higher and lower value; we find that the result remains almost unchanged. The uncertainty in the time lag of maximum correlation is estimated by the time at which the median of block bootstrapped correlations is greater than the lower bound of the confidence interval derived from the block bootstrapping.

We define the index of SPG strength as the principal component of the leading mode of annual mean (detrended) sea surface height (SSH) anomaly over North Atlantic (0-70°W, 30-65°N). Read together with the weights of the leading mode in the central SPG region (Figure B.6), the positive values of this index (hereafter SPGI) correspond to an increase in the SSH, and thus represent a weak SPG. Using altimeter data and ocean model hindcast, SPGI has previously been shown to represent variability in SPG strength (Häkkinen & Rhines, 2004; Hátún et al., 2005) although the methodology for computing SPG index from SSH data is now being debated (Foukal & Lozier, 2017; Hátún & Chafik, 2018). The SPGI has also been shown to be a proxy for changes in SPG strength in a 2000-year coupled model simulation (Zhang, 2008).

We also peform a regression analysis to reconstruct North Sea salinity using multiple predictors. As such, we first split the simulated North Sea salinity time series into two parts: 1853-1950 and 1951-2005. Regression co-efficients are estimated from the former time period, and the same coefficients are then used to reconstruct North Sea salinity for the later time period. The bootstrap procdure as described above is also used here to estimate the confidence bounds.

B.2.3 *Model Evaluation: North Atlantic-North Sea Connections in MPI-ESM1.2-LR*

To identify North Atlantic-North Sea connections in MPI-ESM1.2-LR, we first explore mean large scale circulation patterns and salinity profiles in key regions. Earlier versions of this model have been shown to realistically represent the large scale mean circulation in the North Atlantic (Jungclaus et al., 2013). Our analysis also suggests that the simulated mean upper ocean circulation in the North Atlantic in MPI-ESM1.2-LR (Figure B.1) has qualitative resemblance with observations (e.g. Orvik & Niiler (2002)). Consistent with observations, two branches of the NAC enter the eastern North Atlantic as the Iceland branch and the Rockall Trough branch (Figure B.1a). The Rockall Trough branch is, however, more diffused than what observations suggest (Orvik & Niiler, 2002). Nevertheless, the Rockall Trough branch intensifies

when it enters the FSC, which is also seen in observations. This model has a strong Iceland Branch which turns eastwards after crossing the ISR and feeds the FSC. A relatively weak yet continuous current which links northern Irish shelf to the North Sea is also simulated by the model.

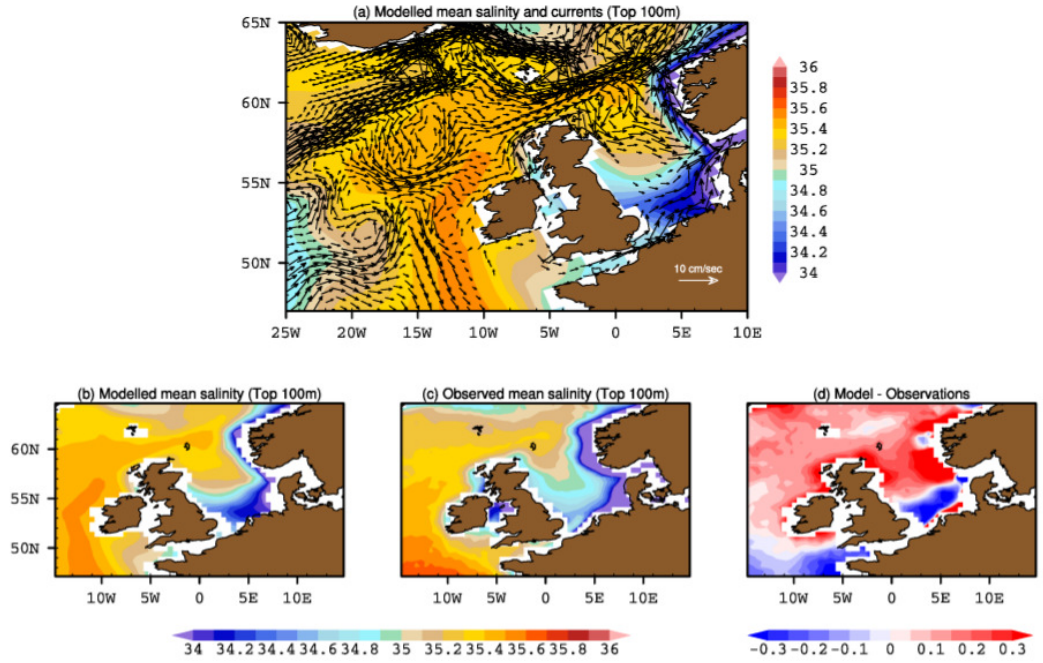

Figure B.1: (a) Modelled mean salinity ([psu], color) and currents ([cm/s], arrows) averaged over top 100m meters of the water column. Current vectors <1cm/s are not shown. (b) Modelled mean, (b) Observed (KNSC) mean, and (c) bias of salinity [psu] in the NWES region.

The North Sea circulation is cyclonic with inflows from the wide open entrance in the north, and from the English Channel in the south. The northern North Sea inflow comprises of three main inflows: the Fair-Isle inflow, the East Shetland inflow and the Norwegian Trench inflow (Turrell et al., 1996). The Norwegian Trench inflow is known to contribute the most to the northern North Sea inflow (Winther & Johannessen, 2006). In the model, this separation is not so distinct, however the model is able to reproduce northern inflows that progress cyclonically towards the central North Sea. Strong inflows are present east of Scotland and also along the western side of the Norwegian Trench. The model also shows a fresh outflow along the whole Norwegian Trench.

Recently, Pätsch et al. (2017) carried out a thorough analysis of the performance of MPIOM (with a different grid configuration) in the North Sea. Their results suggest that MPIOM performs satisfactorily over most of the North Sea although with discrepancies near coasts. Note that while the MPIOM grid resolution in that study was higher than in the present study, the model was forced using observed meteorological forcings, and hence air-sea interactions were not taken into consideration. A similar model configuration used by Mathis et al. (2017) is also unsuitable for the present analysis because, in that model configuration, air-sea interaction is considered over the eastern North Atlantic region only. Such configuration is unsuitable to examine the influence of SPG circulation on the North Sea because the SPG is strongly influenced by basin-wide atmospheric variability. Therefore, given the global coupled

model configuration used in the present study, we focus on the SPG variability, the shelf break and northern and central parts of the North Sea, and exclude the coastal regions.

The simulated mean upper ocean salinity field is shown in Figure B.1. Northward extension of saline subtropical water is seen in the eastern North Atlantic . In the North Sea, northern parts are largely influenced by Atlantic Water and hence salinity values here exceed 35.0 psu while southern and coastal regions are mainly influenced by river runoff and are therefore relatively fresher. Moreover, Atlantic water entering from the northern opening has its maximum southward extent down to 55°N in the North Sea, beyond which Atlantic salinity signature is diluted by fresh water runoff to the North Sea.

Comparison of upper 100 meter modelled mean salinity with observations suggests that the model overestimates salinity over most of the eastern North Atlantic (Figure B.1d). Major challenges for the model are present in the Norwegian Trench outflow region and in the southern North Sea, however, both these regions are not the focus of the present study. The climatological salinity bias in the Rockall Trough, FSC and northern North Sea is relatively lower than near shallow coastal regions.

The hydrography and circulation in the key regions of eastern North Atlantic and the North Sea derived from the model are expected to resemble mean features of observations. Therefore, we examine subsurface salinity on three sections (see Figure B.2d for locations) in the eastern North Atlantic. In the eastern North Atlantic, the core of Atlantic inflow extends down to 800m in the water column close to the Irish shelf edge (Figure B.2a) and dilutes westwards, thus resembling observations in this region (Holliday et al., 2015). This core is seen in the FSC close to the Scottish shelf edge extending down to 400m (Figure B.2b). Observation suggest that the saline Atlantic core is present much closer to the Scottish (Shetland) side of the FSC extending from the surface down to 300 m (Berx et al., 2013). The shoaling of saline core from the Rockall Trough to the FSC indicates that the inflow is guided by topography and geostrophically forced. In the model, the continuity of this saline core into the North Sea is first revealed at a zonal section between Scotland and Norway where high salinity water extends till the western edge of the Norwegian Trench (Figure B.2c). Here, the most saline Atlantic water enters through the central parts of this section and fresh water leaves through the Norwegian Trench.

The analysis of subsurface velocity field shows that the two branches of NAC, the Iceland and Rockall Trough branch, extend deeper down in the water column in the Iceland basin and shallower in the Rockall Trough respectively (Figure B.3a). As noted earlier, the Rockall Trough branch is more sluggish than the Iceland branch in this model simulation. The intensification of Rockall Trough branch is also revealed when it enters the FSC (Figure B.3b). The maximum along channel velocities ($>$ 10 cm/s) in the FSC are present in the top 200 meters and are seen towards the middle of the channel while observations (1995-2009 mean) suggest maximum along channel velocities ($>$ 20cm/s) to be present more towards the Scottish shelf edge (Berx et al., 2013). A part of the inflow in the FSC branches off into the North Sea and is seen in Figure B.3c as a depth independent broad inflow. On this North Sea section, the inflow has its highest intensity west of the western Norwegian Trench (between 300-400 km, east of Scottish east coast). The Norwegian Trench shows outflow waters from surface down to the bottom. The model gives an outflow on the shallower western parts of the

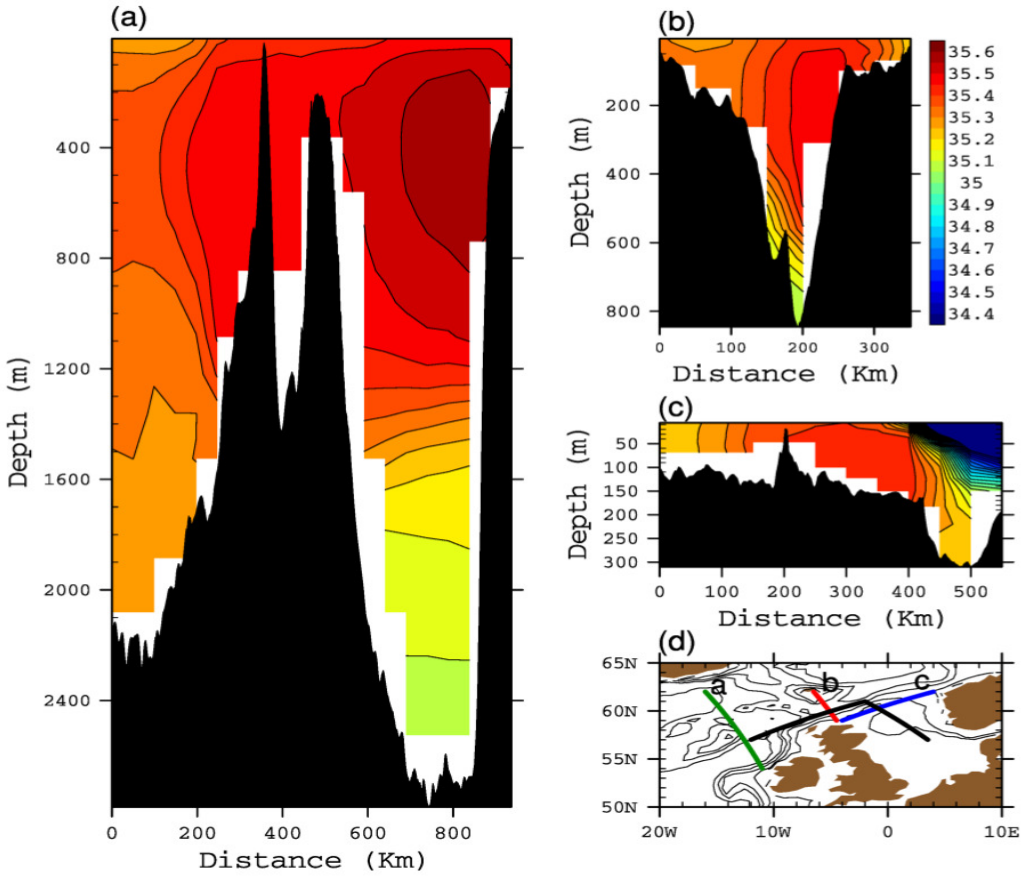

Figure B.2: Salinity [psu] on a section across (a) Rockall Trough, (b) FSC and at (c) North Sea entrance. (d) The location of the various sections used in this study. Green: Rockall Trough, Red: FSC and Blue: North Sea entrance. The bold black line from Rockall Trough to central North Sea represents the section on which Figure B.7 is based. The thin black lines in Figure B.2d are the 100, 200, 1000 and 2000 meter isobaths.

Norwegian Trench where an inflow is know to be present. The long term (1850-2005) mean volume transport through the FSC in in this model is 5.5 Sv which is higher than the observed short term estimates of 3.5 to 4 Sv (Berx et al., 2013). The total northern inflow into the North Sea is about 1.6 Sv which is close to known estimates of 1.7 to 2 Sv (Hjøllo et al., 2009). This suggests that while challenges remain, the model is in overall agreement with respect to the location and intensity of various inflows.

The continuity of the saline core of Atlantic water into the Rockall Trough and FSC, and finally into the North Sea raises questions about the source of high salinity in the model. That the saline core moves close to the shelf edge points to the region south of Rockall Trough as a potential source region and the ESC as the conduit. A property-property diagram of a region south of Rockall Trough and west of Bay of Biscay is shown in Figure B.4. This region is selected as it sits in the intergyre region between the SPG and the subtropical gyre. Two salinity maxima are seen in the Temperature-Salinity (T-S) diagram, a shallower one at about 360m and the deeper one at about 900m. The upper salinity maximum has salinity exceeding 35.70 psu, the highest at these latitudes and therefore, this highly saline water is considered

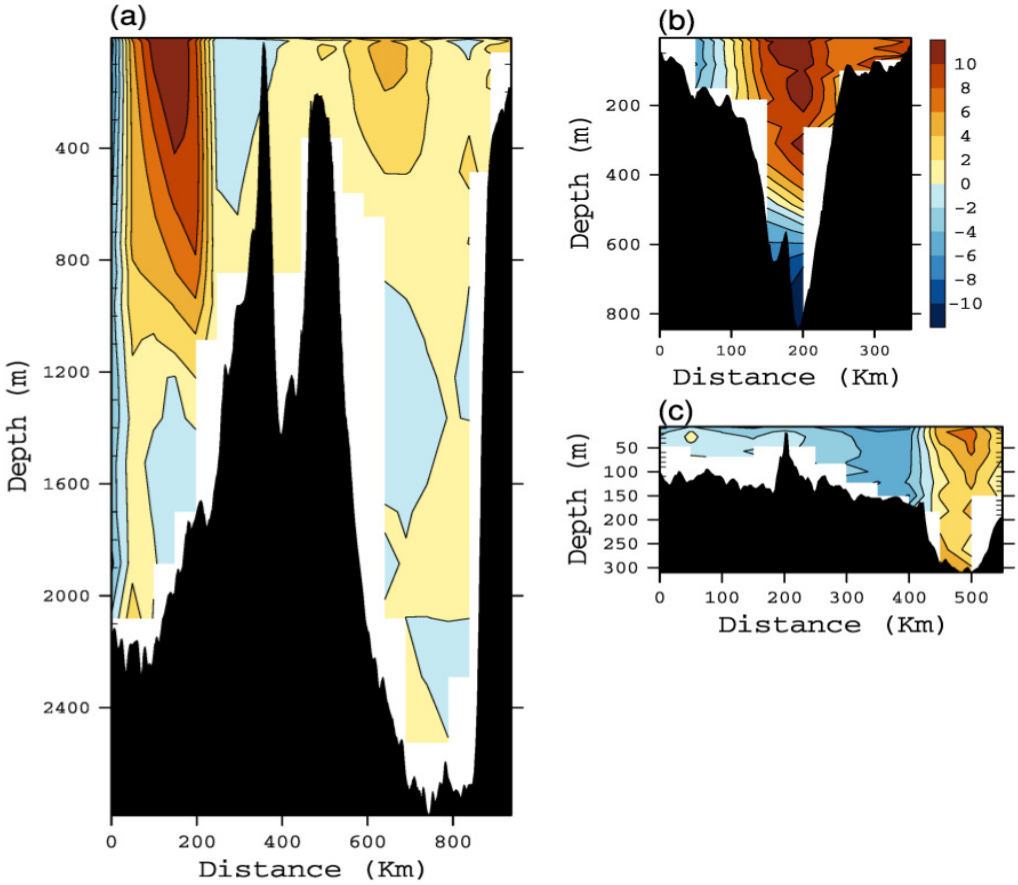

Figure B.3: Velocity (cm/s) perpendicular to a section across (a) Rockall Trough, (b) FSC and at (c) North Sea entrance. For Rockall Trough and FSC, u-component of the velocity is shown, and for North Sea, v-component is shown.

here as the model equivalent of ENAW. The deeper salinity maximum ($\sigma_0 = 27.3$), with a corresponding oxygen minimum, is a vestige of MOW as seen in another T-S analysis south of 40°N (figure not shown), which is also known to propagate northwards (Lozier & Stewart, 2008; Sarafanov et al., 2008). Further analysis shows that both salinity maxima merge north of 50°N and enter the Rockall Trough as a single saline core. The salinity of this modelled saline core diminishes downstream as it mixes with ambient water masses of subpolar origin.

In summary, MPI-ESM1.2-LR reproduces surface and subsurface salinity, circulation and inflow characteristics in the eastern North Atlantic and the North Sea. Challenges remain, however, near the shallower southern and eastern parts of the North Sea. Nevertheless, we only focus on the northern parts of the North Sea and the eastern North Atlantic, where the model is able to reproduce major currents and the associated spreading of North Atlantic water masses. In subsequent sections, we analyze how the variability in the northward penetration of the saline core of Atlantic inflow depends on SPG strength.

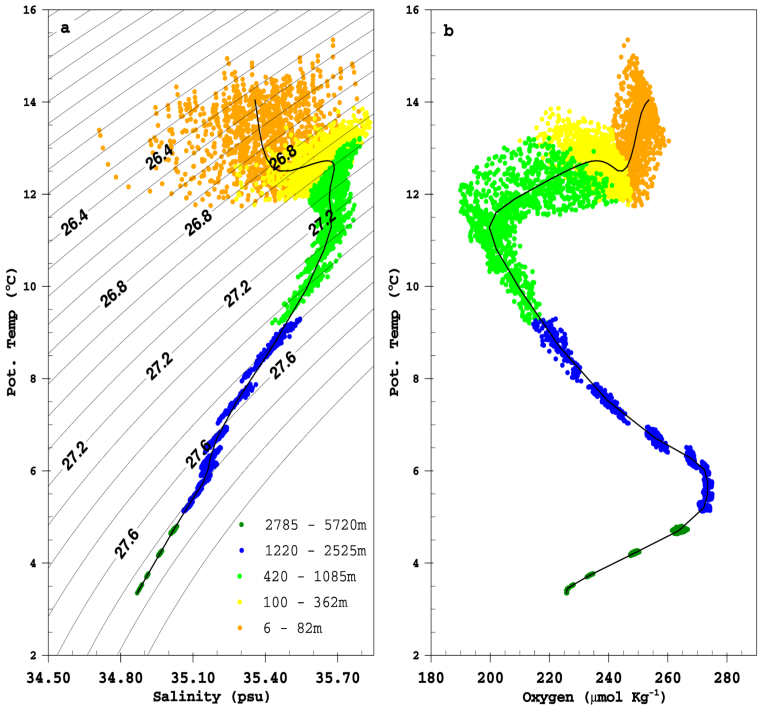

Figure B.4: (a) Temperature-Salinity and (b) Temperature-Oxygen diagram for the region south of Rockall Trough and west of Bay of Biscay (12-20°W, 42-50°N). In the left panel, a salinity maximum is seen at depths shallower than 500m; this is the model equivalent of the highly saline ENAW.

B.3 RESULTS

B.3.1 *The SPG Strength and Salinity Variations in Eastern North Atlantic*

The SPG circulation is coupled to atmospheric variability and the overturning circulation. The dynamical changes in the SPG are captured by the leading mode of SSH variability in the North Atlantic which explains 20 percent of total variance in this simulation (Figure B.5a), and resembles to some extent the well known dipole pattern seen in both observations (Häkkinen & Rhines, 2004) and simulation with a general circulation model (Zhang, 2008). A large part of the variability associated with this pattern is present along the Gulf Stream (GS)/NAC region while some part of the variability is also seen in the southeastern periphery and the SPG center with a tendency opposite to that of the GS/NAC region. Note that the weights in the GS/NAC region are stronger than those presented in earlier studies (Häkkinen & Rhines, 2004; Zhang, 2008). Further analysis reveals that in this model simulation, the southern boundary of the SPG undergoes profound meridional shifts in the Newfoundland basin, which are captured by this leading mode, and thus strong weighting is present along the GS/NAC path.

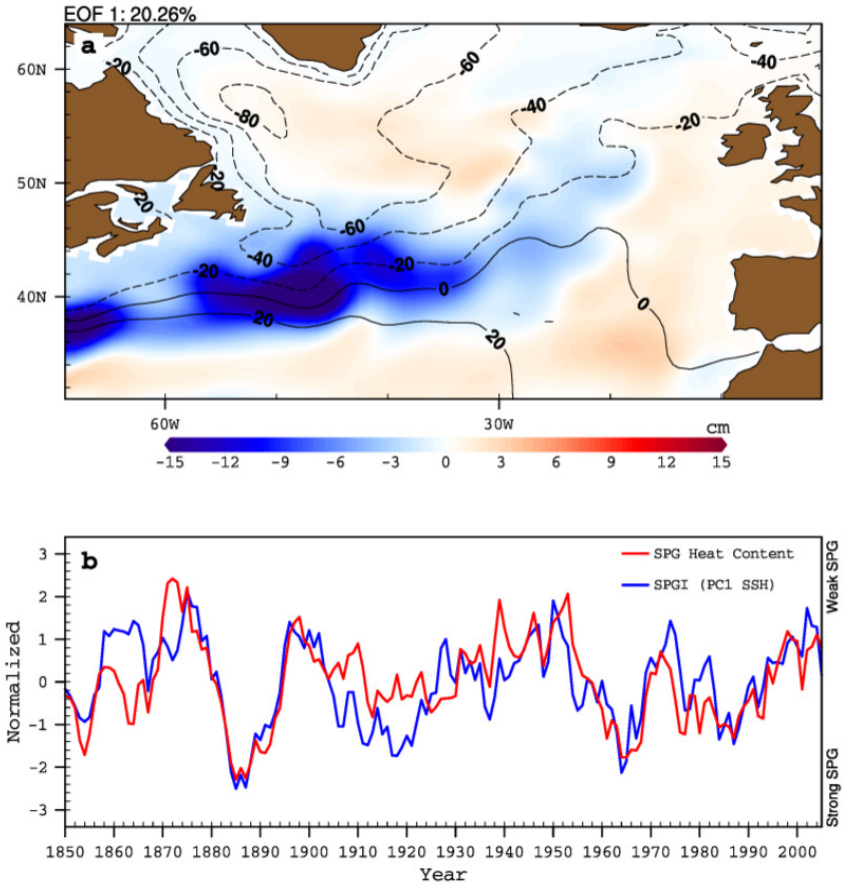

Figure B.5: (a) The pattern of the first empirical orthogonal function of the SSH anomalies in the North Atlantic. Overlayed black lines are the mean SSH contours. (b) Time series (normalized) of the subpolar gyre (SPG) heat content of top 700m and the SPGI. The heat content is averaged over the domain:(10-60°W, 50-62°N)

The evolution of the SPG strength in MPI-ESM1.2-LR (Figure B.5b) is consistent with the present understanding of evolution of heat and currents in the subpolar North Atlantic. The reduction of upper SPG heat content (densification) and the lowering of SSH at the gyre center both indicate a strengthening gyre and vice versa (Häkkinen & Rhines, 2004). That the temporal evolution of the leading mode of the SSH variability in the North Atlantic (0-70°W, 30-65°N) in our model simulation is robust is further confirmed by the high correlation between the SPGI and upper ocean heat content of the SPG (10-60°W, 50-62°N) (Table 1).

Table B.1: Pearson's correlation coefficients (r) among various variables, the lag at which r is maximum (Lag), the estimated degree of freedom (df) and the associated p-value (p) based on two tailed t-test. Median value of the block bootstrapped Pearson's correlation coefficients (r*) and the lag at which r* is maximum (Lag*). The numbers in square brackets give the uncertainty range. Uncertainty in lag is estimated only for those variables which are statistically significantly correlated (bold).

		Unfiltered						10-yr Low Pass
Var1	Var2	Lag	df	r	p	Lag*	r*	r*
SPGI	SPG Heat Content	0	48	0.71	0.000001	0 [0, 1]	**0.71** [0.53, 0.83]	**0.74** [0.51, 0.87]
	FSC inflow	0	63	0.12	0.3489		0.13 [-0.07, 0.36]	0.26 [-0.08, 0.58]
	FSC Saline inflow	1	27	0.66	0.0002	0 [0, 2]	**0.64** [0.47, 0.77]	**0.82** [0.66, 0.91]
	NS inflow	2	116	0.21	0.0236		0.16 [-0.02, 0.35]	0.33 [-0.07, 0.61]
	NS Saline inflow	2	48	0.45	0.00133	0 [0, 4]	**0.37** [0.11, 0.57]	**0.65** [0.35, 0.88]
	RT Salinity	1	40	0.37	0.0187	0 [0, 2]	**0.35** [0.12, 0.55]	**0.49** [0.22, 0.71]
	FSC Salinity	1	37	0.53	0.0007	0 [0, 2]	**0.51** [0.34, 0.66]	**0.71** [0.52, 0.83]
	NS Salinity	3	56	0.42	0.0013	2 [0, 5]	**0.28** [0.08, 0.46]	**0.47** [0.16, 0.73]
NS inflow	NS Salinity	0	111	0.34	0.0003	0 [0, 2]	**0.34** [0.20, 0.46]	**0.37** [0.09, 0.60]
RT Salinity	FSC Salinity	1	48	0.49	0.0004	0 [0, 2]	**0.43** [0.23, 0.60]	**0.64** [0.46, 0.77]
	NS Salinity	1	66	0.49	0.00003	1 [0, 3]	**0.39** [0.19, 0.54]	**0.61** [0.34, 0.77]
FSC Salinity	NS Salinity	1	53	0.39	0.0039	1 [0, 3]	**0.34** [0.13, 0.53]	**0.54** [0.32, 0.72]

To test the relationship between the SPGI and salinity in the eastern North Atlantic, we perform a composite analysis of top 500m average salinity for strong and weak SPG states (Figure B.6). The freshening in the Iceland Basin and Rockall Trough is concomitant with a strengthening SPG which facilitates the eastward extension of fresh subpolar water masses (Figure B.6a). On the other hand, the westward retreat of fresh upper layer concomitant with a weakening SPG circulation allows subtropical waters to dominate this region and propagate far northward across the ISR (Figure B.6b). The changes in the subpolar gyre structure, however subtle, become clearer when the isolines of SSH are compared (contour lines in Figure B.6a and B.6b). The westward retreat of isolines of SSH in the eastern North Atlantic signifies a contracted SPG. This limits the eastward extension of subpolar water masses which would otherwise counter the influence of subtropical water masses (Hátún et al., 2005; Bersch et al., 2007). Therefore, the Rockall Trough, FSC and northern North Sea all have a saline upper layer regime when the SPG is weak, and the SPGI captures this connection. From the North Sea perspective, the SPGI thus represents the temporal evolution of large scale oceanic variability upstream of the ISR, the impact of which is investigated further.

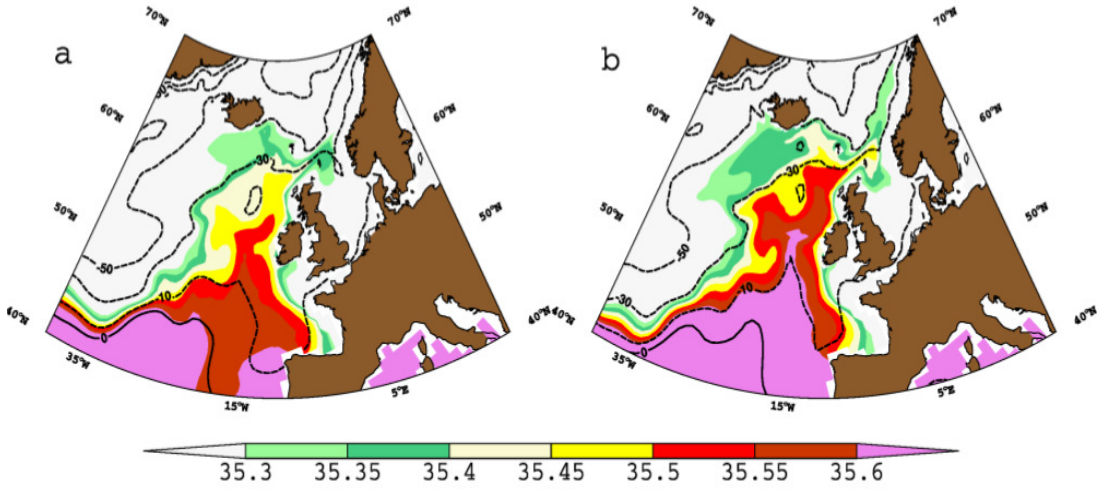

Figure B.6: Composites of the top 485m salinity ([psu], color) and SSH ([cm], contours) in the North Atlantic. Composites of (a) strong SPG and (b) weak SPG, are based on ± 1 standard deviation of SPGI.

The composite analysis of the relation between the SPGI and the upper layer salinity in the region of interest does not provide information regarding consistency in time. To this extent, we show propagation of upper layer salinity along a section (black line in Figure B.2d) from northern Rockall Trough to central North Sea through the FSC (Figure B.7a). The simulation shows periods of saline and low saline influence on this section. The recurring high salinity pulses and their persistence for five to ten years in some cases indicates the presence of a low frequency driving mechanism likely of Atlantic origin. The slope (about one year of propagation time from Rockall Trough to northern North Sea) of these pulses also indicates that they originate south of the ISR (Figure B.7b). This is consistent with the observational study of Glessmer et al. (2014) who showed that in recent decades freshwater anomalies in the Nordic

Sea originated south of ISR, while the role of freshwater anomalies from the Arctic was not substantial. To check if the salinity anomalies on this section are a result of concomitant changes in the local flow field, we look at current speed anomalies on the same section (Figure B.7c). This figure depicts that as compared to salinity anomalies, current speed anomalies vary at a much faster rate. Except during the period 1880-1890, there is no other indication of co-variance between salinity and current speed anomalies. This implies that salinity anomalies have to be tracked upstream to find their generation mechanism.

Salinity (top 100m) in the FSC and northern North Sea largely follows variability in Rockall Trough salinity (Figure B.8a). The correlation coefficients increase when the data is filtered with a 10-year low pass filter (Table 1). The correlations and the time series themselves suggests that it is the decadal to multidecadal variability that is pronounced. On interannual timescale, there are few instances of incoherent deviations, particulaly after mid 1990s. The correlation between unfiltered Rockall Trough and northern North Sea salinity (r= 0.49, at lag 1-year with Rockall Trough leading, also see Table B1) is higher than between FSC and North Sea (r= 0.39, at lag 1-year with FSC leading). This is consistent with observations-based study of Núñez-Riboni & Akimova (2017) who also found a lag of 1-year in salinity anomalies from Rockall Trough to northern North Sea. This implies a close coupling between Rockall Trough and North Sea in the model, which is also suggested by earlier observations (Holliday & Reid, 2001). In the FSC, water masses are transformed due to additional influence of water masses from Faroe Current, and mixing with fresh intermediate waters offshore of Scotland (Turrell et al., 2003). These water mass transformation processes would account for the reduced correlations with the North Sea salinity if these induce distinct modes of variability. Otherwise, atmospheric variability (FSC is shallower than Rockall Trough) could be the cause of reduced correlations between FSC and the North Sea.

A spatial picture of regional co-variance between Rockall Trough salinity and the NWES is illustrated in Figure B.8b,c. At lag 0-year, maximum correlations are limited to the south of ISR. At lag 1-year, maximum correlations are seen along the shelf edge of the NWES. Also, the positive correlations in the North Sea move southward and eastward at lag 1-year. Thus these spatial correlation patterns confirm the advective pathway of Atlantic water from the Rockall Trough to the northern North Sea in this global model (Fig B.1a).

B.3.2 *Hydrographic and Transport Variability*

Having illustrated an influence of SPG strength on northward penetration of subtropical waters, we now focus on the subsurface variability in the key regions and its connection with volume transport variability. In the Rockall Trough, the intermediate layer (1200m-2000m) appears to be out of phase with the upper ocean in its response to the change in the SPG state (Figure B.9a). At these depths LSW is present (cyclonic recirculation at 1200-1600m in Figure B.3a). And it is known from observations that in the eastern North Atlantic, LSW salinity is out of phase with the upper layers because here it evolves at a much slower rate due to long transit times involved in its transport from the Labrador Sea (Bersch et al., 2007). The sill depth of ISR near FSC is about 500m, therefore, we expect only the top 500-700m of the water column to allow for

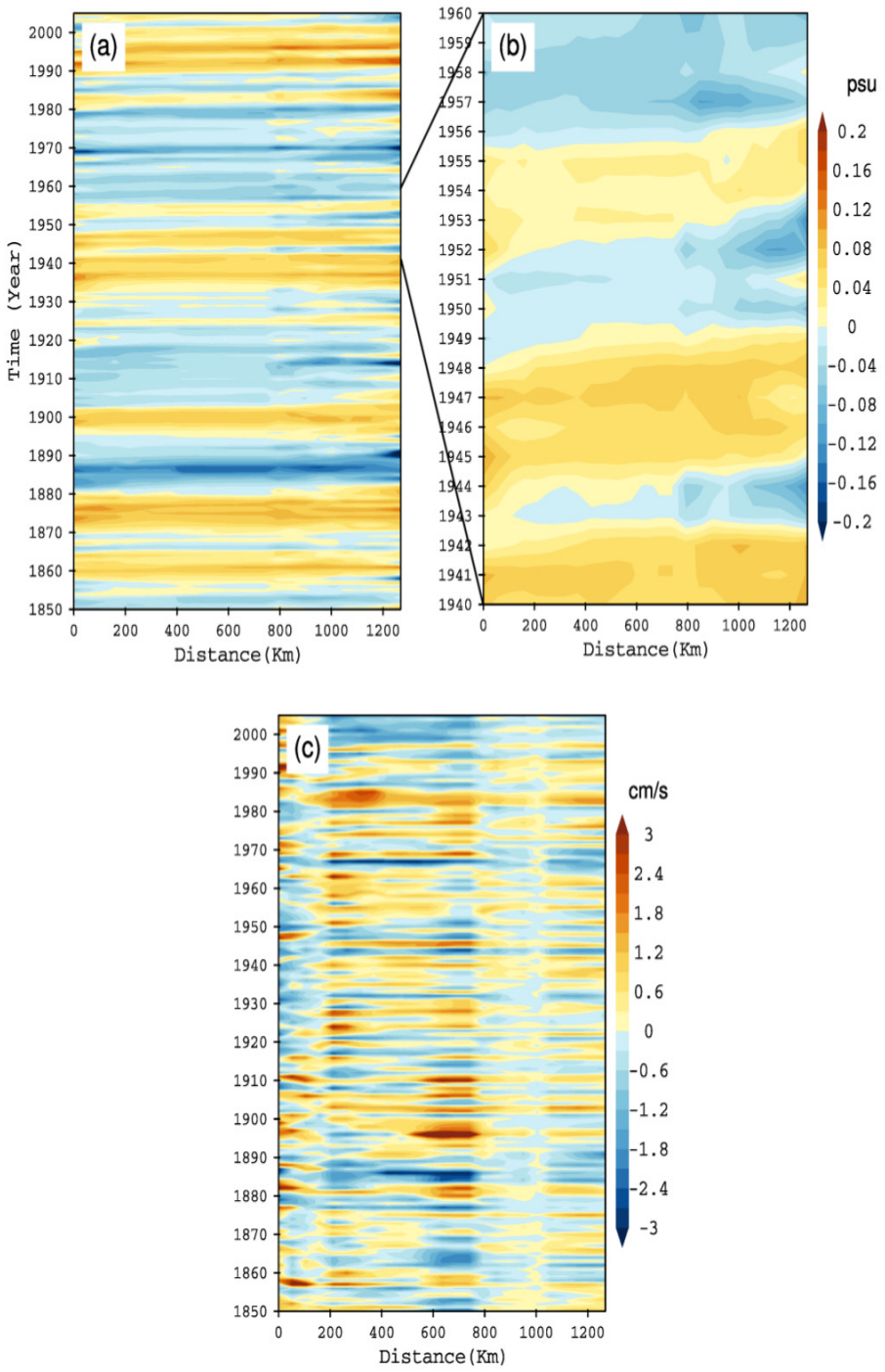

Figure B.7: Hovmöller diagram for top 100m average (a) salinity [psu] and (b) current speed [cm/sec] anomalies along the section from Rockall Trough (0 Km) to the central North Sea shown in Figure B.2d (complete black line). Points on the section shallower than 100m are averaged down to bottom.

northward propagation of salinity anomalies associated with the SPG. Concomitant with a weakening SPG, most of the salinification is seen above 500 m and is most likely the result of higher amounts of modelled ENAW.

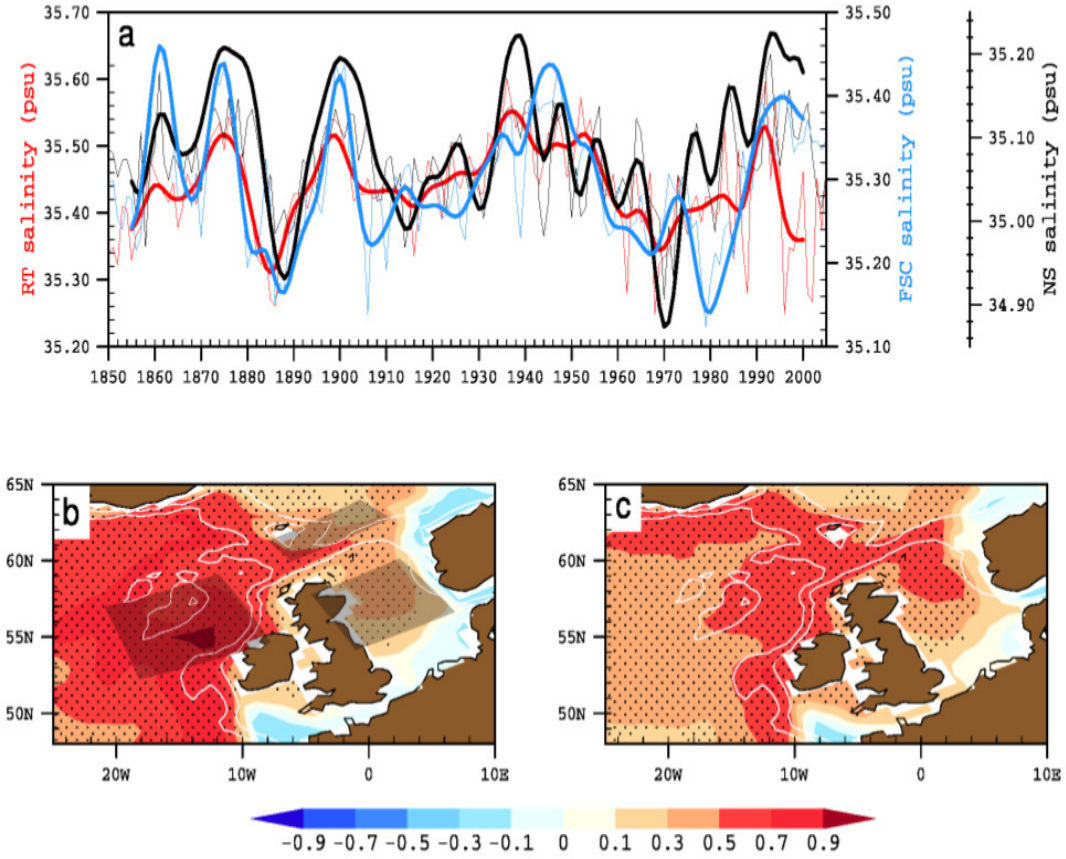

Figure B.8: (a) Time series of top 100m average salinity [psu] in the Rockall Trough, FSC and northern North Sea. (b) Correlation between the Rockall Trough salinity time series and top 100m average salinity at each grid point at lag 0-year. The shaded regions show the respective areas over which the salinity is averaged to get the time series shown in Figure B.8a. (c) Same as Figure B.8b but at lag 1-year. The striplings in Figure B.8b and Figure B.8c represent statistically significant values at 95 percent confidence level. The thin white lines in Figure B.8b and Figure B.8c are the 200 and 1000 meter isobaths.

In the FSC salinity increase is seen throughout the water column with highest amplitudes in the inflow layers (Figure B.9b, also see Figure B.3b for inflow layers). As these composites are based on annual means, the salinity increase in the deep layers which mainly have southward moving dense overflow is very likely due to mixing. The reason being that when the inflowing high salinity water recirculates in this region and strong winter cooling deepens the mixed layer, the surface salinity signal can reach deeper layers. A part of Atlantic inflow through the FSC flows into the North Sea, so this salinity increase is also expected in the northern North Sea. The salinity increase is indeed seen in the northern and central North Sea while the southern and eastern parts have an opposite tendency (Figure B.9c,d). The southern and eastern parts of the North Sea are dominated by inflows from the English Channel and Baltic Sea in the upper layers, and hence do not reflect the connection with the SPG.

Now we assess changes in water mass characteristics into the Rockall Trough, the FSC and and North Sea in relation to the SPG strength. Water mass definitions based

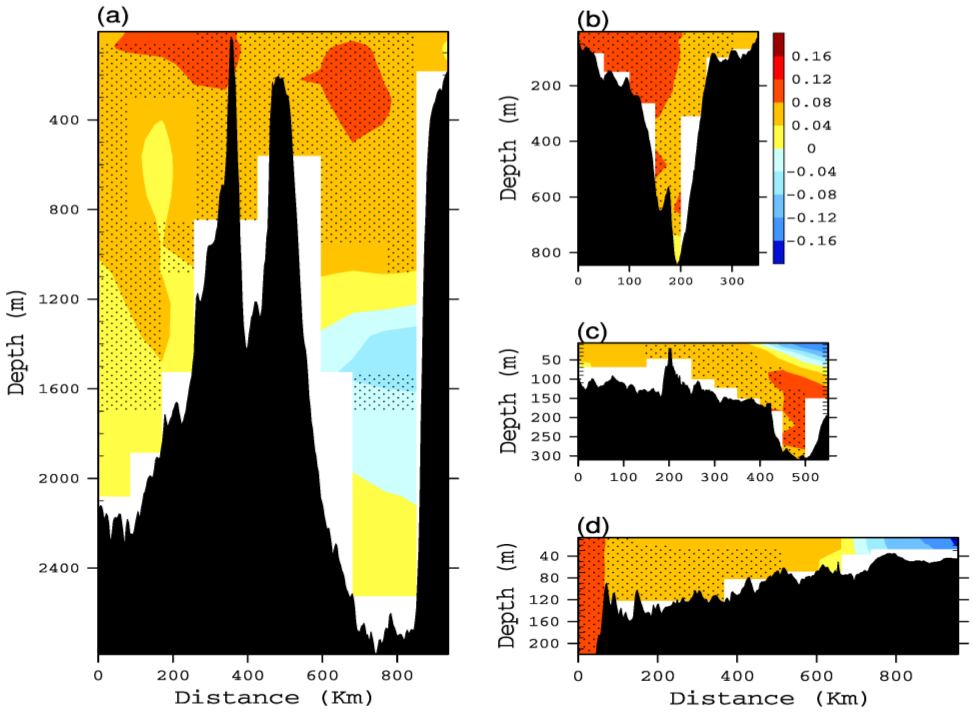

Figure B.9: Composite difference (weak-strong SPG) of salinity [psu] for the section across (a) Rockall Trough, (b) FSC, at the (c) North Sea entrance and through (d) center of North Sea (part of the black line in Figure B.2d from the shelf edge to the central North Sea). Location of all sections is shown in Figure B.2d. The striplings represent statistically significant values at 95 percent confidence level.

on observations cannot be used due to model biases and errors, hence we first assess changes in the volume in T-S space (Figure B.10). In line with results presented earlier, Rockall Trough has a large volume of warm saline water in the upper layers when the SPG is weak and vice versa (Figure B.10a). This also points to the origin of respective water masses: volume changes are mostly concentrated either in the warm-saline part in the T-S space indicating a subtropical origin or in the cold-fresh part indicating a subpolar origin. In the FSC, volume changes occur over a wide range of temperature and salinity (Figure B.10b). Moreover, high amplitudes of SPG related temperature changes are mainly limited to the layers with T$>$ 9.5 °C while salinity increase covers the entire channel. As for the northern North Sea, this region is much shallower compared to the other two regions and hence seasonal heating and winds obscure the SPG signal here. Nevertheless, Figure B.10c does indicate a tendency of North Sea property changes to follow those of Rockall Trough and FSC. Here again, salinity differences are more pronounced than corresponding temperature differences.

The volumetric water mass analysis illustrates an important aspect of subsurface fingerprint of SPG circulation variability. For example, in the northern North Sea we see that only a part of the water column is impacted coherently, and rather than temperature, most of the information about forcing history is in salinity. This now allows us to define a water mass and to quantify changes in its volume transport through the FSC and northern North Sea (Figure B.11). We define the "total" inflow as the volume transport of all northward flowing water into the FSC and all southward flowing water into the North Sea. The "saline" inflow refers to that part of total volume

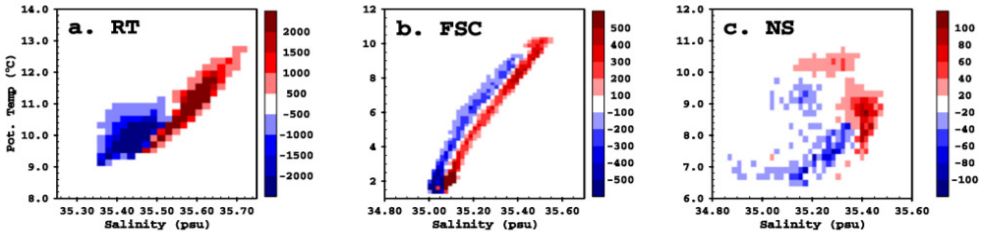

Figure B.10: Composite difference (weak-strong SPG) of top 960m water volume [km^3] for (a) Rockall Trough, (b) FSC and (c) Northern North Sea. For FSC and northern North Sea, depth is down to bottom. The respective regions are shown in Figure B.8b.

transport with salinity greater than a certain threshold (35.40 psu for FSC and 35.30 psu for North Sea) which marks the approximate boundary of volume changes (Figure B.11). The total volume transport into both FSC and North Sea is not significantly correlated with the SPGI (Table B1), and is marked by strong interannual variability. On the other hand, the saline inflow through FSC and North Sea is significantly correlated with SPGI (r= 0.64 and 0.37 respectively). For the North Sea, the change in correlation when only high salinity (> 35.30 psu) water is considered is not large, but nevertheless significant. Note that the "total" and "saline" inflow through North Sea have a coefficient of determination (r^2) of about 45 percent, suggesting that for the North Sea, large part of inflow has high frequency variability. There is a one year lag between the SPGI and FSC saline inflow, and a two year lag with the North Sea saline inflow. The uncertainty associated with the lag identified between the SPGI and North Sea Saline inflow suggests that it is within four years that the impact of changes in SPG circulation is identified the North Sea. This includes the one year propagation time of salinity anomalies from the Rockall Trough to the North Sea.

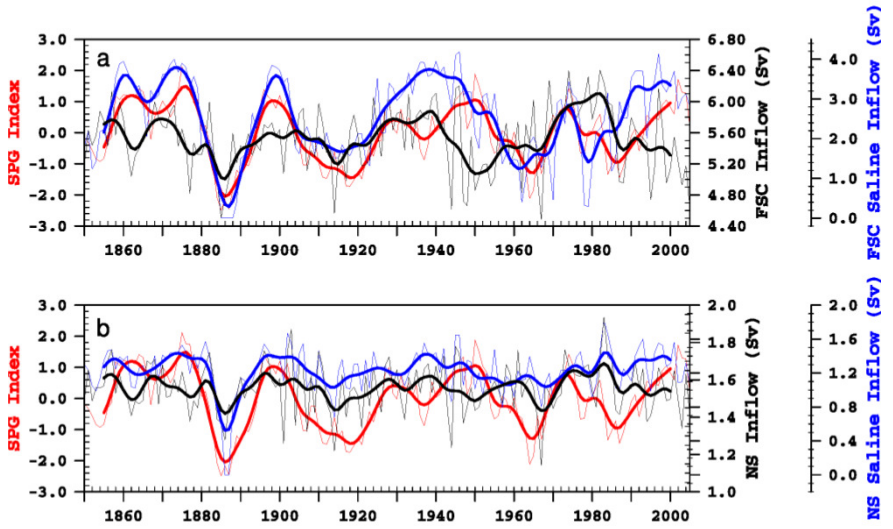

Figure B.11: Time series of SPG index and volume transports into (a) FSC and (b) North Sea. The total volume transport (inflow) comprises all water masses with northward velocities into the FSC (across yellow line in Figure B.2d) and southward into the North Sea (approx. across blue line in Figure B.2d). The "saline" volume transport (Saline inflow) is that part of total inflow with salinity > 35.40 psu for the FSC and salinity > 35.30 psu for the North Sea.

The coherence of SPGI with the FSC Saline inflow peaks at period longer than 20 years (Figure B.12a), and with the North Sea Saline inflow the statistically significant period is between 30-40 years (Figure B.12b). Thus, in this model simulation, it is the decadal to multidecadal variability in the SPG circulation which influences the saline inflow into these two regions. Also, the relatively high correlation between SPGI and North Sea salinity as compared to the correlation between North Sea total inflow and North Sea salinity at decadal timescales and beyond (Table B1) suggests that at least at these timescales, the salinity in North Sea follows SPG variability rather than local acceleration of inflow.

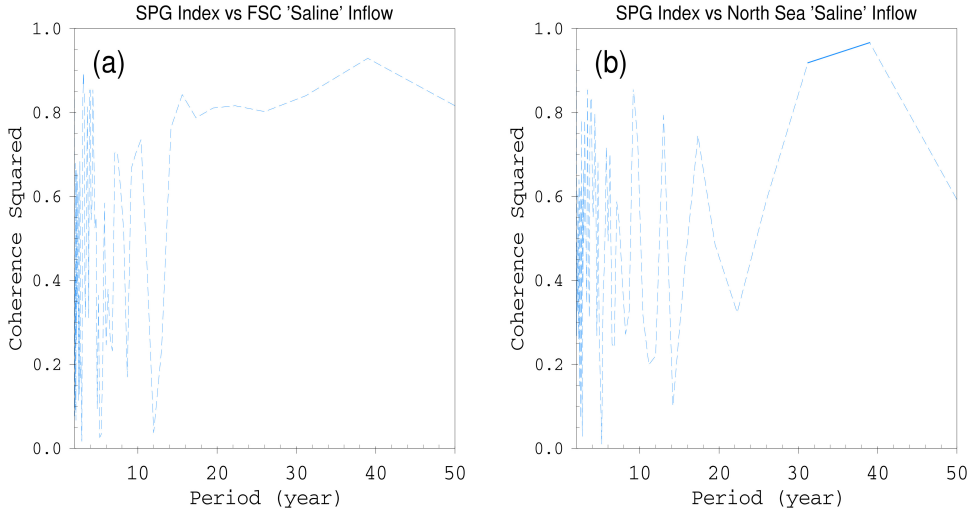

Figure B.12: Square of the spectral coherence between SPGI and (a) FSC Saline inflow and (b) NS Saline inflow. Statistically significant values at 95 percent confidence level are represented by bold solid line.

B.3.3 *Role of Atmospheric Variability*

While we have illustrated that part of the inflow into the FSC and North Sea is influenced by the SPG circulation, a detailed analysis of total FSC and North Sea inflow hints at the role of local atmospheric forcing. Figure B.13 illustrates that the total North Sea inflow is linked to the winds. Periods of strong Atlantic inflow to the North Sea are concomitant with periods of strong southwesterly wind flow. The mean sea level pressure pattern associated with a strong North Sea inflow results in southwesterly winds which pile water onto the shelf through a strong Ekman transport. Similar analysis of relationship between North Sea saline inflow and atmospheric variability shows similar pressure and wind pattern but with lower amplitudes (figure not shown). This suggests that part of the variability in saline inflow not explained by SPGI is explained by atmospheric variability. For the FSC, however, low amplitudes of the pressure pattern in Figure B.13a suggest that the mechanisms driving the total FSC inflow are not entirely wind related (see for example Sandø et al. (2012)).

The impact of large scale atmospheric variability on the NWES is now investigated through a regression analysis (Figure B.14). The large scale atmospheric patterns

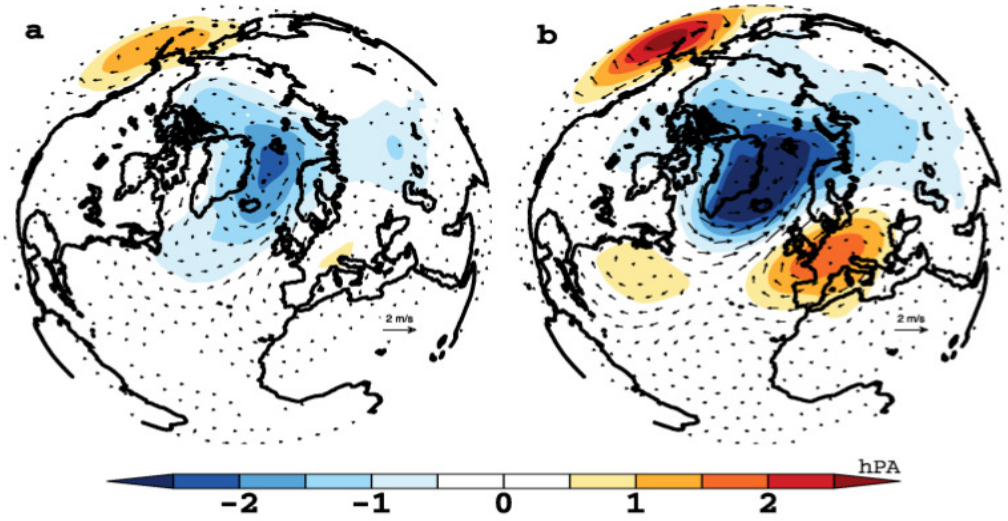

Figure B.13: Composite difference of mean sea level pressure ([hPa], color) and 10-meter winds ([m/s], arrows) for total (a) strong-weak FSC inflow and (b) strong-weak North Sea inflow.

in the North Atlantic in this simulation resemble the NAO (Figure B.14a) and the East Atlantic Pattern (EAP) (Figure B.14b). Over the NWES region, positive NAO is associated with westerly winds (Figure B.14c). Consistent with earlier analysis, westerly winds lead to an increased inflow of Atlantic water across the shelf break, and thus SSH increases in the North Sea (positive regression co-efficients), particularly the southern part. That the fresh Baltic outflow into the North Sea is also restricted due to westerly winds is confirmed by the strong salinification in the Baltic outflow region and along the Norwegian Trench. Thus, a positive NAO leads to an increase in salinity in the North Sea (Figure B.14e) with no lag involved. On the other hand, the atmospheric wind pattern associated with the EAP is such that it has no significant impact on either the Atlantic inflow or the fresh Baltic outflow. As a consequence, there is no significant impact of EAP on salinity in the northern North Sea (Figure B.14f).

As the direct influence of the NAO on North Sea salinity is through the atmospheric winds, the NAO mainly explains short term (interannual) variability in the North Sea salinity time series. This is illustrated through comparison of reconstructed North Sea salinity time series using SPGI and NAO as predictors (Figure B.14g). The regression co-efficients are estimated from the time period 1853-1950 and thereafter the same regression coefficients are used to reconstruct North Sea salinity for the time period 1951-2005 (see section 2.2 on methods). Quite clearly, short term variations in North Sea salinity are captured by that regression model which includes NAO as one of the predictors. On the other hand, long term (decadal to multi-decadal) variations are largely explained by the regression model based on SPGI alone (SPGI leads North Sea salinity by 3 years, see Table B1) which confirms the impact of oceanic variability associated with the SPG circulation on long term variations in North Sea salinity.

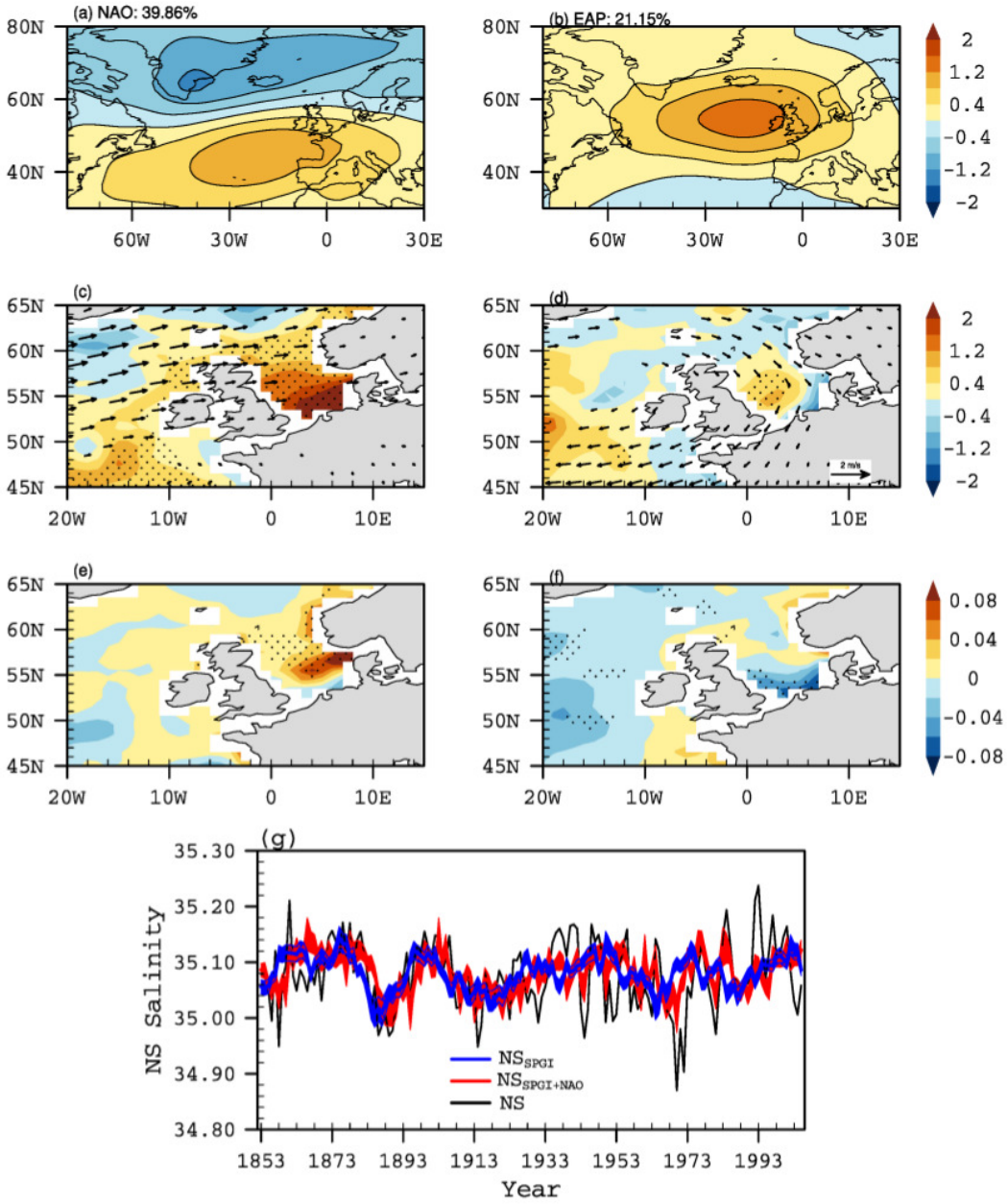

Figure B.14: Modes of variabililty of MSLP: (a) EOF1 (NAO) and (b) EOF2 (EAP). Regression of 10-meter winds (m/s, arrows) and SSH (cm, contours) on normalized (c) NAO (PC1 of MSLP), (d) EAP (PC2 MSLP) index. Regression of salinity (psu) on normalized (e) NAO and (f) EAP index. Only statistically significant regression coefficients are shown (for winds) and stippled (for filled contours). (g) Time series of North Sea salinity (black line), reconstructed NS salinity from regression coefficients based on SPGI (blue line), and NAO and SPGI combined (red line). The thickness of blue and red lines denotes the 95 percent confidence bounds.

B.4 DISCUSSION

We began with the following question: what part of the variability in the North Sea is of Atlantic origin? This question could not have been investigated using a regional model because regional models of the North Sea tend to discount open-ocean signals at their boundaries. This is due to the issues associated with specifying lateral open

boundary conditions. Therefore, the nature of the question at hand and the focus on decadal to multidecadal timescales facilitates the usage of a global model.

The inflowing Atlantic water properties and its transport play a critical role in North Sea variability at timescales longer than those dominated by internal North Sea processes. This remote oceanic control on North Sea was already suggested by Holt et al. (2012) who showed that lateral transport of Atlantic water deficient in nutrient content is an important constraint on primary production. Such realization, therefore, opens up the scope for global models to be used for studying open ocean influence on North Sea via advection of anomalies of remote oceanic origin. However, along with the important prerequisite of being able to resolve broader North Sea circulation characteristics satisfactorily, such analysis using global models would have to be limited to timescales longer than flushing time ($>$ 1 year) of the North Sea.

In this study, using a century long simulation with a global model, we showed that large scale open-ocean circulation has an impact on North Sea inflow. However, there are some caveats that must be considered while interpreting these results. First, we have not assessed the impact of local processes on water mass properties from the Rockall Trough to the North Sea. Second, we have also not looked into the role of changes in the source water mass properties in the North Atlantic, for example in the Labrador Sea or in the vicinity of Bay of Biscay. This analysis also excludes the shallower southern parts of the North Sea where local processes internal to the North Sea are dominant. In these parts of the North Sea, river runoff and tidal mixing dominate. Also, our results are derived from a single model, it would be interesting to examine if other global coupled models show similar SPG-North Sea connections.

Coming back to the results presented in this study, we note that several processes might act together or individually lead to increased salinity levels in the North Sea. These are: a) increased volume transport of Atlantic water, b) increased salinity of the Atlantic water and c) imbalance in the large scale evaporation minus precipitation (E-P) field. As the focus of the present study is on those regions of the North Sea which are away from the coast, river runoff can be excluded as a potential cause. As far as the role of large scale E-P field is concerned, the advective delays from the Rockall Trough rule out that possibility as well. This is because changes in the large scale E-P field would lead to concurrent changes in the surface salinity in the Rockall Trough, FSC and North Sea, which we do not find in our analysis. The large scale E-P field can however enhance or suppress the open ocean signal.

In the present analysis, we identify periods of elevated salinity levels in the Rockall Trough, FSC and the northern North Sea in our simulation, and we show that the recurring high saline periods in these regions are due to the increase in salinity of the Atlantic inflow and not due to the acceleration of the inflow. Although inter annual variability in salinity in the NWES region has often been linked to variability in volume transport (Ellett & Turrell, 1992; Sundby & Drinkwater, 2007; Hjøllo et al., 2009), the persistence of salinity anomalies for multiple years and their recurrence is difficult to explain through changes in volume transport only. One such example is the gradual increase and persistence of high salinity for more than three years in the late 1950s in the NWES which was studied by Dickson (1971). Since his analysis had allowed him to neglect the role of E-P field and river runoff, he had to either show that the volume transport for those years was also increasing from year to year and/or that the source water masses recruited in the inflow stream had a more

southern origin than normal. A persistent pressure anomaly pattern and the resulting air-sea feedback processes were thus conjectured as the mechanism that allowed sustained advective interventions in the eastern North Atlantic which then resulted in increased "southernliness" of the water masses entering the inflow stream to the NWES. However, given observational constraints, it was not still clear if the increased salinity was also due to actual acceleration of the inflow.

The question then arises, why are there periods of high salinity anomalies in the absence of high volume transport anomalies in this simulation? The mechanism identified as the cause of recurring and persistent salinification is the quasi-periodic variability in SPG strength. The "southerliness" of the source water masses is found to be due to higher throughput of subtropical water during those periods when the SPG is weak. Thus, water masses of subtropical origin entering the Atlantic inflow dominate those of subpolar origin which would then lead to elevated salinity levels. Becker et al. (1997) also found peak spectral power between 15 to 20 years in long term temperature and salinity time series of various regions in the NWES. They attributed those spectral peaks to "long-period fluctuations in the North Atlantic circulation system". They speculated that a varying interaction between the SPG and subtropical gyre could lead to elevated salinity levels in the NWES. In the present study, we find that "long-period fluctuations in the North Atlantic circulation system" of 30 to 40 year period are closely related to the strength in the SPG circulation.

Another important aspect of our results is related to the interpretation of the EOF1 mode. The EOF1 mode presented by Häkkinen & Rhines (2004) was based on a short altimeter record and hence does not capture decadal to multi decadal variability associated with the NAC/GS position. Strong weights in the NAC/GS region in the present simulation indicate that meridional shifts in the NAC/GS position lead to heat content changes in the SPG which then spins up/spins down the SPG circulation (see for example Zhang (2008)), and the concomitant reorganization of major current pathways (i.e. expansion and contraction of SPG circulation) in the eastern North Atlantic leads to salinity changes in the NWES. Causes of the meridional shifts in the NAC/GS position and its relationship with the SPG strength are not investigated further in the present paper.

We also show that the atmospheric variability influences North Sea salinity. The direct impact of NAO leads to salinification in the North Sea while the EAP has no significant impact on North Sea salinity in this simulation. It is important to note that while the direct influence of NAO on North Sea salinity is limited to short term variations, NAO can also influence North Sea salinity indirectly through its influence on oceanic circulation in the subpolar North Atlantic. We have not investigated this aspect further in this study, however, we conjecture that the indirect influence of NAO would be opposite to its direct influence. This is because a postive NAO tendency over multiple years leads to strengthening of the SPG circulation, which would then lead to freshening in the eastern North Atlantic and the northern North Sea.

B.5 CONCLUSIONS

Based on our analysis of the connections between the subpolar North Atlantic and the North Sea in a historical simulation with the MPI-ESM-LR, we conclude that:

- A low frequency oceanic perturbation of Atlantic origin drives the re-occurrence and persistence of high salinity pulses on a section from Rockall Trough to the North Sea. In all three regions examined, Rockall Trough, FSC and northern North Sea, salinity varies coherently, albeit with advective delays. The advective delay from Rockall Trough to the northern North Sea is found to be about one year.
- At decadal timescales, the leading mode of SSH variability (20 percent explained variance in this simulation) captures the earlier reported eastern North Atlantic salinity and SPG strength connection.
- While the total volume transport of Atlantic water into the North Sea is wind driven and does not co-vary with SPG strength, the properties of the inflowing Atlantic water are modulated by the variability in Subpolar Gyre strength at decadal to multidecadal timescales (30-40 year period).

The SPG-driven changes in salinity in the eastern North Atlantic and the northern North Sea can influence local hydrographic variability by influencing stratification (Núñez-Riboni & Akimova, 2017) and also influence marine ecosystems in the Rockall Trough (Miesner & Payne, 2018) and the North Sea (Akimova et al., 2016). It also remains to be seen if the influence of SPG variability is present in nutrient concentrations with potential implications for North Sea marine ecosystems. As we have identified oceanic (SPG driven) impacts on the North Sea and as SPG variability has been shown to be predictable with state-of-the-art decadal prediction system at multi-year lead times (Robson et al., 2012a), there might in turn be a potential for the North Sea system too. Current decadal prediction systems are all based on global coupled models. Assessment of such initialized global coupled model simulations in the eastern North Atlantic and in the northern North Sea would illuminate whether the open ocean impacts revealed in the present study also translate into a significant prediction skill.

B.6 ACKNOWLEDGMENTS

This work has benefited from stimulating discussions with Manfred Bersch and technical help from Helmuth Haak. The work of J.B. and A.D. was supported by the Cluster of Excellence CliSAP (EXC177), Universität Hamburg, funded through the Deutsche Forschungsgemeinschaft (DFG, German Research Foundation). This work was also funded by the DFG under Germany's Excellence Strategy – EXC 2037 'Climate, Climatic Change, and Society' – Project Number: 390683824, contribution to the Center for Earth System Research and Sustainability (CEN) of Universität Hamburg (JB, AD). The authors thank Michael Botzet for carrying out the model simulations. The authors also thank three anonymous reviewers whose comments greatly improved the manuscript. The authors also thank the German Computing Center (DKRZ) for providing their computing resources. Model data are accessible at the DKRZ (www.dkrz.de/up). The authors do not report any conflict of interest.

C

DECADAL PREDICTION OF BARENTS SEA COD STOCK THROUGH AN OCEANIC LINKAGE WITH THE SUBPOLAR GYRE

This appendix contains a paper, which is intended to be submitted to Frontiers in Marine Sciences as:

Koul, V., Schrum, C., Arthun, M., Brune, S. and Baehr, J. (2019), "Decadal Prediction of Barents Sea Cod Stock through an Oceanic Linkage with the Subpolar Gyre", Frontiers in Marine Science (to be submitted).

The contribution of Vimal Koul (V.K.) and others to this paper is as follows:
V.K., C.S and J.B. conceived the work. V.K performed the analysis and wrote the paper. V.K. was guided by M.A. on statistical Cod predictability analysis. S.B. carried out the hindcast and assimilation experiments. C.S. and J.B. provided guidance on the overall direction of the work. All authors reviewed the manuscript.

Decadal Prediction of Barents Sea Cod Stock through an Oceanic Linkage with the Subpolar Gyre

Vimal Koul[1,2], Corinna Schrum[3], Marius Arthun[4], Sebastian Brune[1] and Johanna Baehr[1]

[1]Institute of Oceanography, Center for Earth System Research and Sustainability, Universität Hamburg, Germany

[2]International Max Planck Research School on Earth System Modelling, Max Planck Institute for Meteorology, Germany

[3]Helmholtz Zentrum Geesthacht, Institute of Coastal Research, Germany

[4]Geophysical Institute, University of Bergen, Bergen, Norway

(To be submitted)

In the North Atlantic, overwhelming evidence suggests strong climate-ecosystem linkages which can lend predictability to marine resources. However, a considerable gap remains between the success of decadal climate predictions and marine ecosystem predictions. The main challenge towards bridging this gap is posed by the poor performance of global coupled models in the shallow shelf seas, such as the Barents Sea, where some of the highly productive fisheries reside. It is also unclear whether initialized climate predictions provide significantly better predictions than uninitialized predictions in the shelf seas at interannual to decadal timescales. Here, for the first time, we assess decadal predictability of Cod biomass in the Barents Sea using climate predictions from a global Earth System Model (ESM). We show that a high predictive potential emerges from a strong positive relationship between Cod biomass in the Barents Sea and low frequency variability in the Subpolar Gyre (SPG) temperature. We demonstrate that by combining dynamical predictions of SPG temperature from the ESM with the statistical SPG-Cod relationship, the biomass of this stock can be predicted 11-years in advance. Such an extended prediction horizon can not be achieved by using uninitialized predictions of SPG temperature. Overall, our results reveal that it is possible to translate predictability from the physical environment to marine resources, and we forecast that environmental conditions in the decade 2016-2026 would be detrimental for Barents Sea Cod.

C.1 INTRODUCTION

The impact of decadal climate variability on marine ecosystems and its predictability presents great opportunities for sustainable long term management of marine resources. Conventionally, environmental variables have been excluded from ecosystem resource management procedures because of the assumption that exploitation dominates such resources (Skern-Mauritzen et al., 2016; Stock et al., 2011). With the growing evidence of climate driven responses in key aspects of marine ecosystems, such as fish abundace and distribution (Stenseth et al., 2002; Chavez et al., 2003; Drinkwater et al., 2003; Lehodey et al., 2006; Brander, 2010), there is real potential in utilizing climate-ecosystem connections to predict spatio-temporal variability in fish stocks (Stock et al., 2011; Tommasi et al., 2017b; Payne et al., 2017). The necessity to assess climate based marine ecosystem predictability stems not only from the strategic management perspective but also from the limitations of present ecosystem forecast procedures, which either discount or can not foresee the changes in climatic conditions (Pershing et al., 2015; Skern-Mauritzen et al., 2016). Regions with strong climate-ecosystem connections might lend predictability to fish stocks, provided, climate variability in these regions is predictable. Such an investigation on decadal predcitability in fish atocks, derived from the predictability of the physical environment, has not been carried out.

In the North Atlantic Subpolar gyre (SPG), decadal variability of the physical environment is highly predictable using global coupled models (Matei et al., 2012; Msadek et al., 2014; Robson et al., 2018). However, the prediction of fish abundance in the biologically productive shelf seas of the eastern North Atlantic, such as the Barents Sea, has remained considerably behind the predictability of the physical environment of the SPG. Challenges came from the complexity and feedbacks within the foodwebs (Glaser et al., 2014; Subbey et al., 2014) and the impact of fishing mortality on many fish stocks in the North Atlantic (Hutchings, 1995; Myers et al., 1997; Frank et al., 2016; Sguotti et al., 2019). However, while the interaction between the inherent non-linearity in foodweb and fishing mortality may limit the prediction horizon over short time scales, the integrated impact of decadal climate variability in the SPG on fluctuations in fish abundance might provide a predictive potential.

The prospect of decadal prediction of fish abundance emerging from the predictability of physical environment in the SPG can arise from the influence of SPG circulation on the adjoining shelf seas (Koul et al., 2019a). While, climate-based statistical predcition of Barents Sea Cod stock shows promisng skill (Årthun et al., 2018), such prediction only exploits the observed advective delay of oceanic anomalies from the North Atlantic to the Barents Sea. It is unknown whether the dynamical prediction of the physical environment of the SPG can be transfered to fish abundance. The variability in the size and strength of the SPG and its interaction with the meridional overturning circulation creates hydrographic anomalies in the eastern subpolar North Atlantic (Bersch, 2002; Hátún et al., 2005; Häkkinen et al., 2011b). Both observations and global coupled models agree that these anomalies are advected downstream by the Atlantic inflow across the Greenland-Scotland Ridge (GSR, Holliday et al. (2008), Årthun & Eldevik (2016), and Koul et al. (2019a)), where these anomalies influence local hydrography. The properties of the Atlantic inflow are known to influence marine ecosystem in the eastern North Atlantic shelf seas, such as the Barents Sea. through

temperature related effects on recruitment, food availability, fecundity, growth and migration patterns (Ottersen et al., 1994; Beaugrand & Kirby, 2010; Drinkwater et al., 2010).

Recent success in the prediction of fish abundance and distribution have been achieved at seasonal lead times (Payne et al., 2017). These seasonal predictions benefit not only from high resolution of the underlying models which forecast environmental variables but also from the robust mechanistic understanding of climate-ecosystem relationship at these timescales. However, for decadal predictions, along with the low resolution of the underlying global coupled models in the shelf regions, there are multitude of challenges that have impeded the translation of decadal predictions of climate to marine resources (Tommasi et al., 2017b). For example, global coupled models poorly represent northward propagation of oceanic anomalies across the GSR (Langehaug et al., 2017). Further limitations are posed by the exclusion or inadequate parameterization of shelf-sea related processes in global coupled models. While the recent assessment of decadal predictability of climatic conditions in the shelf regions using global models instills confidence (Tommasi et al., 2017c), the looming question on the added value of decadal predictions for marine ecosystem predictions has remained unanswered.

In the present contribution, we use decadal predictions of temperature from an Earth System Model to reveal decadal predictability of the Barents Sea Cod stock. The focus of this study is on the prediction skill of total stock biomass of Barents Sea Cod, a quantity that reflects the integrated impact of climate. Our investigation builds on the promising forecast of Barents Sea Cod biomass using observations (Årthun et al., 2018), and here, we provide new insights into the source of prediction skill in Barents Sea Cod biomass. Supported by new estimates of dynamical prediction skill in eastern North Atlantic hydrography, our analysis provides novel insights into what kind of climate predictions are best suited for predicting marine resources in these regions.

C.2 MODEL DETAILS AND METHODS

C.2.1 *Model Details*

The Max Planck Institute Earth System Model (MPI-ESM) is used in its low resolution (LR) setup in the present study (MPI-ESM-LR, Giorgetta et al. (2013)). The ocean general circulation component of MPI-ESM-LR, the Max Planck Institute Ocean Model (MPIOM, Jungclaus et al. (2013)), is a free surface model with primitive equation solved on an Arakawa C-grid, and with hydrostatic and Boussinesq approximations. It has a total of 40 z-levels in the vertical with closely spaced upper levels; the surface layer thickness is 12 meters. The MPIOM setup used in the study has a rotated grid configuration (GR15) for which the singularity at the North Pole is replaced over Greenland. This has the advantage that horizontal resolution is enhanced north of 50°N, reaching 15Km near Greenland. The resolution increases gradually to 1.5 degrees towards the equator. Embedded in MPIOM is also the ocean biogeochemistry component, the Hamburg Ocean Carbon Cycle model (HAMOCC, Ilyina et al. (2013)). Among other processes, HAMOCC incorporates phosphate and oxygen cycles, and defines the marine food web based on nutrients, phytoplankton, zooplankton and

detritus (NPZD) based approach. The atmospheric general circulation component of MPI-ESM1.2-LR is the European Center-Hamburg (ECHAM, Stevens et al. (2013)). In MPI-ESM1.2-LR, the ECHAM is run at a horizontal resolution of T63 and with 47 vertical levels, the model top being at 0.01hPa. The land surface-atmosphere interactions are simulated by the land vegetation module JSBACH (Reick et al., 2013) which is embedded in ECHAM.

C.2.2 *Methods*

C.2.2.1 *Decadal Prediction System*

We use one set of retrospective initialized decadal predictions (hindcasts) from the MiKlip project (Marotzke et al., 2016; Polkova et al., 2019), carried out with the MPI-ESM-LR. 10-year long ensemble hindcasts with 16 members are started on 1^{st} November every year from 1960-2016. The initial conditions for each member come from an assimilation experiment (1958-2016) with an oceanic ensemble Kalman filter (EnKF) and atmospheric nudging. The oceanic EnKF in MPI-ESM-LR (Brune et al., 2015, 2018) assimilates monthly profiles of temperature and salinity from EN4 (Good et al., 2013). Simultaneously, atmospheric vorticity, divergence, temperature and surface pressure are nudged to ERA40/ERAInterim re-analyses (Uppala et al., 2005; Dee et al., 2011). It should be noted that neither sea surface temperature from satellite observations nor atmospheric temperature below 900 hPa are assimilated in order to allow for a model-consistent assimilation across the atmosphere-ocean boundary. The assimilation experiment as well as the initialized hindcasts use observed solar irradiation, volcanic eruptions, and atmospheric greenhouse gas concentrations (RCP4.5 concentrations from 2006 onward) as boundary conditions, taken from CMIP5 (Taylor et al., 2012).

An additional 16-member uninitialized historical simulations (1850-2005) taken from the MPI-ESM-LR Grand Ensemble (Maher et al., 2019) are analysed to isolate the skill due to external forcing. These historical simulations are performed under natural and anthropogenic forcings derived from observations covering a total of 156 years (1850-2005). For comparison with initialized hindcasts, these historical simulations are extended with a future RCP4.5 concentrations from 2006-2020. The natural forcing includes solar insolation, variations of the Earth orbit, tropospheric aerosol, stratospheric aerosols from volcanic eruptions, and seasonally varying ozone. The anthropogenic forcing includes the well mixed gases CO_2, CH_4, N_2O, CFC-11, and CFC-12 as well as O_3, and anthropogenic sulfate aerosols. Atmospheric CO_2 concentrations are prescribed and the carbon cycle is not interactive. It must be noted that this historical simulation is started from a pre-industrial control run and is not initialized from observations. Therefore, the internal variability in this model simulation may not be in phase with observations, and hence may not reproduce the observed timing of certain climatic events which are related to internal (natural) variability.

C.2.2.2 *Regression Analysis*

In order to predict the evolution of Total Stock Biomass (TSB) of Barents Sea Cod (C_{TSB}), we construct a simple linear regression model with Temperature (T) as the predictor (independent variable) and the C_{TSB} as the predictand (dependent variable):

$$C_{TSB}(y) = \beta_o + \beta_1 T(y - L) + \epsilon, \tag{C.1}$$

where y is the year, L is the lag in years at which the correlation between C_{TSB} and T is maximum, β_o is the intercept, β_1 is the slope and ϵ is the error term.

The regression model is trained on output from the assimilation experiment and the resulting regression coefficients are applied to the ensemble mean temperatures from the initialized and uninitialized hindcasts. This is done to isolate the training and testing data sets. The uncertainties in regression coefficients (slopes and intercepts) are estimated using a bootstrapping methodology. First, 10,000 new predictor and predictand time series of the same length as the original time series are constructed by random sampling with replacement from 80% of parent time series, while preserving their relationship. These new time series are then used to get 10,000 estimates of regression coefficients. The 95% confidence interval is the 2.5^{th} and 97.5^{th} percentile range of these 10,000 regression coefficients. We also applied the cross validation method on the assimilation output to test various simple and multiple regression models in order to identify the best performing predictor (see Årthun et al. (2018)). In addition to the SPG temperature, we use two other predictors. One is the Atlantic Multidecadal Oscillation (AMO) index, defined as the detrended area averaged sea surface temperature over the North Atlantic (0:70°N, 0:90°W). The other predictor is the subsurface (50-200 meter) temperature of the Atlantic inflow at the Barents Sea Opening. The lag (L) in the above equation is calculated separately for each predictor before testing various simple and multiple linear regression models based on these three predictors.

C.2.2.3 *Hindcast Skill and Hindcast Uncertainty*

We use anomaly correlation coefficient (ACC) as the measure of skill of ensemble mean initialized hindcasts and uninitialized historical simulations against annual mean observations for the period (1960-2016). Prior to calculating ACC, the both linear trend and lead-year dependent climatology are removed from the initialized hindcast to account for the lead-year dependent drift in the hindcasts. The uncertainty in hindcast skill is determined using a block bootstrapping approach. The block bootstrapping is done only in time and not across ensemble members. We use a 5-year overlapping block bootstrap to account for the autocorrelation in the time series. The estimated uncertainties are not sensitive to a reasonable choices of block length that allow sufficient number of blocks for sampling. Through random resampling with replacement, 10,000 new block-bootstrapped time series of predictions and observation are used to obtain 10,000 new estimates of ACCs. The 95% confidence interval is the 2.5^{th} and 97.5^{th} percentile range of these 10,000 ACCs.

Observations of temperature and salinity for the period 1960-2016 are from the EN4 gridded dataset (Good et al., 2013), while the observed Cod time series (1946-2016) is obtained from the International Council for the Exploration of the Sea. Prior to

correlation analysis, annual mean values are calculated, and the long term mean and linear trend is removed.

C.3 RESULTS

C.3.1 *Decadal Prediction of the Physical Environment*

We begin with the assessment of the prediction skill of the physical environment in the North Atlantic. The annual upper ocean temperature (0-500m) shows high hindcast skill in the SPG, as well as in the eastern North Atlantic (Figure C.1). In general, the skill degrades as the prediction horizon moves farther from the year of initialization (i.e. at longer lead-years). Furthermore, most of the skill in the North Atlantic, including North Sea and Barents Sea, can be explained by the long term linear trend during the verification period (1970-2016). A noticeable exception is the SPG where the multi-year skill is largely intact irrespective of the trend. Within the SPG, most of the skill is present west of 20 °W and degrades sharply towards the east. Detrending also improves the skill in the SPG where internal variability dominates the forced response. Thus, it appears that initialization is the dominant source of predictability of the upper ocean heat content within the SPG, while the long term trend, arising from the external forcings, seems to dominate predictability north of the Greenland-Scotland Ridge (GSR, Figure C.1).

In the case of annual upper ocean salinity, hindcast skill is not dominated by the long term linear trend (Figure C.2). Within the SPG, highest skill is present southwest of Iceland, which is different from the region of maximum skill for temperature. Also, in this case, hindcast skill in the regions north of the GSR is comparable to that in the SPG, and does not degrade as was the case for temperature. Skill is particularly high along the pathways of Atlantic inflow in the Nordic Seas. The existence of such trend-independent hindcast skill along the Atlantic inflow across the GSR suggests that the majority of the skill is derived from initialization and slow dynamics of the ocean circulation. Salinity, being a passive tracer in the eastern North Atlantic, preserves the memory of initialization far longer than temperature.

The preceding results suggest that external forcing is not the dominant source of hindcast skill for the SPG temperature. To support this result, a more rigorous estimate of the hindcast skill is presented in Figure C.3. Consistent with preceding results, hindcast skill for SPG temperature and salinity is significantly higher when the model is initialized compared to when the model is driven with external forcing only (see Methods). At lead-year 4, the hindcast skill due to initialization even outperforms the skill due to persistence. On the other hand, for temperature in the inflow layer (50-200m) at the Barents Sea Opening, the hindcast skill is high at lead-year 1 but then drops sharply at later lead years, and the hindcast skill is not significantly different than either persistence or uninitialized externally forced simulation. However, the hindcast skill for salinity in this region is higher than the externally forced skill and significantly higher than persistence at lead-years 4 to 7. These results therefore point towards large difference in hindcast skill between temperature ans salinity north of the GSR in MPI-ESM-LR.

In order to understand the cause behind the low hindcast skill in temperature north of the GSR, we now diagnose the heat budget in these regions. A heat budget analysis

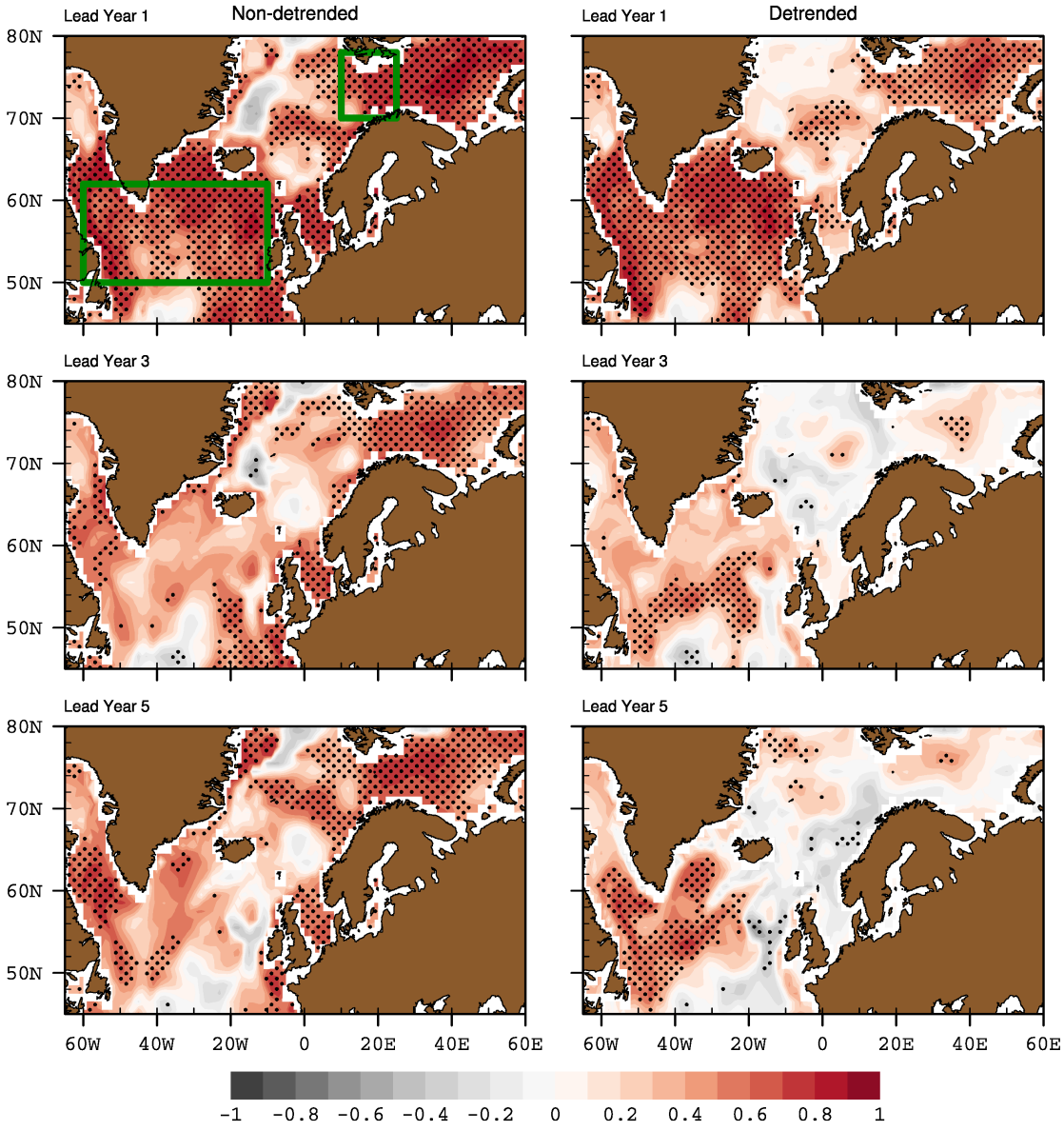

Figure C.1: Anomaly correlation coefficient (ACC) for initialized upper 500 meter temperatures against observations at lead-year 1, 3 and 5. ACCs for non-detrended (left column) and detrended (right column) temperature are shown. Grid points shallower than 500m are averaged till bottom. Stippling denotes statistically significant skill at 95% confidence interval.

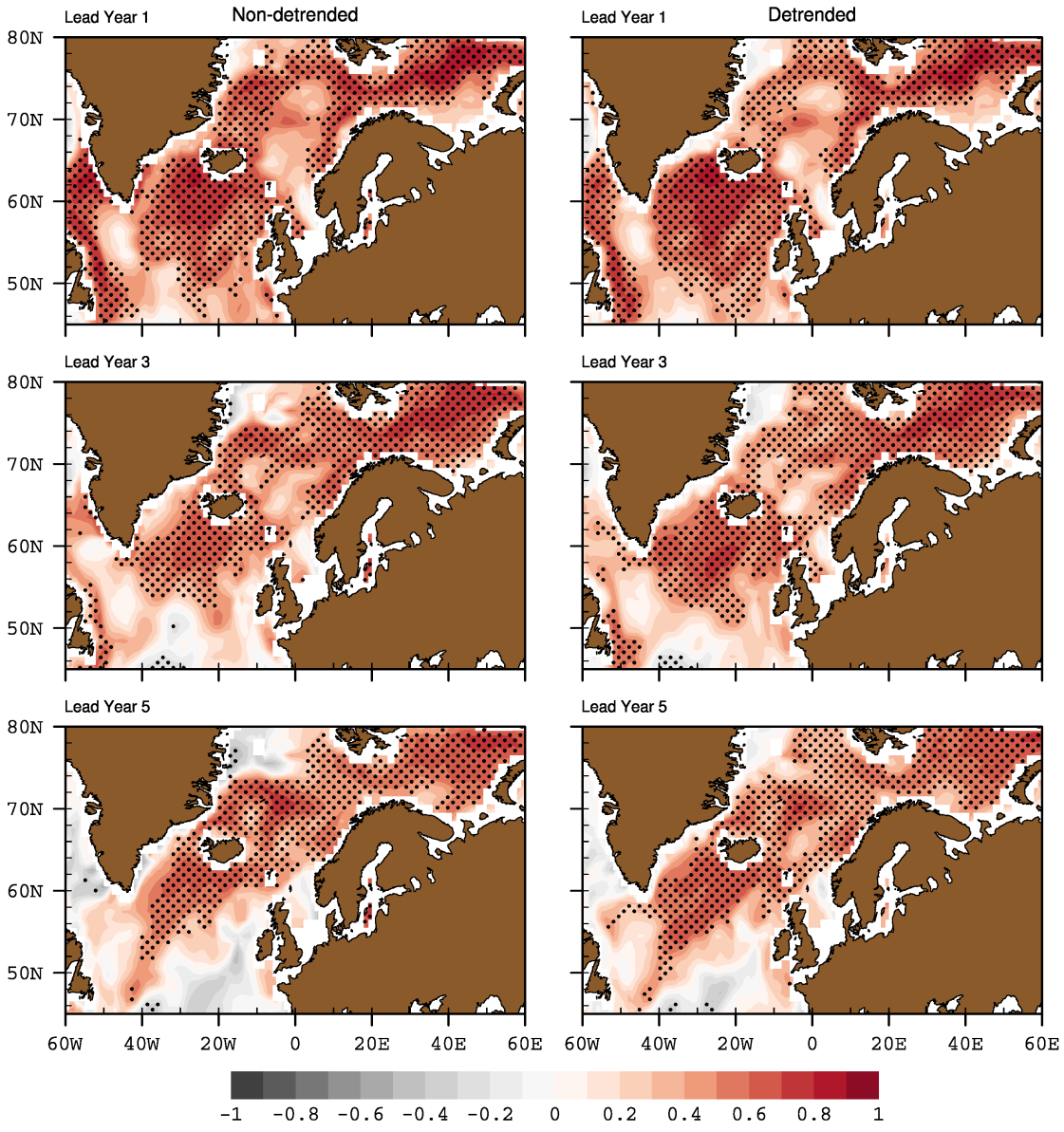

Figure C.2: Anomaly correlation coefficient (ACC) for initialized upper 500 meter salinity against observations at lead-year 1, 3 and 5. ACCs for non-detrended (left column) and detrended (right column) salinity are shown. Grid points shallower than 500m are averaged till bottom. Stippling denotes statistically significant skill at 95% confidence interval.

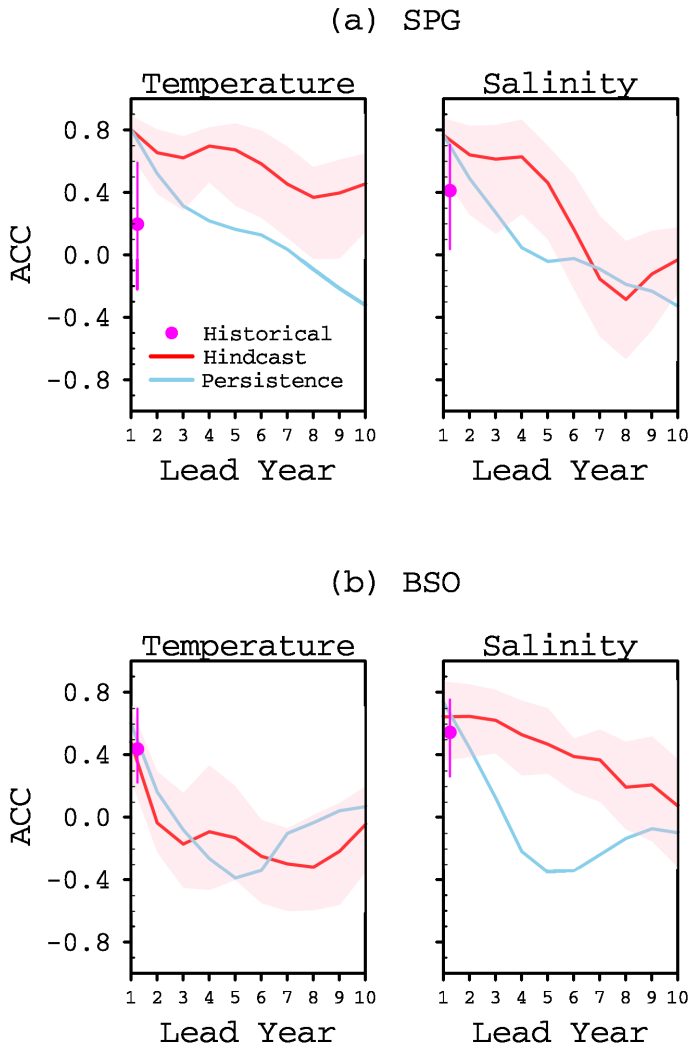

Figure C.3: ACC as a function of lead-year for initialized hindcasts (red), persistence (blue) and historical simulation (magenta dot) for temperature and salinity in (a) SPG and (b) Barents Sea Opening. The locations of these regions are shown by green boxes in Figure C.1a. The shading and whiskers depict 95% confidence intervals.

of upper 500 meter of the SPG is performed to assess the impact of assimilation procedure and the contribution of freshwater flux, surface heat fluxes and ocean heat convergence in driving the changes in ocean heat content (Figure C.4). The vertical heat flux at 500 meter is neglected for this analysis. The assimilation procedure introduces additional sources and sinks of heat which impact the heat budget, however, we find that this impact is small compared to the contribution due to surface heat fluxes and heat convergence at lateral boundaries. The contribution to heat content variability from the surface freshwater flux is also negligible. Diagnosis of SPG heat content variability hints at a dominant role of oceanic heat convergence at the northern and southern boundaries of the SPG. Large variability present in the ocean heat convergence term matches the extended periods of cooling and warming in the SPG. In the 1960s, pronounced reduction in the oceanic heat convergence is followed by cooling in the SPG, while during this period, surface heat fluxes show low to moderate variability. From early 2000s, reduction in oceanic heat content is followed by cooling in the SPG. During this period surface heat fluxes show low to moderate variability, which does not explain the recent SPG cooling. In fact, the correlation between 5-year running mean heat content tendency (delHC) and the net surface heat flux term (NHflux) is 0.02 while the correlation between delHC and the oceanic heat convergence term (OHCG) is 0.73. Consistent with analysis in other decadal prediction systems (Msadek et al., 2014; Robson et al., 2018), our analysis also suggests that initialization of oceanic parameters is responsible for high predictability in the SPG.

North of the GSR, at the Barents Sea Opening, heat budget analysis also suggests a dominant role of oceanic heat convergence (Figure C.5). In this region, correlation between 5-year running mean delHC and NHflux is lower (0.38) than the correlation between delHC and OHCG (0.68). However, while the ocean plays an important role in determining temperature variability at longer timescales, this does not translate into high prediction skill in temperature in this region, as was the case with SPG (Figure C.3). This discrepancy might be related to either initialization errors or propagation of oceanic thermal anomalies across the GSR in MPI-ESM-LR. Nevertheless, the high skill in salinity across the GSR points to advection of oceanic anomalies from the SPG to the far eastern North Atlantic.

In summary, decadal hindcast skill in the SPG temperature and salinity can be largely derived from oceanic initial conditions and the predictive component of external forcings, and not from the external forcing alone. At the Barents Sea Opening, persistence and external forcing dominate hindcast skill of temperature and salinity in inflow layers, except for lead-years 4 to 7 for salinity. The continuity of high hindcast skill in salinity, which is a more conservative tracer than temperature, from the SPG to the Barents Sea Opening, suggests an oceanic linkage between these regions. This is consistent with the recent study by (Koul et al., 2019a) who showed that in MPI-ESM-LR, decadal variability associated with strengthening and weakening of the SPG circulation impacts shelf seas in the eastern North Atlantic.

C.3.2 *Decadal Prediction of Barents Sea Cod (Gadus morhua)*

In the SPG, the decadal variability in temperature is larger than the interannual variability (Hermanson et al., 2014). The emergence of remarkable hindcast skill

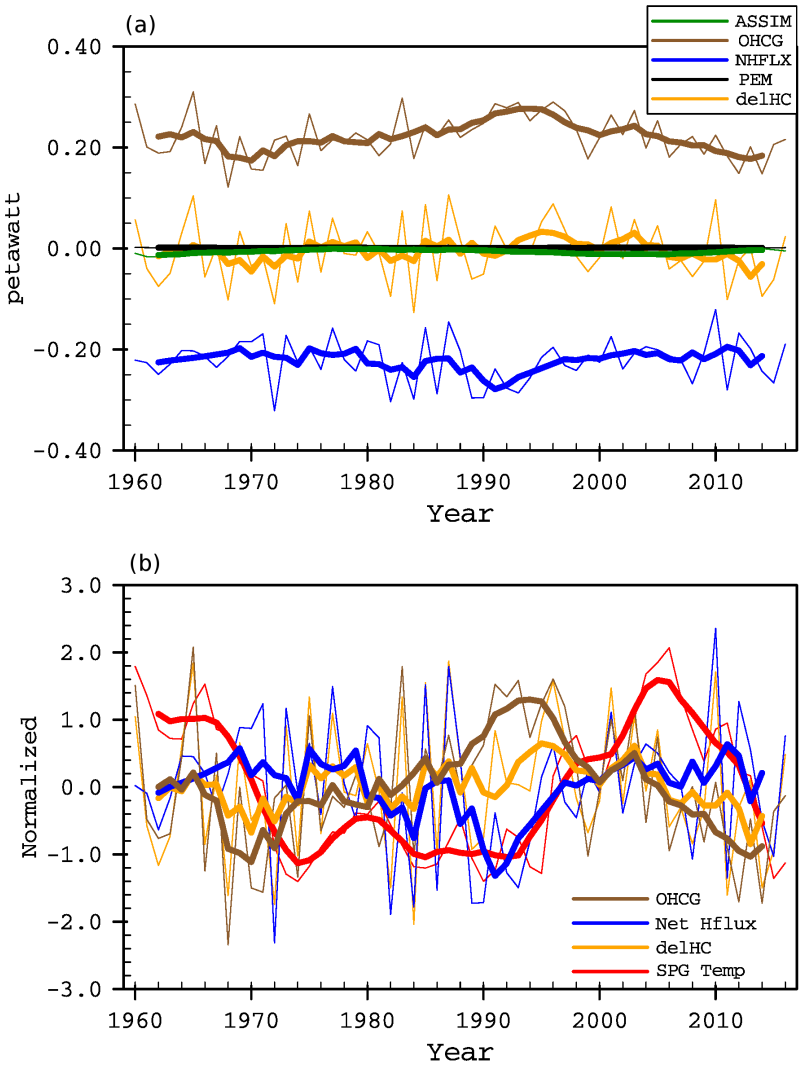

Figure C.4: (a) Time series of the heat budget terms in the SPG region (50:62°N, 10:60°W) for the upper 500 meters in the assimilation run. Contribution to heat budget comes from surface heat fluxes (NHFLX, blue), assimilation nudging (ASSIM, green), freshwater flux at the surface (PEM, black) and the ocean heat convergence from the lateral boundaries (OHCG, brown). The heat content tendency (delHC) is shown in yellow. All values are in Petawatt (1 PW = 10^{15}W). Thin lines show annual mean values and bold lines show 5-year running means. (b) Normalized heat budget terms NHFLX, OHCG and delHC and SPG temperature (0-500m, red)

.

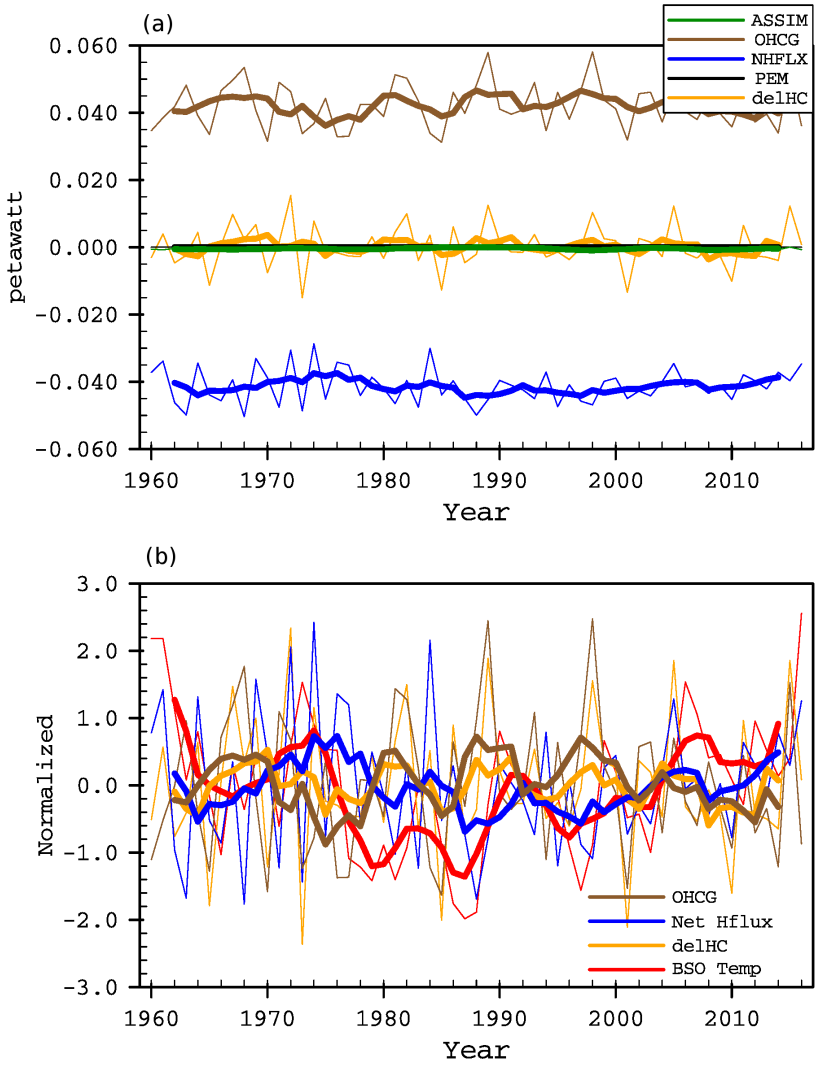

Figure C.5: As in Figure C.4 but for Barents Sea Opening (smaller green box in Figure C.1a).

in SPG properties and its linkage to Barents Sea raises the question whether such profound decadal variability can influence marine resources to the extent that they too exhibit multiyear predictability. The low hindcast skill in temperature at the Barents Sea Opening precludes its application to Cod predictability. Therefore, as a first step, we test the robustness of Cod-SPG linkage using SPG temperature from the assimilation run (see Methods). From the time series of SPG temperature and Barents Sea Cod (Figure C.6a), it is evident that the cooling of SPG in the 1960s precedes the decline in Barents Sea Cod in the 1970s. Furthermore, the recent decadal shift in the SPG – warming from 1995 to 2005 and cooling from 2005 onward – seems to be mirrored by the Barents Sea Cod: a rise from mid 2005 to 2014 and the beginning of a decline thereon. We find a significantly high positive correlation between Barents Sea Cod and SPG temperature (Figure C.6b). Consistent with the observational analysis of (Årthun et al., 2018), the correlation between the SPG temperature (leading) and Barents Sea Cod stock (lagging) peaks at a lag of 7 years (r=0.79, $p < 0.05$). High correlation values are spread throughout the SPG which suggests that basin wide oceanic variability in the SPG influences Barents Sea Cod 7 years later.

Further diagnosis of SPG-Cod relationship suggests that their correlation remains high down to 700 meters in the SPG (Figure C.6c). The hindcast skill (ACC) for SPG temperature at lead-year 4 is maximum between 200-500 meters. Compared to surface layers, this depth range also corresponds to low root mean square errors in the hindcast. The choice of lead-year 4 is guided by our finding that at this lead-year the hindcast skill for SPG temperature is high and statistically significant than both persistence and the historical skill (see Figure C.3a). All of these consideration suggest that subsurface SPG temperature might be the best predictor for Barents Sea Cod biomass. To test this hypothesis, we use temperature at 500 meter depth and area averaged over the SPG domain from the assimilation run as a predictor for Cod biomass, and we compare its performance with other predictors (Figure C.7). The other two predictors are the AMO and subsurface temperatures at the Barents Sea Opening (see Methods). The existence of a 7-year lagged SPG-Cod relationship clearly makes the case for a simple linear regression model that would "predict" Cod biomass using SPG temperature as a predictor. The comparison of various regression models suggests that the regression model based on SPG temperature alone outperforms all other regression models based on various combinations of predictors.

Now, we focus on assessing predictability of Barents Sea Cod Stock at decadal lead times by combining the dynamical prediction of SPG temperature with the statistical SPG-Cod relationship. Since the dynamical model does not have biological variables as output, we feed the statistical model with lead-year 4 hindcasts of SPG temperature. Inb, the results from the dynamical-statistical prediction clearly illustrate that the Barents Sea Cod is predictable 11 years in advance (Figure C.8). Lead-year 4 SPG hindcast predicts Barents Sea Cod 7 years later, thus giving a prediction horizon of 11 years beyond which the prediction quality degrades. The prediction from the dynamical-statistical model also outperforms persistence forecast, which is statistically insignificant at a lead-time of 8 years (blue dot in Figure C.8a). Note that limiting the training period for the regression model to 1995-2016 gives similar results (figure not shown).

Can this prediction skill be achieved using historical SPG temperature instead of the hindcasts? To assess this, we run the statistical model with historical SPG temperature

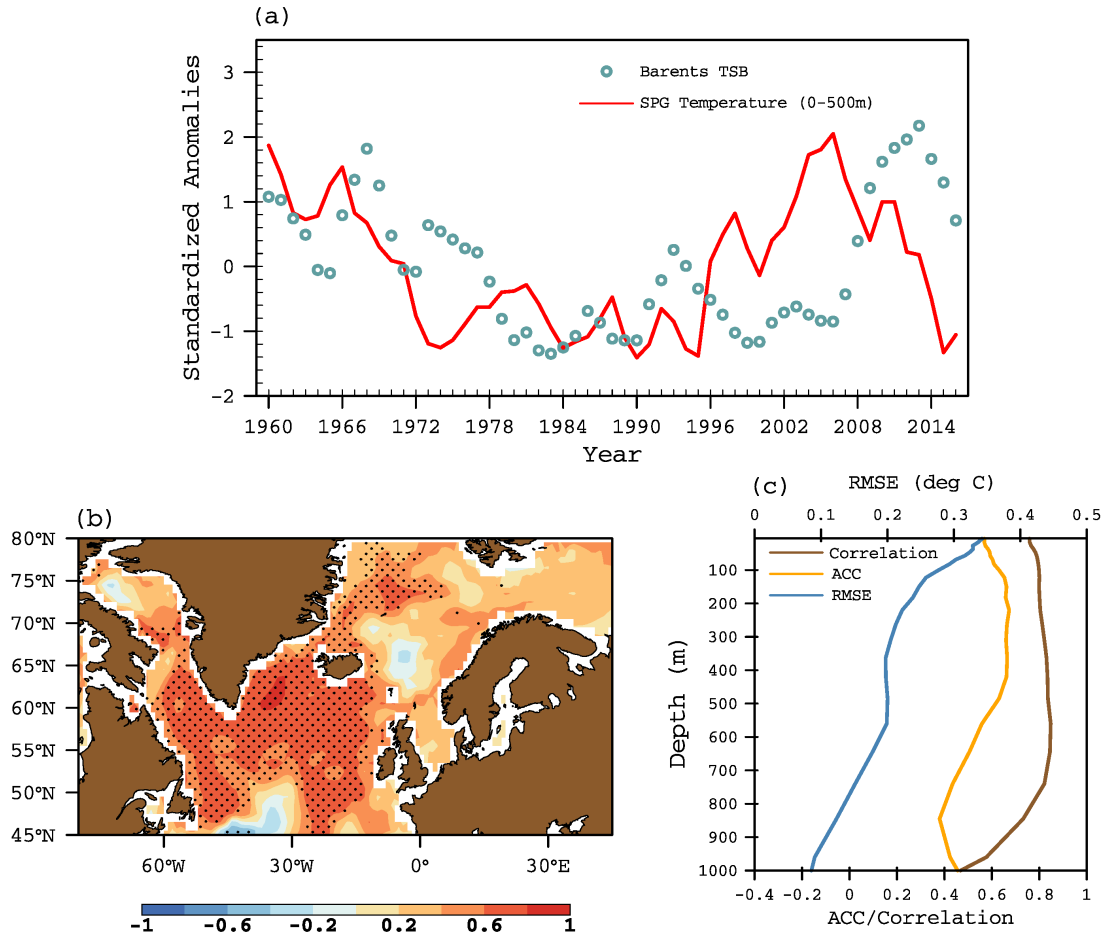

Figure C.6: (a) Time series of SPG temperature and Total Stock Biomass (TSB) of Barents Sea Cod. (b) Correlation of upper 500 m temperature at each grid point with observed time series of TSB of Barents Sea Cod. The temperature field is shifted backward in time by 7-years before correlating with the Barents Sea Cod. Stippling denotes statistically significant correlation at 95% confidence level. (c) Correlation, ACC and root mean square error (RMSE) between area-averaged SPG temperature (leading) at various depth levels and TSB of Barents Sea Cod at lag-7.

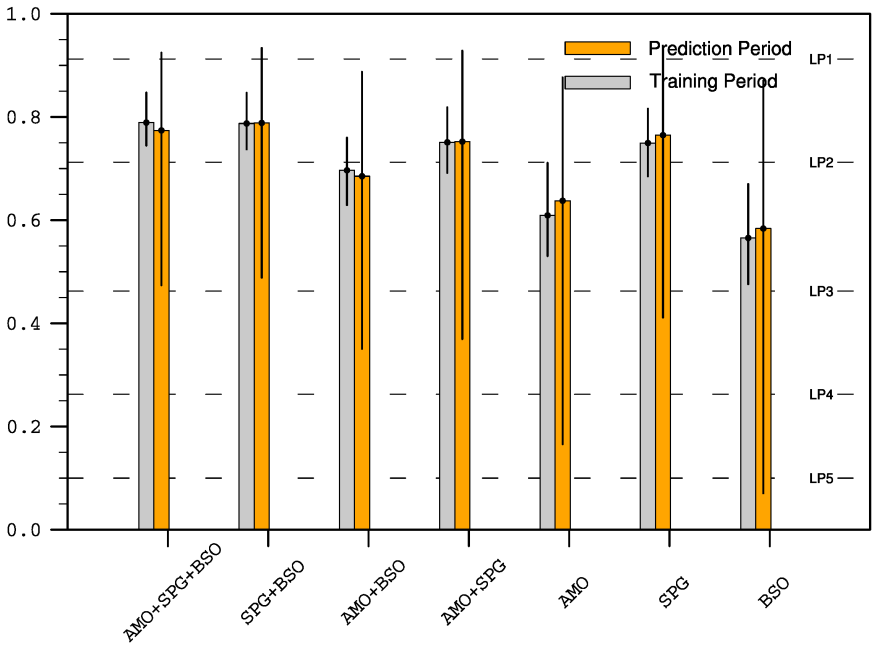

Figure C.7: Cross validated ACCs of Total Stock Biomass of Barents Sea Cod using various predictors from the assimilation run. Training period ACCs are shown in grey and prediction period in orange. The prediction horizon is 7-years for predictions based on AMO and SPG temperature (500m), and 2-years for BSO temperature (50-200m). Dashed horizontal lines indicate predictions based on persistence. AMO–Atlantic Multidecadal Oscillation, SPG–Subpolar Gyre, BSO–Barents Sea Opening, LP–Lagged Persistence

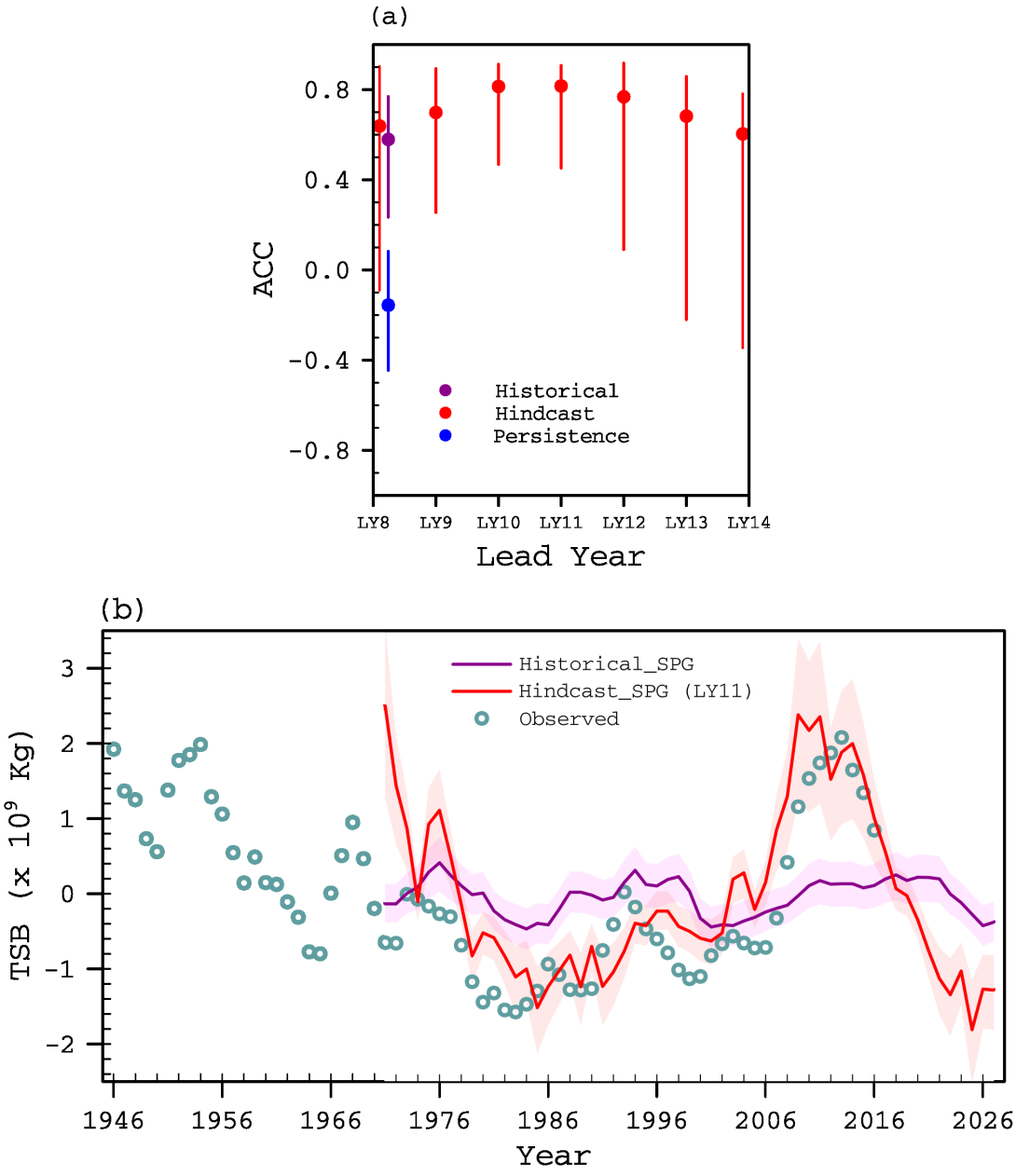

Figure C.8: (a) ACC of hindcast Barents Sea Cod against observations for the period 1971-2016 (red dots). The ACC of the Lag-8 persistence forecast is shown by blue dot and that of the historical simulation is shown by the magenta dot. The whiskers denote 95% uncertainly bounds in ACCs. (b) Reconstructed (1971-2016) and forecast (2016-2027) time series of Barents Sea Cod (red) from LY-11 initialized hindcasts (LY-4 dynamical hindcast of SPG temperature (500m) combined with 7-year lagged linear regression) and historical simulation (magenta) for the period 1971 to 2027. Shading denotes 95% uncertainly bounds. The green circles show observed time series of Barents Sea Cod from 1946-2016.

as input. The correlation skill associated with historical simulation is lower but not statistically different from the hindcast skill. However, the variability in the reconstructed Barents Sea Cod time series using historical simulation is suppressed (magenta line in Figure C.8b). This reconstructed time series fails to capture the recent decadal shift in the Barents Sea Cod Stock, which as shown above follows internal variability in SPG temperature. While these results confirm that there is value in using initialized hindcasts, these results also provide first such evidence that initialized hindcasts can be deployed for prediction of marine resources through climate-ecosystem linkages.

C.4 SUMMARY AND DISCUSSION

Sustainable management of fish stocks in the eastern North Atlantic requires a reliable assessment of future fish stocks. In order to predict future evolution of fish stocks, contemporary stock assessment models mainly rely on estimating future recruitment using spawner biomass of previous years and assuming a certain mortality rate. Incorporating environmental information in such assessment models might not improve their prediction skill because of large uncertainties associated with recruitment-climate relationship, and also because these uncertainties might grow in a warming climate (Myers, 1998; Stock et al., 2011). However, ecosystem characteristics such as the total stock biomass assessed in the present study reflect the integrated effect of large scale climate on fish stocks, and hence the low frequency variability in total stock biomass might be predictable. Our study attempts to bridge the gap between environmental and fisheries prediction by assessing such variable.

The physical climate of the North Atlantic, particularly the heat and salt content of the Subpolar Gyre (SPG), has repeatedly been shown to exhibit multiyear to decadal predictability (Robson et al., 2018; Yeager et al., 2015; Hermanson et al., 2014; Msadek et al., 2014). Consistent with these reports, the 16-member decadal prediction system based on MPI-ESM-LR (see Methods) reveals significantly high skill in the SPG heat and salt content. In the SPG, initialized hindcasts perform better than both uninitialized historical simulation and persistence. There are, however, differences in the source of skill in the shelf seas adjoining the SPG. First, we find that the hindcast skill in temperature north of GSR does not benefit from initialization and most of the skill in temperature north of the GSR is explained by the long term trend. Second, we find that the impact of trend on the skill in predicting salinity is small. This, and a recent finding that the influence of local processes on salinity does not dilute the memory of large scale variability carried by the inflowing atlantic water (Koul et al., 2019a) in MPI-ESM-LR, extends high predictability originating in the SPG to the Barents Sea salinity.

In the present contribution, we assess the feasibility of decadal prediction of Cod stock in the Barents Sea using predictions of the environmental conditions from the MPI-ESM-LR. Such an extended prediction relies on two conditions: (a) that there is robust relationship between Cod and the physical environment and (b) that the physical environment is predictable at multiyear lead times. We find a strong positive correlation between SPG temperature and Cod biomass in the Barents Sea. The strong correlation between temperature and Cod biomass is justified by the direct and indirect effect of temperature on life history of Cod in the Norwegian-

Barents Sea ecosystem (Ottersen et al., 1994; Brander, 1995). While the details of how the temperature influences Barents Sea Cod are well known (see for example Hamre (1994), Ottersen et al. (1994), and Drinkwater et al. (2010)), the importance of the pronounced low frequency variability associated with the SPG, which lends predictability to the Barents Sea Cod, is worth highlighting here. The hydrography of Norwegian-Barents Seas is related to the Atlantic inflow via the Faroe-Shetland Channel. When the SPG circulation is weak, the proportion of subtropical waters in the Atlantic inflow through the Faroe-Shetland Channel increases (Larsen et al., 2012; Koul et al., 2019a). The resulting increase in the transport of warm and saline water masses pushes the ice edge northwards (Årthun et al., 2012; Fossheim et al., 2015), which leads to increased productivity through extended periods of increased primary production and also due to expansion of feeding grounds. Low frequency changes in temperature in the Barents Sea are also known to impact prey availability of Barents Sea Cod (Hamre, 1994).

While a 7-year predictability horizon in Barents Sea Cod stock has been shown to emerge from observations of sea surface temperatures (SST) in the North Atlantic (Årthun et al., 2018), in the present study, we extend the predictability horizon to 11-years using dynamically-predicted subsurface SPG temperature as a predictor. The largest correlations of Barents Sea cod with temperature, in the assimilation run, are found with SPG temperature. Additionally, we reveal that subsurface SPG temperature at 500 meter is a better predictor of Cod biomass than either AMO or local temperatures at the Barents Sea Opening. At first it might seem counter-intuitive that remote oceanic temperatures are better predictors of Barents Sea Cod biomass than local temperatures. But it is entirely possible that the impact of oceanic anomalies advected into the Barents Sea is more pronounced in Cod Stock, because, fishes are not as geographical limited as is our definition of local temperature variability. Furthermore, our results emphasize the importance of initialization of oceanic conditions in the SPG. The uninitialized historical predictions fail to capture decadal fluctuations in Barents Sea Cod stock. Further confidence in our results is derived from the fact that these predictions are based on ensemble mean of a 16-member ensemble (see Methods), which samples the uncertainty associated with the future evolution of the climate system.

We have attempted to bridge the gap between decadal climate predictions and marine ecosystem predictions. The methodology applied here is based on correlational analysis of environment-ecosystem connections. We remind the reader that a degree of caution must be exercised while interpreting the future success of our predictions of Barents Sea Cod. An underlying assumption in our methodology is that the SPG-Cod linkage will remain stable in the near future. This assumption will not hold in case the future harvest rates are high enough to dominate the variability in the Barents Sea Cod stock. By incorporating the impact of fishing pressure, prediction errors can be further minimized. The SPG-Cod linkage identified here must also be re-tested in future as new data accumulate.

C.5 CONCLUSIONS

Based on the results presented in this study, we conclude that:

1. In the 16-member decadal prediction system based on the MPI-ESM-LR, initialized hindcasts of SPG-temperature show higher skill than both persistence and uninitialized hindcasts. North of the Greenland-Scotland Ridge (GSR) the hindcast skill in temperature drops remarkably. In these regions, most of the skill is explained by the long term trend. However, the hindcast skill of salinity does not depend on the long term trend and remains high across the GSR along the Atlantic water pathways.

2. There is a strong positive correlation between SPG temperatures and Barents Sea Cod. The variability in SPG temperature is reflected in Barents Sea Cod biomass 7 years later.

3. The total stock biomass of Barents Sea Cod can be predicted 11-years in advance, and we forecast that Barents Sea Cod stock would decline in the decade 2016-2026 due to unfavourable temperatures during this time.

Various incentives as well as the lessons learnt from past failures have motivated the efforts toward the decadal prediction of marine resources. Foremost is the added value that such predictions can bring to the integrated approach for sustainable management of fish stocks in the near future. For example, reliable predictions of fish biomass would enable the adjustment of future catch targets to account for climate-driven fluctuations in productivity (Sharp, 1987; Mills et al., 2013; Tommasi et al., 2017a). Climate-informed fishery management could also benefit from rapid advances in multiyear prediction of other fishery-related variables such as net primary production by global earth system models (Séférian et al., 2014). The present contribution emphsizes that proper representation of Subpolar Gyre variability in such models is the key to long term predictions in the North Atlantic.

C.6 ACKNOWLEDGEMENTS

This work was funded through a research collaboration between Helmholtz Zentrum Geesthacht and Universität Hamburg. The work of J.B. was supported by the Cluster of Excellence CliSAP (EXC177), Universität Hamburg, funded through the Deutsche Forschungsgemeinschaft (DFG, German Research Foundation). This work was also funded by the DFG under Germany's Excellence Strategy EXC 2037 "Climate, Climatic Change, and Society" Project 390683824, contribution to the Center for Earth System Research and Sustainability (CEN) of Universität Hamburg (J.B.). The authors thank the German Computing Center (DKRZ) for providing their computing resources.

BIBLIOGRAPHY

Akimova, Anna, Ismael Nunez-Riboni, Alexander Kempf & Marc H Taylor (2016). "Spatially-resolved influence of temperature and salinity on stock and recruitment variability of commercially important fishes in the North Sea." In: *PloS one* 11.9, e0161917.

Alheit, Jürgen, Priscilla Licandro, Steve Coombs, Alberto Garcia, Ana Giráldez, Maria Teresa Garcia Santamaría, Aril Slotte & Athanassios C Tsikliras (2014). "Reprint of "Atlantic Multidecadal Oscillation (AMO) modulates dynamics of small pelagic fishes and ecosystem regime shifts in the eastern North and Central Atlantic"." In: *Journal of Marine Systems* 133, pp. 88–102.

Årthun, M, T Eldevik, LH Smedsrud, Ø Skagseth & RB Ingvaldsen (2012). "Quantifying the influence of Atlantic heat on Barents Sea ice variability and retreat." In: *Journal of Climate* 25.13, pp. 4736–4743.

Årthun, Marius & Tor Eldevik (2016). "On anomalous ocean heat transport toward the Arctic and associated climate predictability." In: *Journal of Climate* 29.2, pp. 689–704.

Årthun, Marius, Bjarte Bogstad, Ute Daewel, Noel S Keenlyside, Anne Britt Sandø, Corinna Schrum & Geir Ottersen (2018). "Climate based multi-year predictions of the Barents Sea cod stock." In: *PloS one* 13.10, e0206319.

Asbjørnsen, Helene, Marius Årthun, Øystein Skagseth & Tor Eldevik (2019). "Mechanisms of ocean heat anomalies in the Norwegian Sea." In: *Journal of Geophysical Research: Oceans* 124.4, pp. 2908–2923.

Barrier, Nicolas, Julie Deshayes, Anne-Marie Treguier & Christophe Cassou (2015). "Heat budget in the North Atlantic subpolar gyre: impacts of atmospheric weather regimes on the 1995 warming event." In: *Progress in Oceanography* 130, pp. 75–90.

Beaugrand, Gregory & Richard R Kirby (2010). "Climate, plankton and cod." In: *Global Change Biology* 16.4, pp. 1268–1280.

Becker, G & H Dooley (1995). "The 1989/91 high salinity anomaly in the North Sea and adjacent areas." In: *OCEAN CHALLENGE-CHALLENGER SOCIETY FOR MARINE SCIENCE* 6, pp. 52–57.

Becker, Gerd A & Manfred Pauly (1996). "Sea surface temperature changes in the North Sea and their causes." In: *ICES Journal of Marine Science* 53.6, pp. 887–898.

Becker, Gerd A, Alexander Frohse & Peter Damm (1997). "The northwest European shelf temperature and salinity variability." In: *Ocean Dynamics* 49.2, pp. 135–151.

Bersch, Manfred (2002). "North Atlantic Oscillation–induced changes of the upper layer circulation in the northern North Atlantic Ocean." In: *Journal of Geophysical Research: Oceans* 107.C10.

Bersch, Manfred, Igor Yashayaev & Klaus Peter Koltermann (2007). "Recent changes of the thermohaline circulation in the subpolar North Atlantic." In: *Ocean Dynamics* 57.3, pp. 223–235.

Berx, B, B Hansen, S Østerhus, KM Larsen, T Sherwin & K Jochumsen (2013). "Combining in situ measurements and altimetry to estimate volume, heat and salt transport variability through the Faroe–Shetland Channel." In: *Ocean Science* 9.4, pp. 639–654.

Berx, Barbara & Mark Payne (2017). "The Sub-Polar Gyre Index-a community data set for application in fisheries and environment research." In: *Earth System Science Data* 9.1, pp. 259–266.

Beverton, RJH & SJ Holt (1957). "On the dynamics of exploited fish populations." In: *Fishery Invest. UK Ser., II* 19, pp. 1–533.

Böning, Claus W, Markus Scheinert, Joachim Dengg, Arne Biastoch & Andreas Funk (2006). "Decadal variability of subpolar gyre transport and its reverberation in the North Atlantic overturning." In: *Geophysical Research Letters* 33.21.

Borchert, Leonard F, Wolfgang A Müller & Johanna Baehr (2018). "Atlantic Ocean Heat Transport Influences Interannual-to-Decadal Surface Temperature Predictability in the North Atlantic Region." In: *Journal of Climate* 31.17, pp. 6763–6782.

Born, Andreas, Thomas F Stocker & Anne Britt Sandø (2016). "Transport of salt and freshwater in the Atlantic Subpolar Gyre." In: *Ocean Dynamics* 66.9, pp. 1051–1064.

Brander, KM (1995). "The effect of temperature on growth of Atlantic cod (Gadus morhua L.)" In: *ICES Journal of Marine Science* 52.1, pp. 1–10.

Brander, Keith (2010). "Impacts of climate change on fisheries." In: *Journal of Marine Systems* 79.3-4, pp. 389–402.

Brune, Sebastian, Lars Nerger & Johanna Baehr (2015). "Assimilation of oceanic observations in a global coupled Earth system model with the SEIK filter." In: *Ocean Modelling* 96, pp. 254–264.

Brune, Sebastian, André Düsterhus, Holger Pohlmann, Wolfgang A Müller & Johanna Baehr (2018). "Time dependency of the prediction skill for the North Atlantic subpolar gyre in initialized decadal hindcasts." In: *Climate dynamics* 51.5-6, pp. 1947–1970.

Burkholder, Kristin C & M Susan Lozier (2014). "Tracing the pathways of the upper limb of the North Atlantic Meridional Overturning Circulation." In: *Geophysical Research Letters* 41.12, pp. 4254–4260.

Carmack, Eddy & Paul Wassmann (2006). "Food webs and physical–biological coupling on pan-Arctic shelves: unifying concepts and comprehensive perspectives." In: *Progress in Oceanography* 71.2-4, pp. 446–477.

Chavez, Francisco P, John Ryan, Salvador E Lluch-Cota & Miguel Ñiquen (2003). "From anchovies to sardines and back: multidecadal change in the Pacific Ocean." In: *science* 299.5604, pp. 217–221.

Curry, Ruth G & Michael S McCartney (2001). "Ocean gyre circulation changes associated with the North Atlantic Oscillation." In: *Journal of Physical Oceanography* 31.12, pp. 3374–3400.

Cushing, DH (1990). "Plankton production and year-class strength in fish populations: an update of the match/mismatch hypothesis." In: *Advances in marine biology*. Vol. 26. Elsevier, pp. 249–293.

Daewel, Ute & Corinna Schrum (2017). "Low-frequency variability in North Sea and Baltic Sea identified through simulations with the 3-D coupled physical–biogeochemical model ECOSMO." In: *Earth System Dynamics* 8.3, p. 801.

Daewel, Ute, Corinna Schrum & Alok Kumar Gupta (2015). "The predictive potential of early life stage individual-based models (IBMs): an example for Atlantic cod Gadus morhua in the North Sea." In: *Marine Ecology Progress Series* 534, pp. 199–219.

Dee, Dick P, SM Uppala, AJ Simmons, Paul Berrisford, P Poli, S Kobayashi, U Andrae, MA Balmaseda, G Balsamo, d P Bauer, et al. (2011). "The ERA-Interim reanalysis:

Configuration and performance of the data assimilation system." In: *Quarterly Journal of the royal meteorological society* 137.656, pp. 553–597.

Delandmeter, Philippe & Erik Van Sebille (2019). "The parcels v2. 0 Lagrangian framework: new field interpolation schemes." In: *Geosci. Model Dev. Discuss*.

Delworth, T, S Manabe & RJ Stouffer (1993). "Interdecadal variations of the thermohaline circulation in a coupled ocean-atmosphere model." In: *Journal of Climate* 6.11, pp. 1993–2011.

Dickson, Robert R (1971). "A recurrent and persistent pressure-anomaly pattern as the principal cause of intermediate-scale hydrographic variation in the European shelf seas." In: *Deutsche Hydrografische Zeitschrift* 24.3, pp. 97–119.

Dong, Buwen & Rowan T Sutton (2005). "Mechanism of interdecadal thermohaline circulation variability in a coupled ocean–atmosphere GCM." In: *Journal of climate* 18.8, pp. 1117–1135.

Drinkwater, Kenneth F (2005). "The response of Atlantic cod (Gadus morhua) to future climate change." In: *ICES Journal of Marine Science* 62.7, pp. 1327–1337.

Drinkwater, Kenneth F, Andrea Belgrano, Angel Borja, Alessandra Conversi, Martin Edwards, Charles H Greene, Geir Ottersen, Andrew J Pershing & Henry Walker (2003). "The response of marine ecosystems to climate variability associated with the North Atlantic Oscillation." In: *Geophysical Monograph-American Geophysical Union* 134, pp. 211–234.

Drinkwater, Kenneth F, Gregory Beaugrand, Masahide Kaeriyama, Suam Kim, Geir Ottersen, R Ian Perry, Hans-Otto Pörtner, Jeffrey J Polovina & Akinori Takasuka (2010). "On the processes linking climate to ecosystem changes." In: *Journal of Marine Systems* 79.3-4, pp. 374–388.

Eden, Carsten & Jürgen Willebrand (2001). "Mechanism of interannual to decadal variability of the North Atlantic circulation." In: *Journal of Climate* 14.10, pp. 2266–2280.

Ellett, DJ & WR Turrell (1992). "Increased salinity levels in the NE Atlantic." In: *ICES COUNCIL MEETING PAPERS, ICES, COPENHAGEN(DENMARK), 1992, 12*.

Eveson, J Paige, Alistair J Hobday, Jason R Hartog, Claire M Spillman & Kirsten M Rough (2015). "Seasonal forecasting of tuna habitat in the Great Australian Bight." In: *Fisheries Research* 170, pp. 39–49.

Flatau, Maria K, Lynne Talley & Pearn P Niiler (2003). "The North Atlantic Oscillation, surface current velocities, and SST changes in the subpolar North Atlantic." In: *Journal of Climate* 16.14, pp. 2355–2369.

Fossheim, Maria, Raul Primicerio, Edda Johannesen, Randi B Ingvaldsen, Michaela M Aschan & Andrey V Dolgov (2015). "Recent warming leads to a rapid borealization of fish communities in the Arctic." In: *Nature Climate Change* 5.7, p. 673.

Foukal, Nicholas P & M Susan Lozier (2017). "Assessing variability in the size and strength of the North Atlantic subpolar gyre." In: *Journal of Geophysical Research: Oceans*.

Frank, Kenneth T, Brian Petrie, William C Leggett & Daniel G Boyce (2016). "Large scale, synchronous variability of marine fish populations driven by commercial exploitation." In: *Proceedings of the National Academy of Sciences* 113.29, pp. 8248–8253.

Frankignoul, Claude, Julie Deshayes & Ruth Curry (2009). "The role of salinity in the decadal variability of the North Atlantic meridional overturning circulation." In: *Climate dynamics* 33.6, pp. 777–793.

Gent, Peter R, Jurgen Willebrand, Trevor J McDougall & James C McWilliams (1995). "Parameterizing eddy-induced tracer transports in ocean circulation models." In: *Journal of Physical Oceanography* 25.4, pp. 463–474.

Giorgetta, Marco A, Johann Jungclaus, Christian H Reick, Stephanie Legutke, Jürgen Bader, Michael Böttinger, Victor Brovkin, Traute Crueger, Monika Esch, Kerstin Fieg, et al. (2013). "Climate and carbon cycle changes from 1850 to 2100 in MPI-ESM simulations for the Coupled Model Intercomparison Project phase 5." In: *Journal of Advances in Modeling Earth Systems* 5.3, pp. 572–597.

Glaser, Sarah M, Michael J Fogarty, Hui Liu, Irit Altman, Chih-Hao Hsieh, Les Kaufman, Alec D MacCall, Andrew A Rosenberg, Hao Ye & George Sugihara (2014). "Complex dynamics may limit prediction in marine fisheries." In: *Fish and Fisheries* 15.4, pp. 616–633.

Glessmer, Mirjam Sophia, Tor Eldevik, Kjetil Våge, Jan Even Øie Nilsen & Erik Behrens (2014). "Atlantic origin of observed and modelled freshwater anomalies in the Nordic Seas." In: *Nature Geoscience* 7.11, p. 801.

Good, Simon A, Matthew J Martin & Nick A Rayner (2013). "EN4: Quality controlled ocean temperature and salinity profiles and monthly objective analyses with uncertainty estimates." In: *Journal of Geophysical Research: Oceans* 118.12, pp. 6704–6716.

Hagemann, Stefan & L Dümenil Gates (2003). "Improving a subgrid runoff parameterization scheme for climate models by the use of high resolution data derived from satellite observations." In: *Climate Dynamics* 21.3-4, pp. 349–359.

Häkkinen, Sirpa & Peter B Rhines (2004). "Decline of subpolar North Atlantic circulation during the 1990s." In: *Science* 304.5670, pp. 555–559.

Häkkinen, Sirpa, Peter B Rhines & Denise L Worthen (2011a). "Atmospheric blocking and Atlantic multidecadal ocean variability." In: *Science* 334.6056, pp. 655–659.

– (2011b). "Warm and saline events embedded in the meridional circulation of the northern North Atlantic." In: *Journal of Geophysical Research: Oceans* 116.C3.

Haltuch, MA, EN Brooks, J Brodziak, JA Devine, KF Johnson, N Klibansky, RDM Nash, MR Payne, KW Shertzer, S Subbey, et al. (2019). "Unraveling the recruitment problem: A review of environmentally-informed forecasting and management strategy evaluation." In: *Fisheries Research*.

Hamre, Johannes (1994). "Biodiversity and exploitation of the main fish stocks in the Norwegian-Barents Sea ecosystem." In: *Biodiversity & Conservation* 3.6, pp. 473–492.

Hare, Jonathan A (2014). "The future of fisheries oceanography lies in the pursuit of multiple hypotheses." In: *ICES Journal of Marine Science* 71.8, pp. 2343–2356.

Hátún, H & L Chafik (2018). "On the recent ambiguity of the North Atlantic subpolar gyre index." In: *Journal of Geophysical Research: Oceans*.

Hátún, H, Katja Lohmann, Daniela Matei, Johann H Jungclaus, S Pacariz, M Bersch, A Gislason, J Ólafsson & PC Reid (2016). "An inflated subpolar gyre blows life toward the northeastern Atlantic." In: *Progress in Oceanography* 147, pp. 49–66.

Hátún, Hjálmar, Anne Britt Sandø, Helge Drange, Bogi Hansen & Heðinn Valdimarsson (2005). "Influence of the Atlantic subpolar gyre on the thermohaline circulation." In: *Science* 309.5742, pp. 1841–1844.

Hátún, Hjálmar, MR Payne, G Beaugrand, PC Reid, AB Sandø, H Drange, B Hansen, JA Jacobsen & D Bloch (2009). "Large bio-geographical shifts in the north-eastern

Atlantic Ocean: From the subpolar gyre, via plankton, to blue whiting and pilot whales." In: *Progress in Oceanography* 80.3, pp. 149–162.

Helland-Hansen, Bjørn & Fridtjof Nansen (1909). *The Norwegian Sea: its physical oceanography based upon the Norwegian researches 1900-1904*. Det Mallingske bogtrykkeri.

Herbaut, Christophe & Marie-Noëlle Houssais (2009). "Response of the eastern North Atlantic subpolar gyre to the North Atlantic Oscillation." In: *Geophysical Research Letters* 36.17.

Hermanson, Leon, Rosie Eade, Niall H Robinson, Nick J Dunstone, Martin B Andrews, Jeff R Knight, Adam A Scaife & Doug M Smith (2014). "Forecast cooling of the Atlantic subpolar gyre and associated impacts." In: *Geophysical research letters* 41.14, pp. 5167–5174.

Hjøllo, Solfrid Sætre, Morten D Skogen & Einar Svendsen (2009). "Exploring currents and heat within the North Sea using a numerical model." In: *Journal of Marine Systems* 78.1, pp. 180–192.

Hjort, Johan (1914). "Fluctuations in the great fisheries of northern Europe viewed in the light of biological research." In: ICES.

Hobday, Alistair J, Jason R Hartog, Claire M Spillman & Oscar Alves (2011). "Seasonal forecasting of tuna habitat for dynamic spatial management." In: *Canadian Journal of Fisheries and Aquatic Sciences* 68.5, pp. 898–911.

Holliday, N Penny & Philip C Reid (2001). "Is there a connection between high transport of water through the Rockall Trough and ecological changes in the North Sea?" In: *ICES Journal of Marine Science: Journal du Conseil* 58.1, pp. 270–274.

Holliday, N Penny, SL Hughes, S Bacon, A Beszczynska-Möller, B Hansen, A Lavin, H Loeng, KA Mork, S Østerhus, T Sherwin, et al. (2008). "Reversal of the 1960s to 1990s freshening trend in the northeast North Atlantic and Nordic Seas." In: *Geophysical Research Letters* 35.3.

Holliday, NP (2003). "Air-sea interaction and circulation changes in the northeast Atlantic." In: *Journal of Geophysical Research: Oceans* 108.C8.

Holliday, NP, SA Cunningham, C Johnson, SF Gary, C Griffiths, JF Read & T Sherwin (2015). "Multidecadal variability of potential temperature, salinity, and transport in the eastern subpolar North Atlantic." In: *Journal of Geophysical Research: Oceans* 120.9, pp. 5945–5967.

Holt, JT, M Butenschon, SL Wakelin, Y Artioli & JI Allen (2012). "Oceanic controls on the primary production of the northwest European continental shelf: model experiments under recent past conditions and a potential future scenario." In: *Biogeosciences* 9, pp. 97–117.

Holt, Jason, Patrick Hyder, Mike Ashworth, James Harle, Helene T Hewitt, Hedong Liu, Adrian L New, Stephen Pickles, Andrew Porter, Ekaterina Popova, et al. (2017). "Prospects for improving the representation of coastal and shelf seas in global ocean models." In: *Geoscientific Model Development* 10.1, pp. 499–523.

Hunt Jr, George L, Kenneth F Drinkwater, Kevin Arrigo, Jørgen Berge, Kendra L Daly, Seth Danielson, Malin Daase, Haakon Hop, Enrique Isla, Nina Karnovsky, et al. (2016). "Advection in polar and sub-polar environments: Impacts on high latitude marine ecosystems." In: *Progress in Oceanography* 149, pp. 40–81.

Hurrell, James W, Yochanan Kushnir, Geir Ottersen & Martin Visbeck (2003). "An overview of the North Atlantic oscillation." In: *Geophysical Monograph-American Geophysical Union* 134, pp. 1–36.

Hutchings, Jeffrey A (1995). "The biological collapse of Atlantic cod off Newfoundland and Labrador: an exploration of historical changes in exploitation, harvesting technology, and management." In: *The North Atlantic Fishery: Strengths, Weaknesses, and Challenges*.

Ilyina, Tatiana, Katharina D Six, Joachim Segschneider, Ernst Maier-Reimer, Hongmei Li & Ismael Núñez-Riboni (2013). "Global ocean biogeochemistry model HAMOCC: Model architecture and performance as component of the MPI-Earth system model in different CMIP5 experimental realizations." In: *Journal of Advances in Modeling Earth Systems* 5.2, pp. 287–315.

Jackson, Laura C, K Andrew Peterson, Chris D Roberts & Richard A Wood (2016). "Recent slowing of Atlantic overturning circulation as a recovery from earlier strengthening." In: *Nature Geoscience* 9.7, p. 518.

Johnson, Clare, Mark Inall & Sirpa Häkkinen (2013). "Declining nutrient concentrations in the northeast Atlantic as a result of a weakening Subpolar Gyre." In: *Deep Sea Research Part I: Oceanographic Research Papers* 82, pp. 95–107.

Jungclaus, JH, Nils Fischer, Helmuth Haak, K Lohmann, J Marotzke, D Matei, U Mikolajewicz, D Notz & JS Storch (2013). "Characteristics of the ocean simulations in the Max Planck Institute Ocean Model (MPIOM) the ocean component of the MPI-Earth system model." In: *Journal of Advances in Modeling Earth Systems* 5.2, pp. 422–446.

Jungclaus, Johann H, Katja Lohmann & Davide Zanchettin (2014). "Enhanced 20th century heat transfer to the Arctic simulated in context of climate variations over last millennium." In: *Climate of the Past* 10, pp. 2201–2213.

Kaplan, Isaac C, Gregory D Williams, Nicholas A Bond, Albert J Hermann & Samantha A Siedlecki (2016). "Cloudy with a chance of sardines: forecasting sardine distributions using regional climate models." In: *Fisheries Oceanography* 25.1, pp. 15–27.

Koul, Vimal, C Schrum, A Düsterhus & J Baehr (2019a). "Atlantic Inflow to the North Sea Modulated by the Subpolar Gyre in a Historical Simulation With MPI-ESM." In: *Journal of Geophysical Research: Oceans* 124.3, pp. 1807–1826.

Koul, Vimal, C Schrum, M Årthun, S Brune & J Baehr (2019b). "Decadal Prediction of Barents Sea Cod Stock through an Oceanic Linkage with the Subpolar Gyre." In: *Frontiers in Marine Science (to be submitted)*.

Koul, Vimal, J-E Tesdal, M Bersch, H Hatun, S Brune, L Borchert, H Haak, C Schrum & J Baehr (2019c). "Unravelling the Choice of the North Atlantic Subpolar Gyre Index." In: *Nature Scientific Reports (under review)*.

Lange, Michael & Erik van Sebille (2017). "Parcels v0. 9: prototyping a Lagrangian ocean analysis framework for the petascale age." In: *arXiv preprint arXiv:1707.05163*.

Langehaug, HR, Daniela Matei, T Eldevik, K Lohmann & Y Gao (2017). "On model differences and skill in predicting sea surface temperature in the Nordic and Barents Seas." In: *Climate Dynamics* 48.3-4, pp. 913–933.

Langehaug, Helene R, Anne Britt Sandø, Marius Årthun & M Ilıcak (2019). "Variability along the Atlantic water pathway in the forced Norwegian Earth System Model." In: *Climate dynamics* 52.1-2, pp. 1211–1230.

Langford, Sally, Samantha Stevenson & David Noone (2014). "Analysis of low-frequency precipitation variability in CMIP5 historical simulations for southwestern North America." In: *Journal of Climate* 27.7, pp. 2735–2756.

Larsen, Karin Margretha H, Hjálmar Hátún, Bogi Hansen & Regin Kristiansen (2012). "Atlantic water in the Faroe area: sources and variability." In: *ICES Journal of Marine Science* 69.5, pp. 802–808.

Lehodey, P, J Alheit, M Barange, T Baumgartner, G Beaugrand, K Drinkwater, J-M Fromentin, SR Hare, G Ottersen, RI Perry, et al. (2006). "Climate variability, fish, and fisheries." In: *Journal of Climate* 19.20, pp. 5009–5030.

Lohmann, Katja, Helge Drange & Mats Bentsen (2009). "A possible mechanism for the strong weakening of the North Atlantic subpolar gyre in the mid-1990s." In: *Geophysical Research Letters* 36.15.

Lorbacher, Katja, Joachim Dengg, Claus W Böning & Arne Biastoch (2010). "Regional patterns of sea level change related to interannual variability and multidecadal trends in the Atlantic meridional overturning circulation." In: *Journal of Climate* 23.15, pp. 4243–4254.

Lozier, M. Susan & Nicole M. Stewart (2008). "On the Temporally Varying Northward Penetration of Mediterranean Overflow Water and Eastward Penetration of Labrador Sea Water." In: *J. Phys. Oceanogr.* 38.2097–2103.

Maher, Nicola, Sebastian Milinski, Laura Suarez-Gutierrez, Michael Botzet, Mikhail Dobrynin, Luis Kornblueh, Jürgen Kröger, Yohei Takano, Rohit Ghosh, Christopher Hedemann, et al. (2019). "The Max Planck Institute Grand Ensemble: Enabling the Exploration of Climate System Variability." In: *Journal of Advances in Modeling Earth Systems* 11.7, pp. 2050–2069.

Mantua, Nathan J, Steven R Hare, Yuan Zhang, John M Wallace & Robert C Francis (1997). "A Pacific interdecadal climate oscillation with impacts on salmon production." In: *Bulletin of the american Meteorological Society* 78.6, pp. 1069–1080.

Marotzke, Jochem, Wolfgang A Müller, Freja SE Vamborg, Paul Becker, Ulrich Cubasch, Hendrik Feldmann, Frank Kaspar, Christoph Kottmeier, Camille Marini, Iuliia Polkova, et al. (2016). "MiKlip: a national research project on decadal climate prediction." In: *Bulletin of the american meteorological society* 97.12, pp. 2379–2394.

Marshall, John, Helen Johnson & Jason Goodman (2001). "A study of the interaction of the North Atlantic Oscillation with ocean circulation." In: *Journal of Climate* 14.7, pp. 1399–1421.

Marsland, Simon J, Helmuth Haak, Johann H Jungclaus, Mojib Latif & Frank Röske (2003). "The Max-Planck-Institute global ocean/sea ice model with orthogonal curvilinear coordinates." In: *Ocean modelling* 5.2, pp. 91–127.

Martin, Elinor R, Chris Thorncroft & Ben BB Booth (2014). "The multidecadal Atlantic SST—Sahel rainfall teleconnection in CMIP5 simulations." In: *Journal of Climate* 27.2, pp. 784–806.

Matei, Daniela, Holger Pohlmann, Johann Jungclaus, Wolfgang Müller, Helmuth Haak & Jochem Marotzke (2012). "Two tales of initializing decadal climate prediction experiments with the ECHAM5/MPI-OM model." In: *Journal of Climate* 25.24, pp. 8502–8523.

Mathis, Moritz, Alberto Elizalde, Uwe Mikolajewicz & Thomas Pohlmann (2015). "Variability patterns of the general circulation and sea water temperature in the North Sea." In: *Progress in Oceanography* 135, pp. 91–112.

Mathis, Moritz, Alberto Elizalde & Uwe Mikolajewicz (2017). "Which complexity of regional climate system models is essential for downscaling anthropogenic climate change in the Northwest European Shelf?" In: *Climate Dynamics*, pp. 1–23.

Mauritzen, C, Solfrid Sætre Hjøllo & Anne Britt Sandø (2006). "Passive tracers and active dynamics: A model study of hydrography and circulation in the northern North Atlantic." In: *Journal of Geophysical Research: Oceans* 111.C8.

McCarthy, Gerard D, Ivan D Haigh, Joël J-M Hirschi, Jeremy P Grist & David A Smeed (2015). "Ocean impact on decadal Atlantic climate variability revealed by sea-level observations." In: *Nature* 521.7553, pp. 508–510.

Meehl, Gerald A, Lisa Goddard, George Boer, Robert Burgman, Grant Branstator, Christophe Cassou, Susanna Corti, Gokhan Danabasoglu, Francisco Doblas-Reyes, Ed Hawkins, et al. (2014). "Decadal climate prediction: an update from the trenches." In: *Bulletin of the American Meteorological Society* 95.2, pp. 243–267.

Michalsen, K, Geir Ottersen & Odd Nakken (1998). "Growth of North-east Arctic cod (Gadus morhua L.) in relation to ambient temperature." In: *ICES Journal of Marine Science* 55.5, pp. 863–877.

Miesner, Anna K & Mark R Payne (2018). "Oceanographic variability shapes the spawning distribution of blue whiting (Micromesistius poutassou)." In: *Fisheries Oceanography* 27.6, pp. 623–638.

Mills, Katherine E, Andrew J Pershing, Curtis J Brown, Yong Chen, Fu-Sung Chiang, Daniel S Holland, Sigrid Lehuta, Janet A Nye, Jenny C Sun, Andrew C Thomas, et al. (2013). "Fisheries management in a changing climate: lessons from the 2012 ocean heat wave in the Northwest Atlantic." In: *Oceanography* 26.2, pp. 191–195.

Mork, Kjell Arne, Øystein Skagseth & Henrik Søiland (2019). "Recent Warming and Freshening of the Norwegian Sea Observed by Argo Data." In: *Journal of Climate* 32.12, pp. 3695–3705.

Msadek, Rym, TL Delworth, A Rosati, W Anderson, G Vecchi, Y-S Chang, K Dixon, RG Gudgel, W Stern, A Wittenberg, et al. (2014). "Predicting a decadal shift in North Atlantic climate variability using the GFDL forecast system." In: *Journal of Climate* 27.17, pp. 6472–6496.

Myers, Ransom A (1998). "When do environment–recruitment correlations work?" In: *Reviews in Fish Biology and Fisheries* 8.3, pp. 285–305.

Myers, Ransom A, Jeffrey A Hutchings & Nicholas J Barrowman (1997). "Why do fish stocks collapse? The example of cod in Atlantic Canada." In: *Ecological applications* 7.1, pp. 91–106.

Núñez-Riboni, Ismael & Anna Akimova (2017). "Quantifying the impact of the major driving mechanisms of inter-annual variability of salinity in the North Sea." In: *Progress in oceanography* 154, pp. 25–37.

Nye, Janet A, Jason S Link, Jonathan A Hare & William J Overholtz (2009). "Changing spatial distribution of fish stocks in relation to climate and population size on the Northeast United States continental shelf." In: *Marine Ecology Progress Series* 393, pp. 111–129.

Olafsdottir, Anna H, Kjell Rong Utne, Jan Arge Jacobsen, Teunis Jansen, Guðmundur J Óskarsson, Leif Nøttestad, Bjarki Þ Elvarsson, Cecilie Broms & Aril Slotte (2019). "Geographical expansion of Northeast Atlantic mackerel (Scomber scombrus) in the Nordic Seas from 2007 to 2016 was primarily driven by stock size and constrained by low temperatures." In: *Deep Sea Research Part II: Topical Studies in Oceanography* 159, pp. 152–168.

Olsen, Esben Moland, Geir Ottersen, Marcos Llope, Kung-Sik Chan, Grégory Beaugrand & Nils Chr Stenseth (2010). "Spawning stock and recruitment in North Sea

cod shaped by food and climate." In: *Proceedings of the Royal Society B: Biological Sciences* 278.1705, pp. 504–510.

Orvik, Kjell Arild & Peter Niiler (2002). "Major pathways of Atlantic water in the northern North Atlantic and Nordic Seas toward Arctic." In: *Geophysical Research Letters* 29.19.

Ottersen, Geir, Harald Loeng & Askjell Raknes (1994). "Influence of temperature variability on recruitment of cod in the Barents Sea." In: *ICES Marine Science Symposia*. Vol. 198. Copenhagen, Denmark: International Council for the Exploration of the Sea, 1991-, pp. 471–481.

Pacanowski, RC & SGH Philander (1981). "Parameterization of vertical mixing in numerical models of tropical oceans." In: *Journal of Physical Oceanography* 11.11, pp. 1443–1451.

Pätsch, Johannes, Hans Burchard, Christian Dieterich, Ulf Gräwe, Matthias Gröger, Moritz Mathis, Hartmut Kapitza, Manfred Bersch, Andreas Moll, Thomas Pohlmann, et al. (2017). "An evaluation of the North Sea circulation in global and regional models relevant for ecosystem simulations." In: *Ocean Modelling*.

Payne, Mark R, Alistair J Hobday, Brian R MacKenzie, Desiree Tommasi, Danielle P Dempsey, Sascha MM Fässler, Alan C Haynie, Rubao Ji, Gang Liu, Patrick D Lynch, et al. (2017). "Lessons from the first generation of marine ecological forecast products." In: *Frontiers in Marine Science* 4, p. 289.

Pershing, Andrew J, Michael A Alexander, Christina M Hernandez, Lisa A Kerr, Arnault Le Bris, Katherine E Mills, Janet A Nye, Nicholas R Record, Hillary A Scannell, James D Scott, et al. (2015). "Slow adaptation in the face of rapid warming leads to collapse of the Gulf of Maine cod fishery." In: *Science* 350.6262, pp. 809–812.

Piecuch, Christopher G, Rui M Ponte, Christopher M Little, Martha W Buckley & Ichiro Fukumori (2017). "Mechanisms underlying recent decadal changes in subpolar N orth A tlantic O cean heat content." In: *Journal of Geophysical Research: Oceans* 122.9, pp. 7181–7197.

Pinsky, Malin L, Boris Worm, Michael J Fogarty, Jorge L Sarmiento & Simon A Levin (2013). "Marine taxa track local climate velocities." In: *Science* 341.6151, pp. 1239–1242.

Planque, B & T Frédou (1999). "Temperature and the recruitment of Atlantic cod (Gadus morhua)." In: *Canadian Journal of Fisheries and Aquatic Sciences* 56.11, pp. 2069–2077.

Pohlmann, Holger, Michael Botzet, Mojib Latif, Andreas Roesch, Martin Wild & Peter Tschuck (2004). "Estimating the decadal predictability of a coupled AOGCM." In: *Journal of Climate* 17.22, pp. 4463–4472.

Polkova, Iuliia, Sebastian Brune, Christopher Kadow, Vanya Romanova, Gereon Gollan, Johanna Baehr, Rita Glowienka-Hense, Richard J Greatbatch, Andreas Hense, Sebastian Illing, et al. (2019). "Initialization and ensemble generation for decadal climate predictions: A comparison of different methods." In: *Journal of Advances in Modeling Earth Systems* 11.1, pp. 149–172.

Pörtner, Hans-Otto, B Berdal, R Blust, O Brix, A Colosimo, B De Wachter, A Giuliani, T Johansen, T Fischer, Rainer Knust, et al. (2001). "Climate induced temperature effects on growth performance, fecundity and recruitment in marine fish: developing a hypothesis for cause and effect relationships in Atlantic cod (Gadus morhua)

and common eelpout (Zoarces viviparus)." In: *Continental Shelf Research* 21.18-19, pp. 1975–1997.

Pyper, Brian J & Randall M Peterman (1998). "Comparison of methods to account for autocorrelation in correlation analyses of fish data." In: *Canadian Journal of Fisheries and Aquatic Sciences* 55.9, pp. 2127–2140.

Quinn, Terrance J & Richard B Deriso (1999). *Quantitative fish dynamics*. oxford university Press.

Reick, CH, Thomas Raddatz, Victor Brovkin & Veronika Gayler (2013). "Representation of natural and anthropogenic land cover change in MPI-ESM." In: *Journal of Advances in Modeling Earth Systems* 5.3, pp. 459–482.

Robson, JI, RT Sutton & DM Smith (2012a). "Initialized decadal predictions of the rapid warming of the North Atlantic Ocean in the mid 1990s." In: *Geophysical Research Letters* 39.19.

Robson, Jon, Rowan Sutton, Katja Lohmann, Doug Smith & Matthew D Palmer (2012b). "Causes of the rapid warming of the North Atlantic Ocean in the mid-1990s." In: *Journal of Climate* 25.12, pp. 4116–4134.

Robson, Jon, Pablo Ortega & Rowan Sutton (2016). "A reversal of climatic trends in the North Atlantic since 2005." In: *Nature Geoscience* 9.7, p. 513.

Robson, Jon, Irene Polo, Dan LR Hodson, David P Stevens & Len C Shaffrey (2018). "Decadal prediction of the North Atlantic subpolar gyre in the HiGEM high-resolution climate model." In: *Climate dynamics* 50.3-4, pp. 921–937.

Sandø, AB, JE Nilsen, T Eldevik & Mats Bentsen (2012). "Mechanisms for variable North Atlantic–Nordic seas exchanges." In: *Journal of Geophysical Research: Oceans* 117.C12.

Sarafanov, Artem (2009). "On the effect of the North Atlantic Oscillation on temperature and salinity of the subpolar North Atlantic intermediate and deep waters." In: *ICES Journal of Marine Science* 66.7, pp. 1448–1454.

Sarafanov, Artem, Anastasia Falina, Alexey Sokov & Alexander Demidov (2008). "Intense warming and salinification of intermediate waters of southern origin in the eastern subpolar North Atlantic in the 1990s to mid-2000s." In: *Journal of Geophysical Research: Oceans* 113.C12.

Sarafanov, Artem, Anastasia Falina, Alexey Sokov, Vyacheslav Zapotylko & Sergey Gladyshev (2018). "Ship-Based Monitoring of the Northern North Atlantic Ocean by the Shirshov Institute of Oceanology. The Main Results." In: *The Ocean in Motion*. Springer, pp. 415–427.

Schrum, Corinna (2001). "Regionalization of climate change for the North Sea and Baltic Sea." In: *Climate Research* 18.1/2, pp. 31–37.

Séférian, Roland, Laurent Bopp, Marion Gehlen, Didier Swingedouw, Juliette Mignot, Eric Guilyardi & Jérôme Servonnat (2014). "Multiyear predictability of tropical marine productivity." In: *Proceedings of the National Academy of Sciences* 111.32, pp. 11646–11651.

Sguotti, Camilla, Saskia A Otto, Romain Frelat, Tom J Langbehn, Marie Plambech Ryberg, Martin Lindegren, Joël M Durant, Nils Chr. Stenseth & Christian Möllmann (2019). "Catastrophic dynamics limit Atlantic cod recovery." In: *Proceedings of the Royal Society B* 286.1898, p. 20182877.

Sharp, GD (1987). "Climate and fisheries: cause and effect or managing the long and short of it all." In: *South African Journal of Marine Science* 5.1, pp. 811–838.

Shelton, PA & L Hutchings (1982). "Transport of anchovy, Engraulis capensis Gilchrist, eggs and early larvae by a frontal jet current." In: *ICES Journal of Marine Science* 40.2, pp. 185–198.

Sherwin, Toby J, Jane F Read, N Penny Holliday & Clare Johnson (2011). "The impact of changes in North Atlantic Gyre distribution on water mass characteristics in the Rockall Trough." In: *ICES Journal of Marine Science* 69.5, pp. 751–757.

Skern-Mauritzen, Mette, Geir Ottersen, Nils Olav Handegard, Geir Huse, Gjert E Dingsør, Nils C Stenseth & Olav S Kjesbu (2016). "Ecosystem processes are rarely included in tactical fisheries management." In: *Fish and Fisheries* 17.1, pp. 165–175.

Stenseth, Nils C, Atle Mysterud, Geir Ottersen, James W Hurrell, Kung-Sik Chan & Mauricio Lima (2002). "Ecological effects of climate fluctuations." In: *Science* 297.5585, pp. 1292–1296.

Stevens, Bjorn, Marco Giorgetta, Monika Esch, Thorsten Mauritsen, Traute Crueger, Sebastian Rast, Marc Salzmann, Hauke Schmidt, Jürgen Bader, Karoline Block, et al. (2013). "Atmospheric component of the MPI-M Earth System Model: ECHAM6." In: *Journal of Advances in Modeling Earth Systems* 5.2, pp. 146–172.

Stock, Charles A, Michael A Alexander, Nicholas A Bond, Keith M Brander, William WL Cheung, Enrique N Curchitser, Thomas L Delworth, John P Dunne, Stephen M Griffies, Melissa A Haltuch, et al. (2011). "On the use of IPCC-class models to assess the impact of climate on living marine resources." In: *Progress in Oceanography* 88.1-4, pp. 1–27.

Subbey, Sam, Jennifer A Devine, Ute Schaarschmidt & Richard DM Nash (2014). "Modelling and forecasting stock–recruitment: current and future perspectives." In: *ICES Journal of Marine Science* 71.8, pp. 2307–2322.

Sundby, Svein & Kenneth Drinkwater (2007). "On the mechanisms behind salinity anomaly signals of the northern North Atlantic." In: *Progress in Oceanography* 73.2, pp. 190–202.

Sundby, Svein & Odd Nakken (2008). "Spatial shifts in spawning habitats of Arcto-Norwegian cod related to multidecadal climate oscillations and climate change." In: *ICES Journal of Marine Science* 65.6, pp. 953–962.

Taylor, Arnold H & John A Stephens (1998). "The North Atlantic oscillation and the latitude of the Gulf Stream." In: *Tellus A* 50.1, pp. 134–142.

Taylor, Karl E, Ronald J Stouffer & Gerald A Meehl (2012). "An overview of CMIP5 and the experiment design." In: *Bulletin of the American Meteorological Society* 93.4, pp. 485–498.

Tesdal, Jan-Erik, Ryan P Abernathey, Joaquim I Goes, Arnold L Gordon & Thomas WN Haine (2018). "Salinity trends within the upper layers of the subpolar North Atlantic." In: *Journal of Climate* 31.7, pp. 2675–2698.

Tommasi, Désirée, Charles A Stock, Kathleen Pegion, Gabriel A Vecchi, Richard D Methot, Michael A Alexander & David M Checkley Jr (2017a). "Improved management of small pelagic fisheries through seasonal climate prediction." In: *Ecological Applications* 27.2, pp. 378–388.

Tommasi, Desiree, Charles A Stock, Alistair J Hobday, Rick Methot, Isaac C Kaplan, J Paige Eveson, Kirstin Holsman, Timothy J Miller, Sarah Gaichas, Marion Gehlen, et al. (2017b). "Managing living marine resources in a dynamic environment: the role of seasonal to decadal climate forecasts." In: *Progress in Oceanography* 152, pp. 15–49.

Tommasi, Desiree, Charles A Stock, Michael A Alexander, Xiaosong Yang, Anthony Rosati & Gabriel A Vecchi (2017c). "Multi-annual climate predictions for fisheries: an assessment of skill of sea surface temperature forecasts for large marine ecosystems." In: *Frontiers in Marine Science* 4, p. 201.

Turrell, WR, G Slesser, R Payne, RD Adams & PA Gillibrand (1996). "Hydrography of the East Shetland Basin in relation to decadal North Sea variability." In: *ICES Journal of Marine Science: Journal du Conseil* 53.6, pp. 899–916.

Turrell, William R, Bogi Hansen, Sarah Hughes & Svein Østerhus (2003). "Hydrographic variability during the decade of the 1990s in the Northeast Atlantic and southern Norwegian Sea." In: *ICES Marine Science Symposia*. Vol. 219, pp. 111–120.

Uppala, Sakari M, PW Kållberg, AJ Simmons, U Andrae, V Da Costa Bechtold, M Fiorino, JK Gibson, J Haseler, A Hernandez, GA Kelly, et al. (2005). "The ERA-40 re-analysis." In: *Quarterly Journal of the Royal Meteorological Society: A journal of the atmospheric sciences, applied meteorology and physical oceanography* 131.612, pp. 2961–3012.

Walters, Carl J & Jeremy S Collie (1988). "Is research on environmental factors useful to fisheries management?" In: *Canadian Journal of Fisheries and Aquatic Sciences* 45.10, pp. 1848–1854.

Winther, Nina Gjerde & Johnny A Johannessen (2006). "North Sea circulation: Atlantic inflow and its destination." In: *Journal of Geophysical Research: Oceans* 111.C12.

Yeager, Stephen G, Alicia R Karspeck & Gokhan Danabasoglu (2015). "Predicted slowdown in the rate of Atlantic sea ice loss." In: *Geophysical Research Letters* 42.24, pp. 10–704.

Yeager, Stephen, Alicia Karspeck, Gokhan Danabasoglu, Joe Tribbia & Haiyan Teng (2012). "A decadal prediction case study: Late twentieth-century North Atlantic Ocean heat content." In: *Journal of Climate* 25.15, pp. 5173–5189.

Zhang, Liping & Chunzai Wang (2013). "Multidecadal North Atlantic sea surface temperature and Atlantic meridional overturning circulation variability in CMIP5 historical simulations." In: *Journal of Geophysical Research: Oceans* 118.10, pp. 5772–5791.

Zhang, Rong (2008). "Coherent surface-subsurface fingerprint of the Atlantic meridional overturning circulation." In: *Geophysical Research Letters* 35.20.

Zhang, Rong & Geoffrey K Vallis (2007). "The role of bottom vortex stretching on the path of the North Atlantic western boundary current and on the northern recirculation gyre." In: *Journal of Physical Oceanography* 37.8, pp. 2053–2080.

ACKNOWLEDGMENTS

The successful completion of this dissertation has only been possible with the support, guidance and care of many people. First, I would like to express my most sincere gratitude to my supervisor, Johanna Baehr. I consider myself really fortunate to have been exposed to a research envronment nurtured by her wisdom and scientific accumen. Her unwavering support and encouragemnt throughout these last three years has been invaluebale. I am also deeply grateful to my co-supervisor, Corrina Schrum. I learned a lot from the many exciting discussions we have had on various aspects of my research. I thank Corinna for her magnanimity and allowing me the freedom to explore new ideas. Both Johanna and Corinna are the architects of my transformation from a naive researcher to a thinking scientist, and for that I owe them an insurmountable debt of gratitude. Special thanks are also to Manfred Bersch for being the source of immense knowledge and wisdom.

I have also immensly benefited from sharp insights and critical thinking of my Panel Chair, Jochem Marotzke. His course on Academic Writing has had a profound impact on my approach towards research in general. I am also thankful to Helmuth Haak for all the technical help and discussions on ocean modeling.

I am very thankful to my collegues and students of the Climate Modeling group at Universität Hamburg. I am really glad to have shared my office, my luchtime and my stupid jokes with Patrick Pieper, and I have learned a lot of Statisitcs from him too. I have really enjoyed long discussion with Sebastian Brune on my research and on Cricket. Sebastian has inculcated in me a positive attitude towards research, and for that I am really thankful to him. Thanks are also due to André, Leo, Nele, David and Mikhail for being there whenever I needed them. I have cherished the company of Kevin, Tim, Toby and Simon, and their zeal to teach me German.

I am grateful to the International Max Planck Research School on Earth System Modelling. My heatfelt thanks goes to Antje Weitz, Cornelia Kampmann and Michaela Born for always being supportive and helpful.

This dissertation would not have been possible without the support of my friends. Imke, Sally, Sebastian, Johannes and Katherine, all have stood by me throughpout this journey. No words can express heartfelt appreciation for their moral and intellectual support.

Last but not the least, I would like to thank my loving family for all their care and understanding. I would not have reached here without their support, and the support of my best friend and my life partner, Priyanka. The strength of her optimism and belief in me has enabled me to overcome challenges.

VERSICHERUNG AN EIDES STATT – AFFIRMATION ON OATH

Hiermit versichere ich an Eides statt, dass ich die vorliegende Dissertation mit dem Titel: „Decadal Prediction of Shelf-Sea Marine Ecosystems in the North Atlantic: The Role of the Subpolar Gyre“ selbstständig verfasst und keine anderen als die angegebenen Hilfsmittel – insbesondere keine im Quellenverzeichnis nicht benannten Internet-Quellen – benutzt habe. Alle Stellen, die wörtlich oder sinngemäß aus Veröffentlichungen entnommen wurden, sind als solche kenntlich gemacht. Ich versichere weiterhin, dass ich die Dissertation oder Teile davon vorher weder im In- noch im Aus- land in einem anderen Prüfungsverfahren eingereicht habe und die eingereichte schriftliche Fassung der auf dem elektronischen Speichermedium entspricht.

Hamburg, October 2019

Vimal Koul

Hinweis / Reference

Die gesamten Veröffentlichungen in der Publikationsreihe des MPI-M
„Berichte zur Erdsystemforschung / Reports on Earth System Science“,
ISSN 1614-1199

sind über die Internetseiten des Max-Planck-Instituts für Meteorologie erhältlich:
http://www.mpimet.mpg.de/wissenschaft/publikationen.html

All the publications in the series of the MPI -M
„Berichte zur Erdsystemforschung / Reports on Earth System Science“,
ISSN 1614-1199

are available on the website of the Max Planck Institute for Meteorology:
http://www.mpimet.mpg.de/wissenschaft/publikationen.html